

MTB-325-87A
AUGUST 23, 1988

EVALUATION OF CANDIDATE ALLOYS
FOR THE CONSTRUCTION OF
METAL FLEX HOSES IN
THE STS LAUNCH ENVIRONMENT

PREPARED BY:

ENGINEERING DEVELOPMENT DIRECTORATE
MECHANICAL ENGINEERING DIRECTORATE
MATERIALS SCIENCE LABORATORY
MATERIALS TESTING BRANCH

National Aeronautics and
Space Administration

John F. Kennedy Space Center



DOCUMENT NO. MTB-325-87A
DATE: AUGUST 23, 1988

TEST REPORT

Evaluation of Candidate Alloys for the Construction of
Metal Flex Hoses in the STS Launch Environment

ISSUED BY

National Aeronautics and Space Administration
Kennedy Space Center
Materials Testing Branch

PREPARED BY:

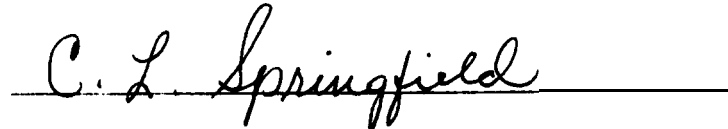


L. G. MacDowell
Materials Testing Branch



C. Ontiveros
NASA/ASEE Summer Faculty Fellow

APPROVED BY:



C. L. Springfield, NASA
Chief, Materials Testing Branch

ACKNOWLEDGMENT: The authors wish to thank Mr. M. D. Springer for his help with monitoring the samples and applying the acid solutions for the salt fog chamber and beach exposure tests.

NOTICE: This document was prepared under the sponsorship of the National Aeronautics and Space Administration. Neither the **United** States Government nor any person acting on behalf of the United States Government assumes any liability resulting from the use of the information contained in this document, or warrants that such use will be free from privately owned rights.

The citation of manufacturer's names, trademarks or other product identification in this document does not constitute an endorsement or approval of the use of such commercial products.

ABSTRACT

Various vacuum jacketed cryogenic supply lines at the Shuttle launch site use convoluted flexible expansion joints. The atmosphere at the launch site has a very high salt content, and during a launch, fuel combustion products include hydrochloric acid. This extremely corrosive environment has caused pitting corrosion failure in the flex hoses, which were made out of **304L** stainless steel. A search was done to find a more corrosion resistant replacement material. This study focused on 19 metal alloys. Tests which were performed include electrochemical corrosion testing, accelerated corrosion testing in a salt fog chamber, long term exposure at 'the beach corrosion testing site, and pitting corrosion tests in ferric chloride solution. Based on the results of these tests, the most corrosion resistant alloys were found to be, in order, Hastelloy C-22, Inconel 625, Hastelloy **C**-276, Hastelloy C-4, and **Inco** Alloy G-3. Of these top five alloys, the Hastelloy C-22 stands out as being the best of the alloys tested, for this application.

TABLE OF CONTENTS

	PAGE
1 .0 INTRODUCTION	1
2.0 MATERIALS AND EQUIPMENT	2
2.1 CANDIDATE ALLOYS	2
2.2 ELECTROCHEMICAL	3
2.3 SALT FOG CHAMBER/ACID DIP	4
2.4 BEACH EXPOSURE/ACID SPRAY	5
2.5 FERRIC CHLORIDE IMMERSION	5
3.0 TEST PROCEDURES	6'
3.1 ELECTROCHEMICAL	6
3.2 SALT FOG CHAMBER/ACID DIP	7
3.3 BEACH EXPOSURE/ACID SPRAY	8
3.4 FERRIC CHLORIDE IMMERSION	9
4.0 TEST RESULTS AND DISCUSSION	9
-1.1 ELECTROCHEMICAL	9
4.2 SALT FOG CHAMBER/ACID DIP	23
4.3 BEACH EXPOSURE/ACID SPRAY	30
4.4 FERRIC CHLORIDE IMMERSION	35
5.0 CONCLUSIONS	39
REFERENCES	39
APPENDIX A	42
APPENDIX B	72

LIST OF ILLUSTRATIONS

Figure	Title	Page
1	'Stable Corrosion Potential	10
2	Unstable Corrosion Potential	11
3	Polarization Resistance Graph	12
4	Cyclic Polarization With Hysteresis Loop	14
5	Cyclic Polarization Without Hysteresis	14
6	Cyclic Polarization With Uniform Corrosion	17
7	Photos After Cyclic Polarization	18
8	Salt Fog Results After 20 Weeks	28
9'	Beach Exposure Results After 251 Days	32
10	Photos After Ferric Chloride Immersion	37
11	Ferric Chloride Immersion - Galvanic Samples	38
Al-A58	Corrosion Potential And Cyclic Polarization	43
Bl-B20	Salt Fog And Beach Exposure Sample Photos	73

LIST OF TABLES

Table	Title	Page
1	Candidate Alloys And Their Compositions	2
2	Properties Of Candidate Alloys	3
3	Autogenous Weld Samples	4
4	Samples Welded To 304L Stainless Steel	5
5	Corrosion Potential	11
6	Polarization Resistance Results	13
i	Area Of Hysteresis Loop	15
8	Critical Pitting Potential	16
9	Protection Potential	16
10	Weight Loss	19
11	Corrosion Potential - 1.0N HCl and 0.1N HCl	20
12	Polarization Resistance Results (1.0N HCl)	20
13	Cyclic Polarization Results (1.0N HCl)	21
14	Summary Of Electrochemical Results	22
15	Salt Fog/Acid Dip Results - 4 Weeks	24
16	Salt Fog/Acid Dip Results - 8 Weeks	25
17	Salt Fog/Acid Dip Results - 12 Weeks	26
18	Salt Fog/Acid Dip Results - 16 Weeks	26
19	Salt Fog/Acid Dip Results - 20 Weeks	27
20	Salt Fog/Acid Dip - Galvanic Welded Results	29
21	Beach Exposure/Acid Spray Results - 60 Days	31
22	Beach Exposure/Acid Spray Results - 251 Days	32
23	Beach Exposure/Acid Spray - Composite Welded	34
24	Ferric Chloride Immersion Results	36
25	Ferric Chloride Immersion - Composite Welded	36

1.0 INTRODUCTION

- 1.1 Flexible hoses are used in various supply lines that service the Orbiter at the launch pad. These convoluted flexible hoses were originally made out of **304L** stainless steel. The extremely corrosive environment of the launch site has caused pitting corrosion in many of these flex hose lines. In the case of vacuum jacketed cryogenic lines, pinhole leaks caused by failure of the flex hose by pitting produces a loss of vacuum and subsequent loss of insulation.
- 1.2 The atmosphere at the launch site has a very high chloride content caused by the proximity of the Atlantic Ocean. During a launch, the products from the fuel combustion reaction include concentrated hydrochloric acid. This combination of chloride and acid leads to a very corrosive environment. This type of environment causes severe pitting in some of the common stainless steel alloys.
- 1.3 A request was made by K. Buehler, DM-MED-43, to find an alternative material for the flex hoses, to reduce the problems associated with pitting corrosion. An experimental study was carried out on 19 candidate alloys, including **304L** stainless steel for comparison. These alloys were chosen on the basis of their reported resistance to chloride environments.
- 1.4 Data is available in the literature on the corrosion resistance of several of the alloys being considered in this study. The data generally is for seawater (**1-3**), chloride solutions (**3-13**), or acids (**8,10,12,14,15**) individually. Some information is available on combinations of these (**8,10,11,13,16**), but experimental results were not found for all of the alloys under the specific conditions of the environment of interest -- **NaCl** combined with **HCl**.
- 1.5 Tests to determine which of the candidate alloys have the best corrosion resistance include electrochemical corrosion testing, accelerated corrosion testing in a salt fog chamber, long term exposure at the beach corrosion testing site, and pitting corrosion tests in ferric chloride solution. This report summarizes the results of these tests for all 19 of the candidate alloys.

- 1.6 For the most corrosion resistant alloys, mechanical tests were also performed to determine the alloys' resistance to cyclic fatigue cracking. Details of **these** mechanical tests may be found in reports MTB-688-87, MTB-028-88, MTB-090-88.

2.0 MATERIALS AND EQUIPMENT

2.1 CANDIDATE ALLOYS

2.1.1 Nineteen alloys were chosen for testing as possible replacement material for the **304L** stainless steel flex hoses. Two of the alloys -- 316L stainless steel and **Monel 400** -- were suggested by personnel from **DM-MED-43**. An additional sixteen alloys were suggested by DM-MSL-2, and **304L** stainless steel was also included for comparison purposes. The 19 candidate alloys **and** their nominal compositions are shown in Table 1. These alloys were chosen for consideration based on their reported resistance to corrosion.

TABLE 1 CANDIDATE ALLOYS AND THEIR NOMINAL COMPOSITIONS (WT%)

ALLOY	Ni	Fe	Cr	ND	Mn*	Co*	Cu	C*	Si*	P*	S*	Other
HASTELLOY C-4	Bal.	3.0	18	17	1.0	2.0		0.61	0.08	0.62	6.61	Ti 0.7
HASTELLOY C-22	Bal.	3.6	22	13	0.5	2.5		0.61	0.08	0.02	0.61	v 0.3, W 3
HASTELLOY C-276	Bal.	7.0	17	17	1.0	2.5		0.01	0.08	0.02	0.01	v 0.3, W 4.5
HASTELLOY B-2	Bal.	2.0	1	28	1.0	1.0		0.01	0.1	0.62	0.61	
INCONEL 600	Bal.	8.0	16		1.0		0.5	0.15	0.5		0.61	
INCONEL 625	Bal.	5.0	23	10	0.5	1.0		0.10	0.5	0.01	6.01	cb 4.1
INCONEL 825	Bal.	22.0	21	3	1.0		2.5	0.65	0.5		0.63	
INCO S-3	Bal.	20.0	22	7	1.0	5.0	2.0	0.02	1.0	0.04	0.03	Cb 0.5, W 1.5
MONEL 400	Bal.	2.5			2.0		31	0.36	0.5		0.02	
ZIRCONIUM 702												Zr 99.2, Hf 4.5
SS 304L	10	Bal.	19		2.0			0.63	1.0			
SS 304LN	10	Bal.	19		2.0			0.03	1.0	0.04	0.03	N 0.13
SS 316L	12	Bal.	17	2.5	2.0			0.63	1.6	0.04	6.03	
SS 317L	13	Bal.	19	3.5	2.0			0.63	1.6			
SS 904L	25	Bal.	21	4.5	2.0		1.5	6.02	1.0	0.04	6.03	
20 Co-3	35	Bal.	26	2.5	2.0		3.5	6.67	1.6			
7Mo + N	4	kl.	28	2	2.0			6.63	6.6	6.63	0.01	N 0.23
ES 2205	5	Bal.	22	3	2.0			6.63	1.6	0.03	6.62	N 6.14
FERRALUM 255	5	Bal.	26	3	1.5		2.0	0.04	1.0	6.64	0.63	N 6.17

* Values are max.

2.1.2 In addition to corrosion resistance, mechanical properties are also important to consider when selecting a new material. Some physical and mechanical properties for the candidate alloys are listed in Table 2.

TABLE 2 PHYSICAL AND MECHANICAL PROPERTIES OF THE CANDIDATE ALLOYS

ALLOY	Density (g/cm ³)	Tensile Strength(ksi)	Yield Strength(ksi)	Modulus of Elasticity(psi)	Hardness	Impact Strength at -320F(ft lb)	Coeff. of Thermal Expansion(in/in F)
HASTELLOY C-4	A M	111	60	31E+06	90 Rb	270	6.0E-06
HASTELLOY C-22	6.69	116	59	30E+06	93 Rb	260	6.33E-06
HASTELLOY C-276 A	%	115	52	30E+06	90 Rb	263	6.2E-06
HASTELLOY B-2	9.22	139	76	31E+06	92 Rb	53	5.6E-06
INCONEL 600	A43	90	37	30E+06	m m	61	7.4E-06
INCONEL 625	8.44	120	60	30E+06	79 Rb	35	7.1E-06
INCONEL 825	6.14	112	64	30E+06	80 Rb	67	7.8E-06
INCO 6-3	6.31	90	35	29E+06	85 Rb	263	A 1E-06
MODEL 400	A63	77	37	26E+06	72 Rb	200	7.7E-06
ZIRCONIUM 702	6.50	36	16	11E+06	77 %	*	2.9E-06
95 304L	A02	79	33	28E+06	70 Rb	71	9.2E-06
95 304LN	8.02	79	33	28E+06	70 Rb	*	9.2E-06
95 316L	8.02	61	34	28E+06	75 Rb	51	9.2E-06
95 317L	8.02	85	35	28E+06	80 Rb	*	8.9E-06
95 904L	8.00	71	31	28E+06	84 Rb	*	AS-06
20 Cr-J	8.08	96	53	28E+06	90 Rb	*	8.3E-06
7Mo +N	7.79	110	61	29E+06	99 Rb	0	6.4E-06
ES 2205	7.80	100	70	28E+06	30 Rc	0	7.9E-06
FERRALIUM 255	7.79	130	100	31E+06	26 Rc	0	6.6606

* Data not available

2.2 ELECTROCHEMICAL

2.2.1 A Model 351-2 Corrosion Measurement System, manufactured by EG&G Princeton Applied Research, was used for all electrochemical measurements.

2.2.2 Specimens were flat coupons 1.59 cm (5/8") in diameter. The specimen holder is designed such that the exposed metal surface area is 1 cm².

2.2.3 The electrochemical cell included a saturated calomel reference electrode (SCE), 2 graphite rod counter electrodes, the metal specimen working electrode, and a bubbler/vent tube. The electrolyte was an aerated solution of HCl plus 3.55wt% NaCl. The concentration of HCl was 0.1N for the first round of testing and was increased to

1.0N for a second round of tests on the more resistant alloys. The solutions were made using deionized water.

2.3 SALT FOG CHAMBER/ACID DIP

2.3.1 An Atlas Corrosive Fog Exposure System Model SF-2000, manufactured by Atlas Electric Devices Company, was used for accelerated exposure. The solution for salt fog exposure was a standard 5% sodium chloride mixture prepared as needed. The dipping solution was a **1.0N** (about 9 vol%) hydrochloric acid/alumina (**Al₂O₃**) mixture. The particle size of the alumina was 0.3 micron. The solution was thoroughly stirred prior to dipping due to the settling of the alumina powder.

2.3.2 Flat specimens exposed to these solutions were 1" x 2" samples of the identified alloys and were approximately **1/8"** thick. One set of samples were base metals with an autogenous weld on one end as identified in Table 3. Another set of specimens were the candidate alloys welded to **304L** stainless steel for galvanic studies and are identified in Table 4. All flat specimens had a **3/8"** hole drilled in the center for mounting purposes. Stress corrosion cracking specimens were standard U-bend samples prepared with a weld in the center of the bend, using the same materials as given in Table 3. The specimens were obtained commercially from Metal Samples Company, RT. 1, Box 152, Munford, AL.

TABLE 3 **AUTOGENOUS WELD SAMPLES**

BASE ALLOY	FILLER	BASE ALLOY	FILLER
HASTELLOY c-4	c-4	SS 304L	ER 308L
HASTELLOY C-22	c-22	SS 304LN	ER 308L
HASTELLOY C-276	C-276	SS 316L	ER 316L
HASTELLOY B-2	B-2	SS 317L	ER 317
INCONEL 600	ERNiCr-3	SS 904L	904L
INCONEL 625	ERNiCrMo-3	20 Cb-3	ER 320
INCONEL 825	ERNiFeCr-1	7Mo . N	ER312Mo
INCO Q-3	Hastelloy G3	Es 2205	ER22.B. 3L
HONEL 400	ERNiCo-7	FERRALIUM 255	F 255
ZIRCONIUM 702	ER2r2		

TABLE 4 **SAMPLES WELDED TO 304L
STAINLESS STEEL**

BASE ALLOY	FILLER	BASE ALLOY	FILLER
HASTELLOY C-4	ERNiCrMo-7	SS 304LN	CR 308L
HASTELLOY C-22	ERNiCrMo-10	SS 316L	CR 316L
HASTELLOY C-276	ERNiCrMo-4	SS 317L	ER 317
HASTELLOY R-2	ERNiMo-7	SS 904L	ER 904L
INCONEL 600	ERNiCr-3	20 Cb-3	ER 320
INCONEL 625	ERNiCr-3	7Mo . N	ER312Mo
INCONEL 825	ERNiCr-3	ES 2205	ER22.8. 3L
INCO 0-3	Hastelloy 0 3	FERRALIUM 255	F 255
MONEL 400	ERNiCr-3		

NOTE : It was not possible to obtain a sample of Zirconium 702 welded to 304L stainless steel

2.4 BEACH EXPOSURE/ACID SPRAY

2.4.1 All exposure was carried out at the KSC Beach Corrosion Test Site which is about 100 feet from the high tide line. The site is located on the Atlantic Ocean approximately 1 mile south of Launch Complex 39A at Kennedy Space Center, Florida.

2.4.2 The acid solution used in the spray operation was 10% hydrochloric acid by volume (about 1.0N) mixed with the 0.3 micron alumina powder to form a slurry. The specimens used in this testing were duplicate specimens as described in the salt fog/acid dip tests.

2.5 FERRIC CHLORIDE IMMERSION

2.5.1 Large glass beakers (600 - 1000 ml) were used to hold the test solution. Specimens were suspended in the solution by a glass cradle. Specimens were 1" x 2" flat samples as described in the salt fog/acid dip tests.

3.0 TEST PROCEDURES

3.1 ELECTROCHEMICAL

- 3.1.1 The test specimens were polished with 600-grit paper, ultrasonically degreased in a detergent solution, dried, and weighed before immersion in the electrolyte.
- 3.1.2 The electrolyte solution was aerated for at least 45 minutes before immersion of a test specimen. Aeration continued throughout the test.
- 3.1.3 Electrochemical tests performed include determining corrosion potential, polarization resistance, and cyclic **polarization**. The polarization resistance test procedure was based on ASTM G59 (17). The cyclic polarization procedure was based on ASTM G61 (18). All three electrochemical tests can be run in sequence on a single specimen.
- 3.1.4 The corrosion potential (E_{corr}) was monitored for 3600 seconds, after which time the potential had usually stabilized.
- 3.1.5 For the polarization resistance test, the potential was varied from **-20mV** to **+20mV** relative to the measured corrosion potential, while the resulting current was recorded. The scan rate was **0.1 mV/sec**. A linear graph of E vs I was made, and the resulting slope (at **I=0**) plus the Tafel constants were used to calculate the corrosion rate in mpy. Tafel constants were found from the cyclic polarization data.
- 3.1.6 The cyclic polarization scan started at -250mV relative to E_{corr} . The scan rate was **0.166 mV/sec**, and the scan was reversed when the current density reached **5 mA/cm²**. The reverse potential scan continued until the potential returned to the starting point of -250mV relative to E_{corr} . A graph was then made of E vs **logI**.
- 3.1.7 It was assumed that since the polarization resistance scan covers a very small

potential range, it should not affect the specimen surface prior to the cyclic polarization. Experiments were run with and without the polarization resistance test, and the results support this assumption.

3.1.8 Specimens were inspected visually and photographed after each cyclic polarization test. Samples were also weighed before and after the tests to determine overall weight loss.

3.2 SALT FOG CHAMBER/ACID DIP

3.2.1 Prior to **mounting**, the new corrosion specimens were visually checked and weighed to the nearest 0.1 milligram on a properly calibrated Mettler AE160 electronic balance. The specimens were then mounted on insulated rods and set in the salt fog chamber at about 15-20 degrees off the vertical.

3.2.2 The specimens were exposed to one week (**168** hours) of salt fog per ASTM B117 (**19**). The temperature of the chamber was controlled at **95° F (35° C) ± 2° F**. After the one week exposure, the specimens were removed and dipped in the hydrochloric acid/alumina mixture to simulate the booster effluent created during launch of the Space Shuttle. After one minute of immersion, the specimens were allowed to drain and dry overnight. Following this dipping procedure, the samples were installed in the salt fog chamber for the next one week cycle.

3.2.3 After a four week/four dip period, the specimens were removed from the mounting rod and inspected. The inspection procedure included cleaning, weighing, and visual characterization of the corrosion taking place. The corroded specimens were first cleaned using a nonabrasive pad and soapy water to remove heavy deposits of alumina. This was followed by chemical cleaning per ASTM **G1 (20)** to remove tightly adhering corrosion products. After cleaning, the specimens were allowed to dry overnight

before weighing. The specimens were weighed to the nearest 0.1 milligram on the Mettler electronic balance. The coupons were visually inspected with the naked eye and under 40x magnification. All observations were recorded in terms of appearance, sheen, pit severity/density, and stress cracking phenomena. After the inspection, the specimens were remounted and returned to the chamber for the next four week/four dip cycle of testing.

3.3 BEACH EXPOSURE/ACID SPRAY

- 3.3.1 The beach exposure test procedure was based on ASTM **G50 (21)**, with the addition of an acid spray. The new duplicate specimens were first visually inspected and weighed to the nearest 0.1 milligram as was stated before. The coupons were mounted on short insulated rods that were attached to a Plexiglas sheet. The orientation of the specimens was face side up and boldly exposed to the environment to receive the full extent of sun, rain, and sea spray. The U-bend specimens were mounted on 36" long insulated rods and secured with nylon tie wraps. Both the Plexiglas sheet and the insulated rods were mounted on test stands at the beach corrosion test site using nylon tie wraps. The specimens were mounted facing east towards the ocean at a 45 degree angle.
- 3.3.2 Approximately every two weeks, the specimens received an acid spray with the solution described. The acid spray thoroughly wet the entire surface and was allowed to remain on the surface of the specimens until it dried or was rinsed off by rain.
- 3.3.3 After the first exposure period of 60 days, the specimens were brought to the laboratory for inspection. The inspection procedure was the same as that for the salt fog testing. The samples were remounted and returned to the beach site for continued exposure testing.

3.4 FERRIC CHLORIDE IMMERSION

3.4.1 The ferric chloride immersion test procedure was based on ASTM G48, Method A (22). The test solution was made by dissolving 100 grams of reagent grade ferric chloride ($\text{FeCl}_3 \cdot 6\text{H}_2\text{O}$) in 900 ml of distilled water. The solution was then filtered to remove insoluble particles and allowed to cool to room temperature.

3.4.2 Samples were measured to calculate exposed surface area, cleaned, rinsed, and weighed before immersion in the test solution. Each sample was placed in a glass cradle and lowered into the test solution. The beaker was covered with a watch glass and left for 72 hours.

3.4.3 After 72 hours, the samples were removed and rinsed with water. Corrosion products were removed, and the samples were then dipped in acetone or alcohol and allowed to air dry. Each specimen was weighed and examined visually for signs of pitting and weld decay. Specimens were also examined at low magnification and photographed.

3.4.4 Some of the samples that showed no sign of corrosion were put back into the test solution. These samples were periodically inspected and re-immersed for a total exposure time of 912 hours.

4.0 TEST RESULTS AND DISCUSSION

4.1 ELECTROCHEMICAL

4.1.1 The electrochemical tests were run first with 3.55 wt% NaCl + 0.1N HCl, measuring only corrosion potential and cyclic polarization data. These tests were repeated, with the insertion of the polarization resistance experiment. There was very good agreement between the two sets of experiments, indicating good reproducibility and a negligible effect of the polarization resistance test on the

cyclic polarization results. A general discussion of the results of the three electrochemical tests will now be given, followed by an explanation of the results for each of the 19 individual alloys.

4.1.2 Corrosion potential (E_{corr}) gives an indication of how noble an alloy is in a given environment. Generally, a less negative corrosion potential means that the alloy can be expected to be more resistant to corrosion, in that particular electrolyte, compared to an alloy with a more negative corrosion potential. Thus, alloys can be ranked according to resistance to general corrosion, based on corrosion potential. Figure 1 shows the corrosion potential vs time data for a stable material. Some materials displayed very unstable corrosion potentials, such as shown in Figure 2. Table 5 shows the results for the 19 alloys tested, in order of increasing activity. The potentials are all with respect to the SCE reference and were recorded after 1 hour.

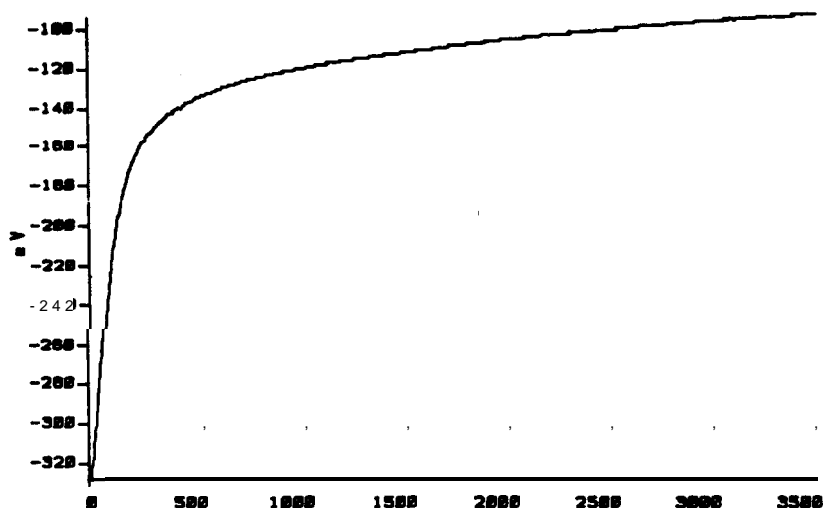


Figure 1 Stable Corrosion Potential

ES 2205 in Aerated 3.55% NaCl - 0.1N HCl
Corrosion Potential (mV) vs Time (seconds)

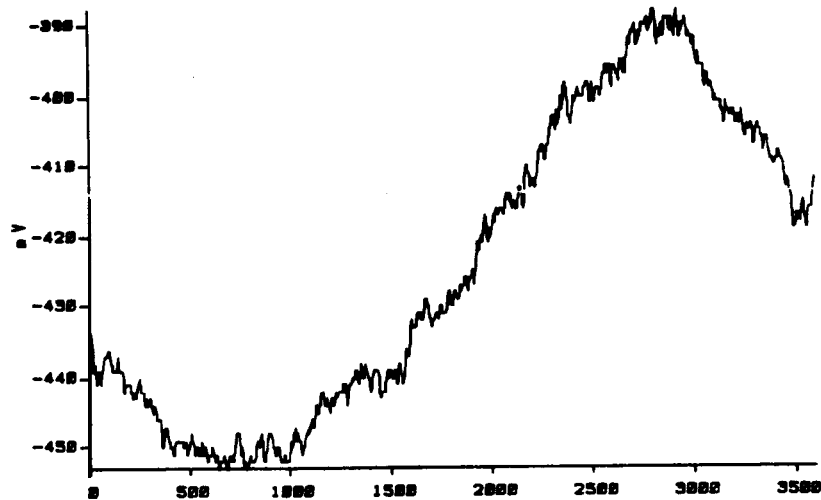


Figure 2 Unstable Corrosion Potential
304LN in Aerated 3.55% NaCl - 0.1N HCl
Corrosion Potential (mV) vs Time (seconds)

TABLE 5 CORROSION POTENTIAL
ELECTROLYTE: 3.55% NaCl - 0.1N HCl

MATERIAL NAME	E _{corr} VOLTS	MATERIAL NAME	E _{corr} VOLTS
INCONEL 625	-0.054	HASTELLOY C-276	-0.133
INCONEL 625	-0.060	FERRALIUM 255	-0.139
7Mo . N	-0.060	20 Cb-3	-0.140
HASTELLOY C-22	-0.068	20 Cb-3	-0.150
Es 2205	-0.072	SS 316L	-0.154
HASTELLOY C-276	-0.085	HASTELLOY B-2	-0.159
7Mo . N	-0.085	HASTELLOY B-2	-0.160
SS 904L	-0.085	MONEL 400	-0.172
HASTELLOY C-22	-0.086	MONEL 400	-0.174
ES 2205	-0.095	MONEL 400	-0.178
INCO o-3	-0.098	SS 316L	-0.187
FERRALIUM 255	-0.102	INCONEL 600	-0.272
INCO G-3	-0.102	INCONEL 600	-0.273
HASTELLOY C-4	-0.105	ZIRCONIUM 702	-0.319
HASTELLOY C-4	-0.106	ZIRCONIUM 702	-0.319
INCONEL 825	-0.106	SS 304L	-0.403
SS 317L	-0.108	SS 304L	-0.405
SS 904L	-0.116	SS 304L	-0.410
INCONEL 825	-0.121	SS 304LN	-0.410
SS 317L	-0.123	SS 304LN	-0.412
SS 317L	-0.132	SS 304L	-0.416

4.1.3 Polarization resistance is used to calculate **the** uniform corrosion rate when **the** potential is close to the corrosion potential. Results of a typical polarization resistance run are shown in Figure 3.

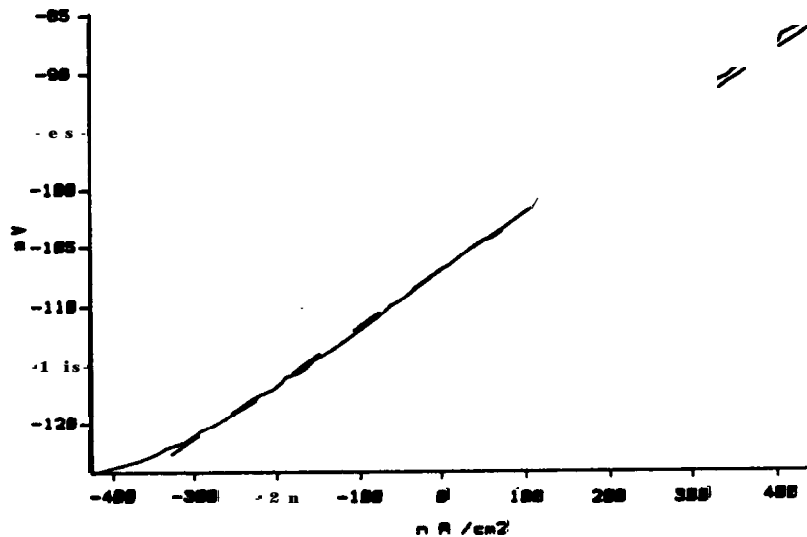


Figure 3 Polarization Resistance Graph
Hastelloy C-4 in Aerated 3.55% NaCl - 0.1N HCl
Potential (mV) vs Current Density (nA/cm²)

According to the Stearn-Geary theory (23), a graph of E vs I should be linear over a current and potential range very close to **I=0** (i.e., close to **E_{corr}**). The slope of this line is R_p in ohms. Corrosion current and uniform corrosion rate are then calculated as follows

$$I_{corr} = \frac{10^6 B_a B_c}{2.3 R_p (B_a + B_c)}$$

$$\text{Corrosion Rate} = \frac{0.13 I_{corr} (\text{E.W.})}{d}$$

where Ba and Bc are the Tafel constants in V/decade, I_{corr} is the corrosion current density in $\mu\text{A}/\text{cm}^2$, E.W. is the equivalent weight in g/equiv, d is density in g/cm^3 , and corrosion rate is in mpy. Table 6 summarizes the polarization resistance results, with the alloys ranked in order of increasing corrosion rate. The polarization resistance results did not correlate with the beach exposure and salt fog chamber results as well as the cyclic polarization results did. In general, the polarization resistance technique works better with metals that display active corrosion behavior. It may not give accurate results for passive metals such as many of the alloys used in this study. So in this case, polarization resistance is not the best electrochemical technique to use to predict actual field exposure corrosion results.

TABLE 6 RESULTS OF POLARIZATION RESISTANCE EXPERIMENTS

ELECTROLYTE: 3.55X NA CL - 0.1N NCL

MATERIAL NAME	Ba V/DEC	Bc V/DEC	Rp OHMS	Icorr AMPS	CORR. RATE MPY
INCONEL 625	0.09	0.10	180000	1.15E-07	0.05
FERRALIUM 255	0.15	0.13	247000	1.23E-07	0.06
7Mo . N	0.19	0.15	240000	1.52E-07	0.07
ZIRCONIUM 702	0.25	0.19	248000	1.89E-07	0.09
INCO G-3	0.21	0.14	140000	2.61E-07	0.12
SS 904L	0.20	0.16	150000	2.57E-07	0.12
20 Cb-3	0.23	0.10	98500	3.08E-07	0.14
ES 2205	0.21	0.18	127000	3.31E-07	0.15
SS 317L	0.23	0.19	131000	3.46E-07	0.16
SS 316L	0.21	0.19	125000	3.47E-07	0.16
HASTELLOY C-22	0.23	0.17	84000	5.06E-07	0.22
INCONEL 625	0.33	0.17	90000	5.42E-07	0.24
HASTELLOY C-4	0.42	0.17	47500	1.11E-06	0.47
HASTELLOY C-276	0.38	0.24	44000	1.45E-06	0.62
SS 304LN	0.11	0.11	6450	3.70E-06	1.69
HASTELLOY B-2	0.05	0.25	1800	1.01E-05	4.16
HONEL 400	0.08	0.30	930	3.00E-05	13.00
INCONEL 600	0.07	0.29	665	3.68E-05	16.50
SS 304L	0.07	0.14	352	5.80E-05	26.00

4.1.4 Cyclic polarization gives an indication of a specimen's resistance to pitting corrosion (18,24), and this method has been used for many systems to determine susceptibility to localized corrosion (4-6,9,11,13,16,18,24,25). Figure 4 shows a curve with the hysteresis effect typical of a material with a low resistance to pitting. Since the potential scan is at a known constant rate,

the potential values can be converted to time, and the area inside the hysteresis loop can be found by integration to give units of **coulombs/cm²**. This area value should be very small for alloys that are highly resistant to pitting, as seen in Figure 5 which is for a material that is very corrosion resistant. In this case, the reverse scan traces almost exactly over the forward scan.

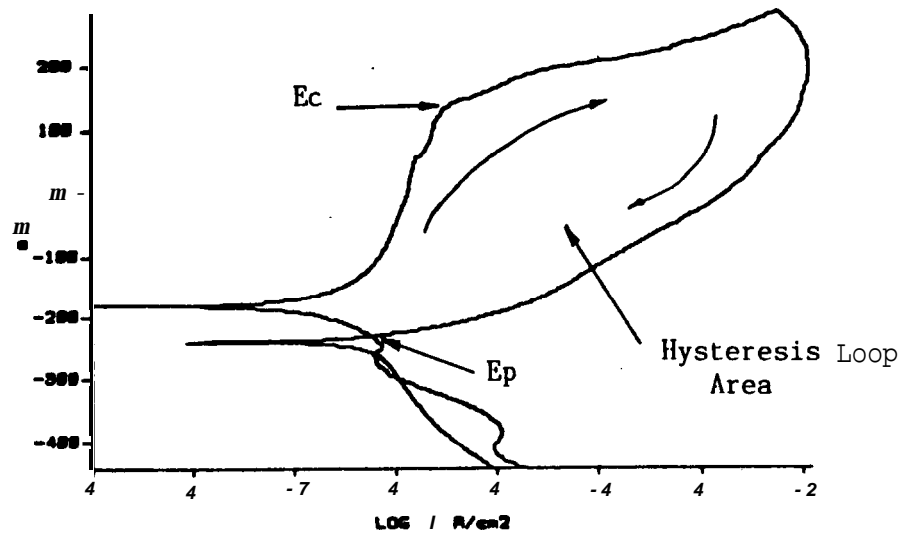


Figure 4 Cyclic Polarization With Hysteresis Loop
316 L in Aerated 3.55% NaCl - 0.1N HCl, mV vs log I(A/cm²)

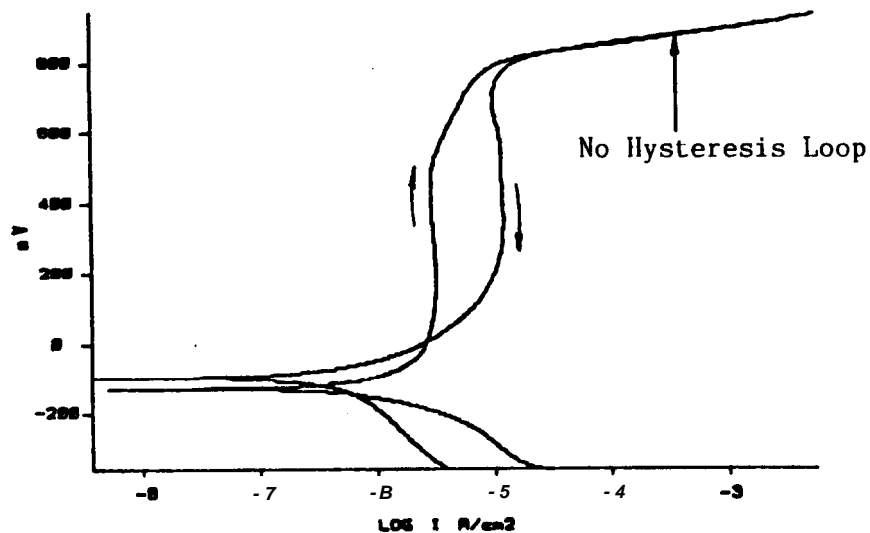


Figure 5 Cyclic Polarization Without Hysteresis
Hastelloy C-4 in Aerated 3.55% NaCl - 0.1N HCl, mV vs log I

Table 7 ranks the alloys according to area of the hysteresis loop.

TABLE 7 AREA OF HYSTERESIS LOOP

ELECTROLYTE: 3.55% NaCl - 0.1N HCl

MATERIAL NAME	AREA OF LOOP COULOMBS	MATERIAL NAME	AREA OF LOOP COULOMBS
HASTELLOY C-22	2.00	SS 904L	7.00
HASTELLOY C-22	2.00	SS 904L	7.00
HASTELLOY C-276	2.00	ZIRCONIUM 702	8.00
HASTELLOY C-4	2.00	INCONEL 625	9.00
HASTELLOY C-4	2.00	INCONEL 625	9.00
INCO G-3	2.00	ZIRCONIUM 702	10.00
INCO G-3	2.00	SS 304L	12.00
FERRALIUM 255	3.00	SS 304L	13.00
FERRALIUM 255	3.00	SS 304LN	13.00
INCONEL 625	3.00	SS 316L	15.00
INCONEL 625	3.00	SS 316L	15.00
INCONEL 600	4.00	SS 317L	15.00
7Mo + N	4.00	SS 304LN	16.00
ES 2205	5.00	SS 317L	20.00
INCONEL 600	5.00	20 Cb-3	21.00
ES 2205	6.00	20 Cb-3	23.00

Two other parameters that apply to cyclic polarization are critical pitting potential (E_c) and protection potential (E_p). At E_c , the current increases dramatically until the reversal point is reached (see Figure 4). The more noble (positive) the value of E_c , the more resistant is the alloy to initiation of localized corrosion. E_p is the point at which the reverse scan intersects the forward scan (see Figure 4). E_p represents repassivation of previously formed pits. In general, localized corrosion can propagate at potentials more noble (positive) than E_p . So, it would be desirable for E_p to be greater than E_{corr} to make it less likely that E_{corr} will exceed E_p , and therefore less likely that localized corrosion will continue. Tables 8 and 9 rank the alloys according to E_c and E_p , respectively.

TABLE 8 CRITICAL • ITTIWO POTENTIAL

ELECTROLYTE: 3.55% NaCl - 0.1N HCL

MATERIAL NAME	Ec VOLTS	MATERIAL NAME	EC VOLTS
FERRALIUM 255	0.810	INCONEL 825	0.270
7Mo + N	0.810	SS 904L	0.230
ES 2205	0.800	ZIRCONIUM 702	0.214
FERRALIUM 255	0.800	SS 317L	0.210
HASTELLOY C-22	0.800	ZIRCONIUM 702	0.205
HASTELLOY C-276	0.800	SS 317L	0.156
HASTELLOY C-4	0.800	20 Cb-3	0.150
INCONEL 625	0.800	SS 316L	0.141
ES 2205	0.790	20 Cb-3	0.136
INCO G-3	0.790	SS 316L	0.110
INCO G-3	0.790	SS 304LN	0.035
INCONEL 625	0.790	INCONEL 600	0.010
HASTELLOY C-22	0.780	INCONEL 600	-0.010
HASTELLOY C-4	0.780	SS 304LN	-0.010
7Mo + N	0.780	SS 304L	-0.093
INCONEL 825	0.309	SS 304L	-0.096
SS 904L	0.291	SS 304L	-0.240

TABLE 9 PROTECTION POTENTIAL

ELECTROLYTE: 3.55% NaCl - 0.1N HCL

MATERIAL NAME	Ep VOLTS	MATERIAL NAME	Ep VOLTS
HASTELLOY C-22	0.900	ZIRCONIUM 702	0.019
INCO G-3	0.860	ZIRCONIUM 702	-0.040
7Mo + N	0.844	20 Cb-3	-0.137
FERRALIUM 255	0.835	INCONEL 825	-0.149
ES 2205	0.830	20 Cb-3	-0.150
HASTELLOY C-22	0.830	SS 304L	-0.200
HASTELLOY C-4	0.830	SS 904L	-0.200
INCONEL 625	0.830	SS 304L	-0.207
HASTELLOY C-4	0.826	SS 317L	-0.207
INCO G-3	0.816	SS 904L	-0.210
FERRALIUM 255	0.810	SS 316L	-0.222
HASTELLOY C-276	0.800	SS 317L	-0.224
INCONEL 625	0.800	SS 316L	-0.229
ES 2205	0.652	SS 304L	-0.242
INCONEL 825	0.143	SS 304LN	-0.278
INCONEL 600	0.068	SS 304LN	-0.280
INCONEL 600	0.040		

4.1.5 Some alloys displayed uniform corrosion, rather than localized pitting or crevice corrosion. This was the case for Monel 400 and Hastelloy B-2. In these instances, the cyclic polarization curves were similar to the one shown in Figure 6. This type of curve does not yield meaningful values for E_c , E_p , or area of the hysteresis loop. Therefore, data for these two alloys do not appear in Tables 7, 8, and 9. Although these two alloys did not suffer localized

corrosion, they did have an unacceptably high uniform corrosion rate, as seen in Table 6.

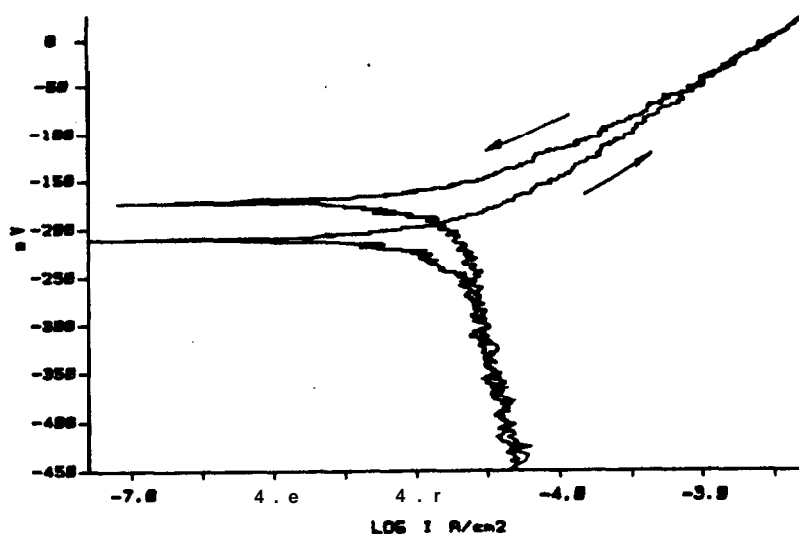


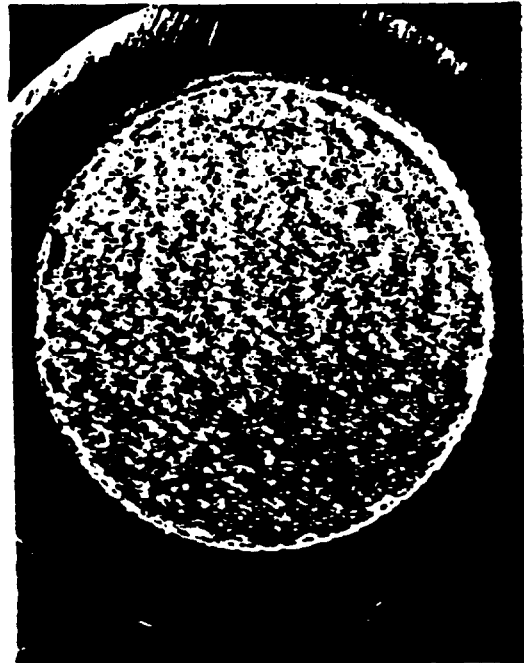
Figure 6 Cyclic Polarization With Uniform Corrosion
Monel 400 in Aerated 3.55% NaCl - 0.1N HCl
Potential (mV) vs Log Current Density (A/cm²)

4.1.6 Visual inspection and inspection under a microscope revealed various levels of pitting corrosion. Crevice corrosion was also observed on several of the samples around the edge of the specimen holder. These visual observations agreed extremely well with the electrochemical results. Some representative photos are shown in Figure 7. Figure 7a, of stainless steel 304L, shows crevice corrosion and pitting. Figure 7b, Inconel 600, shows crevice corrosion, pitting, and uniform corrosion. The Monel 400 in Figure 7c shows uniform corrosion **only**, and the Hastelloy C-276 in Figure 7d shows no signs of corrosion attack.

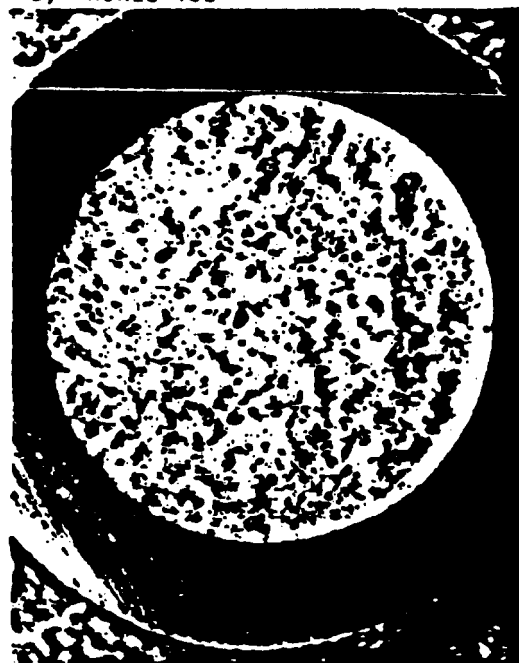
Figure 7 Representative Photos After Cyclic Polarization in 3.55% NaCl + 0.1N HCl



A) 304L



B) INCONEL 600



C) MONEL 400



D) HASTELLOY C-276

4.1.7 Total weight loss was measured for each sample. This is an indication of the amount of corrosion. However, this value can not be used to determine a meaningful general corrosion rate because in most cases the corrosion was not uniform over the entire surface -- it was localized in pitting and/or crevice corrosion. Table 10 shows the weight loss for the alloys tested.

TABLE 10 WEIGHT LOSS
ELECTROLYTE: 3.55% NaCl - 0.1N HCl

MATERIAL NAME	WT LOSS (mg)	MATERIAL NAME	WT LOSS (mg)
FERRALIUM 255	0.3	SS 904L	1.5
HASTELLOY C-22	0.3	SS 904L	1.6
HASTELLOY C-276	0.3	INCONEL 600	1.8
HASTELLOY C-4	0.3	ZIRCONIUM 702	2.0
HASTELLOY C-22	0.4	INCONEL 600	2.1
HASTELLOY C-276	0.4	INCONEL 825	2.1
HASTELLOY C-4	0.4	INCONEL 825	2.2
INCO G-3	0.4	ZIRCONIUM 702	2.5
INCONEL 625	0.4	SS 304LN	3.3
FERRALIUM 255	0.5	SS 304L	3.7
7Mo . N	0.5	SS 316L	3.8
INCONEL 625	0.6	SS 316L	3.8
7Mo . N	0.6	SS 317L	4.0
ES 2205	0.7	SS 304L	4.6
HASTELLOY B-2	0.7	SS 304LN	4.8
INCO G-3	0.7	SS 317L	5.1
ES 2205	1.0	20 Cb-3	5.5
HASTELLOY B-2	1.0	20 Cb-3	5.8
MONEL 400	1.2	MONEL 400	9.5
SS 304L	1.4		

4.1.8 Based on the data in the preceding tables and figures for the first round of tests, the most resistant alloys were determined to be Hastelloy C-4, Hastelloy C-22, Hastelloy C-276, Inconel 625, Inco Alloy G-3, Ferralium 255, 7Mo+N, ES 2205, and 904L. These alloys were then run through the same electrochemical tests using a more aggressive electrolyte of 3.55 wt% NaCl with the HCl concentration increased to 1.0N. Stainless steel 304L was also used, as a basis for comparison.

4.1.9 Table 11 shows the effect on corrosion potential of increasing the acid concentration. The 904L, Ferralium 255, ES 2205, and 7MotN became much more active. Table 12 summarizes the polarization resistance results obtained with the increased acid concentration. For the 904L,

ES 2205, and 7Mo+N alloys, the effect of the increased activity of Table 11 can be seen in the very high corrosion rates given in Table 12, as compared to the results in Table 6. The corrosion rates increased from 0.12 to 36.8 mpy for **904L**, from 0.15 to 180 mpy for ES 2205, and from 0.07 to 457 mpy for **7Mo+N**. As with the results in Table 6, this test separates out some of the poor performers, but it can not rank the alloys accurately.

TABLE 11 CORROSION POTENTIAL IN 1.0N HCl AND IN 0.1N HCl (BOTH WITH 3.55% NaCl)

MATERIAL NAME	E _{corr} (V) 1.0 N	E _{corr} (V) 0.1 N
INCO G-3	-0.051	-0.100
INCONEL 625	-0.058	-0.057
HASTELLOY C-4	-0.098	-0.105
HASTELLOY C-22	-0.106	-0.077
HASTELLOY C-276	-0.108	-0.109
SS 904L	-0.328	-0.100
FERRALIUM 255	-0.421	-0.120
ES 2205	-0.422	-0.084
SS 304L	-0.452	-0.408
7Mo . N	-0.455	-0.072

TABLE 12 POLARIZATION RESISTANCE

ELECTROLYTE: 3.55% NaCl - 1.0N HCL

MATERIAL NAME	B _a V/DEC	B _c V/DEC	R _p OHMS	I _{corr} AMPS	CORR. RATE MPY
FERRALIUM 255	0.03	0.06	43000	2.00E-07	0.09
INCONEL 625	0.29	0.13	84400	4.62E-07	0.21
INCO G-3	0.35	0.13	77500	5.31E-07	0.24
HASTELLOY C-22	0.38	0.14	61700	7.21E-07	0.31
HASTELLOY C-276	0.54	0.15	38700	1.32E-06	0.56
HASTELLOY C-4	0.63	0.16	23800	2.34E-06	1.00
SS 904L	0.06	0.21	257	7.88E-05	36.80
SS 304L	0.06	0.11	167	9.56E-05	43.70
ES 2205	0.15	0.13	79	3.85E-04	180.00
7Mo . N	0.24	0.13	37	9.82E-04	457.00

4.1.10 The cyclic polarization results for the stronger electrolyte are summarized in Table 13, with the alloys ranked according to weight loss. The **304L** sample experienced uniform corrosion. Therefore, results for **304L** do not appear in Table 13, for the reasons mentioned in paragraph 4.1.5 in regard to Figure 6 (i.e., no meaningful values for E_c, E_p, or area).

TABLE 13 CYCLIC POLARIZATION RESULTS

ELECTROLYTE: 3.55% NaCl - 1.0N HCl

MATERIAL NAME	CC VOLTS	CP VOLTS	AREA OF LOOP COULOMBS	WT LOSS (mg)
INCO G-3	0.825	0.899	1.00	0.2
NASTCLOY C-22	0.820	0.866	1.00	0.3
NASTCLOY C-276	0.840	0.840	1.00	0.3
HASTELLOY C-4	0.800	0.870	1.00	0.3
FERRALIUM 255	0.855	0.855	2.00	0.4
INCONEL 625	0.870	0.908	3.00	0.6
SS 904L	0.100	-0.197	7.00	1.6
ES 2205	0.855	-0.145	2.00	2.8
7Mo+N	0.040	0.900	1.00	6.9

The high weight loss values seen in Table 33 for 904L, ES 2205, and 7Mo+N agree with the active corrosion potentials of Table 11 and the high corrosion rates of Table 12. The ES 2205 and 7Mo+N suffered severe uniform corrosion, in addition to pitting, which is why the area values for these two alloys do not correlate with the weight loss values. Since there was uniform corrosion, the area values are not really meaningful, and the weight loss gives a better indication of the extent of corrosion for these two alloys. Visual inspection also agreed with the results of Tables 11, 12 and 13: the 7Mo+N and ES 2205 suffered severe uniform corrosion; the 904L alloy showed increased crevice corrosion compared to the results with the 0.1N HCl solution; the Ferralium 255 showed signs of some general corrosion; and the remaining alloys, Hastelloy C-1, Hastelloy C-22, Hastelloy C-276, Inconel 625, and Inco Alloy G-3, still displayed excellent resistance to both localized and uniform corrosion.

- 4.1.11 The graphical results for corrosion potential and cyclic polarization for each of the alloys are shown in Appendix A, Figures A1 to A58. Graphs are included for the 3.55% NaCl + 0.1N HCl electrolyte for all of the alloys. For the more resistant alloys, the graphs from the 3.55% NaCl + 1.0N HCl electrolyte are also given. All of these results are summarized and briefly explained in Table 14.

TABLE 14 SUMMARY OF ELECTROCHEMICAL RESULTS

ALLOY	3.55% NaCl + 0.1N HCl		3.55% NaCl + 1.0N Hcl	
	FIGURE	COMMENTS	FIGURE	COMMENTS
HASTELLOY C-4	A1	Stable, Noble Ecorr	a3	Stable, Noble Ecorr
	A2	Very Small hysteresis Area Excellent Pitting Resistance	A4	Very Small Hysteresis Area Excellent Pitting Resistance
HASTELLOY C-22	A5	Stable, Noble Ecorr	A7	Stable, Noble Ecorr
	A6	Very Small hysteresis Area Excellent Pitting Resistance	A8	Very Small Hysteresis Area Excellent Pitting Resistance
HASTELLOY C-276	A9	Stable, Fairly Noble Ecorr	A11	Stable, Fairly Noble Ecorr
	A10	Very Small Hysteresis Area Excellent Pitting Resistance	a12	Very Small Hysteresis Area Excellent Pitting Resistance
HASTELLOY B-2	A13	Stable, Slightly ktive Ecorr		
	A14	Uniform Corrosion		
INCONEL 600	A15	Unstable, Fairly ktive Ecorr		
	A16	Uniform Corrosion & Pitting		
INCONEL 625	A17	Stable, Very Noble Ecorr	A19	Stable, Very Noble Ecorr
	A18	Small hysteresis Area Very Good Pitting Resistance	A20	Very Small hysteresis Area Excellent Pitting Resistance
INCONEL 825	A21	Stable, Noble Ecorr		
	A22	Large Area, Low Pitting Resistance		
INCO G-3	A23	Stable, Noble Ecorr	A25	Very Noble Ecorr
	A24	Excellent Pitting Resistance	A26	Excellent Pitting Resistance
MONEL 400	A27	Stable, Slightly ktive Ecorr		
	A28	Uniform Corrosion		
ZIRCONIUM 702	A29	Stable, Fairly ktive Ecorr		
	A30	Low Resistance To Pitting		
SS 304L	A31	Fairly Stable, Active Ecorr	A33	Fairly Stable, Active Ecorr
	A32	Poor Resistance To Pitting	A34	Uniform Corrosion
SS 304LN	A35	Unstable, Active Ecorr		
	A36	Large Hysteresis Area Poor Pitting Resistance		
SS 316L	A37	Fairly Stable, Slightly ktive Ecorr		
	A38	Large Hysteresis Area Very Poor Pitting Resistance		
SS 317L	A39	Stable, Slightly ktive Ecorr		
	A40	Large Hysteresis Area Very Poor Pitting Resistance		
SS 904L	A41	Stable, Noble Ecorr	A43	Fairly Stable, Active Ecorr
	A42	Some Pitting Resistance	A44	Poor Pitting Resistance
20 Cb-3	A45	Fairly Stable, Slightly Active Ecorr		
	A46	Extremely Poor Resistance To Pitting		
7Mo + N	A47	Stable, Noble Ecorr	A49	Stable, Active Ecorr
	A48	Moderate Pitting and Uniform Corrosion	A50	Some Pitting and Uniform Corrosion
ES 2205	A51	Stable, Noble Ecorr	A53	Active, Fairly Stable Ecorr
	A52	Moderate Pitting	A54	Some Pitting, Uniform Corrosion
FERRALIUM 255	A55	Stable, Noble Ecorr	A57	Stable, Active Ecorr
	A56	Small hysteresis Area Very Good Pitting Resistance	A58	Good Pitting Resistance

4.2 SALT FOG CHAMBER/ACID DIP

4.2.1 **After 4 weeks** of salt fog exposure and four acid dips, the coupons were returned to the laboratory for analysis. After a cleaning procedure, the specimens were weighed to determine the weight loss caused by the 4-week exposure. Using the weight loss results and the measured area of the coupons, corrosion rate calculations were made to compare the alloys' resistance to the salt fog/acid dip environment. The formula used to calculate the corrosion rate is

$$\text{CORROSION RATE (MILS PER YEAR)} = \frac{534w}{dAt}$$

where **w** is the weight loss in milligrams, **d** is the metal density in grams per cubic centimeter (**g/cm³**), **A** is the area of exposure in square inches (**in²**), and **t** is the exposure time in hours. This expression calculates the uniform corrosion rate over the entire surface and gives no indication of the severity of localized attack (pitting) occurring on the surface. To determine the severity of this localized attack, the coupons were examined visually with the naked eye and under 40 power magnification. The measured weight loss, the resulting calculated corrosion rate, and the visual observations for each of the alloys for the 4-week cycle are presented in Table 15. As can be seen from the table, several materials clearly separated from the rest and displayed superior corrosion resistance. These materials included three Hastelloy alloys (C-22, C-4, and C-276), Zirconium 702, Inconel 625, and Inco Alloy G-3. The Inco Alloy G-3 marked the point at which the corrosion rates accelerated rapidly for the many stainless steel alloys included in the testing. The visual observations confirmed the corrosion resistance of the top alloys, with no visual deterioration at **40x**. These results were considered important but premature, and the specimens were returned to the salt fog chamber for further exposure.

TABLE 15

RESULTS OF FOUR WEEK EXPOSURE IN 5% SALT FOG AND FOUR DIPS IN 1.0N HCL - ALUMINA

MATERIAL NAME	WGT LOSS(g)	CORR. RATE(MPY)	REMARKS - OBSERVATIONS AT 1X AND 40X
HASTELLOY C-22	0.0007	0.0140	NO PITTING AT 1X - NO PITTING AT 40X
ZIRCONIUM 702	0.0008	0.0210	NO PITTING, BRIGHT SHEEN AT 1X - NO PITTING AT 40X
HASTELLOY c-4	0.0018	0.0290	NO PITTING AT 1X - NO PITTING AT 40X
HASTELLOY c-276	0.0018	0.0340	NO PITTING AT 1X - NO PITTING AT 40X
INCONEL 625	0.0020	0.0400	NO PITTING, BRIGHT SHEEN AT 1X - NO PITTING AT 40X
INCOLOY G-3	0.0059	0.1210	NO PITTING AT 1X - SLIGHT PITTING AT 40X
msl EuroYS- 2	0.0228	0.4150	NO PITTING AT 1X - UNIFORM CORROSION AT 40X
SS904L	0.0300	0.6200	VISIBLE PITTING, NO SHEEN AT 1X - MODERATE PITTING AT 40X
SS304LN	0.0324	0.6320	VISIBLE PITTING, NO SHEEN AT 1X - MODERATE PITTING AT 40X
SS316L	0.0301	0.6400	VISIBLE PITTING, NO SHEEN AT 1X - MODERATE PITTING AT 40X
SS317L	0.0324	0.6970	VISIBLE PITTING, NO SHEEN AT 1X - MODERATE PITTING AT 40X
SS304L	0.0359	0.7300	VISIBLE PITTING, NO SHEEN AT 1X - MODERATE PITTING AT 40X
INCONEL 825	0.0386	0.8080	VISIBLE PITTING, NO SHEEN AT 1X - MODERATE PITTING AT 40X
INCONEL 600	0.0420	0.8770	NO SHEEN AT 1X - NUMEROUS SW PITS AT 40X
7Mo + N	0.0469	1.0600	NO PITTING, NO SHEEN AT 1X - VERY SLIGHT PITTING AT 40X
FERRALIUM 253	0.0476	1.0600	VISIBLE PITTING, SLIGHT SHEEN AT 1X - NUMEROUS SLIGHT PITS AT 40X
ES 2205	0.0675	1.2060	NO PITTING, 1a SHEEN AT 1X - VERY SLIGHT PITTING AT 40X
MONEL 400	0.0893	1.7350	SLIGHT SHEEN AT 1X - SLIGHT PITTING, ETCHED AT 40X
20Cb-3	0.0945	2.6300	VERY VISIBLE CORROSION AT 1X - NUMEROUS LARGE PITS, SOME DEEP AT 40X

4.2.2 Following another 1-week exposure cycle, the specimens were returned to the laboratory for an **8-week** analysis. The same procedures were conducted to clean, weigh, calculate, and observe the specimens. The B-week data is shown in Table 16. As can be seen from the table, not much changed in the ranking of the alloys, with the top six materials clearly superior to the rest. However, the Inco Alloy G-3 started showing signs of pitting at **40x**, but these pits were small. The corrosion rates did not change much since the relationship between weight loss and time should stay fairly constant. However, some materials display a slight reduction in corrosion rate, and this is probably due to a slight slowing of the pitting after an initial accelerated attack. In comparison to the electrochemical data, two materials changed their relative positions in the rankings. The cyclic polarization in **0.1N HCl/3.55% NaCl** showed the Zirconium 702 material to be a poor performer, but in the salt fog/acid dip testing, this material displayed excellent corrosion resistance. On the other hand,

the electrochemical testing in the 1.0N HCl/3.55% NaCl showed the Ferralium 255 to perform well, but in the salt fog/acid dip testing, this material corroded rapidly and pitted badly. The reasons for this behavior are unclear, but continued testing confirmed this result.

TABLE 16

RESULTS OF EIGHT WEEK EXPOSURE IN 5% SALT FOG AND EIGHT DIPS IN 1.0N HCL - ALUMINA

MATERIAL NAME	WGT LOSS(g)	CORR. RATE(MPY)	REMARKS - OBSERVATIONS AT 1X AND 40X
HASTELLOY C-22	0.0015	0.0150	NO PITTING, RIM SHEEN AT 1X - NO PITTING, NO WELD DECAY AT 40X
ZIRCONIUM 702	0.0012	0.0160	SOME STAINING, BRIGHT SHEEN AT 1X - NO PITTING, NO WELD DECAY AT 40X
HASTELLOY C-276	0.0028	a0260	NO PITTING, BRIGHT SHEEN AT 1X - NO PITTING, NO WELD DECAY AT 40X
INCONEL 625	0.0027	0.0270	NO PITTING, BRIGHT SHEEN AT 1X - NO PITTING, NO WELD DECAY AT 40X
HASTELLOY C-4	a0029	0.0280	NO PITTING, BRIGHT SHEEN AT 1X - NO PITTING, NO WELD DECAY AT 40X
INCONEL 6-3	0.0071	0.0730	NO PITTING, SLIGHT SHEEN AT 1X - MODERATE SHALLOW PITTING, SOME PITTING OF WELD AT 40x
HASTELLOY D-2	0.0420	0.3820	NO PITTING, NO SHEEN AT 1X - UNIFORM CORROSION WITH LOCALIZED ATTACK AT 40X
SS304LN	0.0620	0.6050	VISIBLE PITTING, NO SHEEN AT 1X - NUMEROUS PITS, SOME LARGE, NO WELD DECAY AT 40X
SS316L	0.0631	0.6730	VISIBLE PITTING, NO SHEEN AT 1X - NUMEROUS SHALLOW PITS, SOME WELD DECAY AT 40x
SS304L	a0672	0.6930	VISIBLE PITTING, NO SHEEN AT 1X - NUMEROUS PITS, SOME LARGE, NO WELD DECAY AT 40X
SS904L	0.0695	a7200	VISIBLE PITTING, NO SHEEN AT 1X - NUMEROUS LARGE SHALLOW PITS, PITTING OF WELD AT 40X
SS317L	0.0699	0.7520	VISIBLE PITTING, NO SHEEN AT 1X - MODERATE PITTING, SOME WELD DECAY AT 40X
INCONEL 825	0.0854	0.8930	VISIBLE PITTING, NO SHEEN AT 1X - VERY NUMEROUS PI, PITTING OF WELD AT 40X
INCONEL 600	0.0915	0.9420	NO SHEEN AT 1X - UNIFORM ATTACK, NO WELD DECAY AT 40X
7Mo + N	0.0916	1.0350	NO PITTING, NO SHEEN AT 1X - UNIFORM CORROSION, MODERATE WELD DECAY AT 40X
FERRALIUM 255	0.0939	1.0450	VISIBLE PITTING, NO SHEEN AT 1X - UNIFORM ATTACK WITH NUMEROUS PITS, PITTING OF WELD AT 40X
ES 2205	0.1286	1.1500	VISIBLE PITTING, NO SHEEN AT 1X - SLIGHT PITTING WITH CREVICE CORROSION, PITTING OF WELD AT 40X
20Cb-3	0.1705	1.8300	VISIBLE PITTING, NO SHEEN AT 1X - HEAVY PITTING, MANY LARGE AND DEEP, SEVERE PITTING OF WELD AT 40X
INCONEL 400	0.1908	1.8750	NO SHEEN AT 1X - UNIFORM CORROSION, SOME PITTING OF WELD AT 40X

4.2.3

After another 4-week exposure cycle, the specimens were returned to the laboratory for the 12-week analysis. The results of the 12-week testing are shown in Table 17. After 12 weeks in the salt fog chamber and 12 acid dips, a clear trend began to emerge. The corrosion rates were remaining fairly constant with a slight reduction still being displayed by some materials. The alloys were settling into their positions for the ranking of corrosion resistance in this accelerated environment. The Inco Alloy G-3 lost its sheen and continued to display pitting attack and some deterioration of the weld. The observation of very small pits developing on the three Hastelloy materials and one Inconel material were barely detectable and were considered insignificant since the weight loss remained very low.

TABLE 17

RESULTS OF 12 WEEK EXPOSURE TO 5% SALT FOG AND 12 DIPS IN 1.0N HCL - ALUMINA

MATERIAL NAME	WGT LOSS(g)	CORR. RATE(MPY)	REMARKS - OBSERVATIONS AT 1X AND 40X
HASTELLOY C-22	0.0019	0.0120	NO PITTING, BRIGHT SHEEN AT 1X - A FEW SMALL PITS AT 40X
ZIRCONIUM 702	0.0015	0.0130	NO PITTING, BRIGHT SHEEN AT 1X - SLIGHT UNIFORM CORROSION, NO PITTING AT 40X
INCONEL 625	0.0029	0.0190	NO PITTING, BRIGHT SHEEN AT 1X - FEW VERY SMALL PITS AT 40X
HASTELLOY c-276	0.0031	0.0190	NO PITTING, BRIGHT SHEEN AT 1X - FEW VERY SMALL PITS AT 40X
HASTELLOY C-4	0.0036	0.0230	NO PITTING, BRIGHT SHEEN AT 1X - FEW PITS AT 40X
INCOLOY 8-3	0.0080	0.0550	SLIGHT PITTING, NO SHEEN AT 1X - FEW SMALL PITS, UNIFORM CORROSION AT 40X
mslEuovB-2	0.0662	0.4010	NO PITTING, NO SHEEN/STAINED AT 1X - FEW PITS, UNIFORM CORROSION AT 40X
SS304LN	0.1081	0.7030	SOME PITTING, NO SHEEN, VISIBLE RUST AT 1X - NUMEROUS PITS AT 40X
SS304L	0.1031	0.7200	VISIBLE PITTING, NO SHEEN AT 1X - NUMEROUS SMALL PITS, SOME LARGE AND DEEP AT 40X
SS304L	0.1094	0.7490	VISIBLE PITTING, NO SHEEN AT 1X - NUMEROUS LARGE PITS AT 40X
SS316L	0.1071	0.7610	VISIBLE PITTING, NO SHEEN AT 1X - LARGE DEEP PITS, UNIFORM CORROSION AT 40X
SS317L	a.1124	0.8060	SOME LARGE PITS, NO SHEEN AT 1X - LARGE DEEP PITS AT 40X
INCONEL 825	0.1250	0.8720	VISIBLE PITTING, NO SHEEN AT 1X - NUMEROUS LARGE PITS, FAIRLY DEEP AT 40X
FERRALUM 255	0.1294	0.9600	NUMEROUS PITS, NO SHEEN AT 1X - SEVERAL LARGE PITS AT 40X
INCONEL 600	0.1417	0.9730	NO PITTING, NO SHEEN AT 1X - UNIFORM CORROSION AT 40X
ES 2205	0.1926	1.1470	VISIBLE PITTING, NO SHEEN AT 1X - SOME LARGE PITS AT 40X
7Mo + N	0.1547	1.1653	NO PITTING, NO SHEEN AT 1X - FEW LARGE DEEP PITS, UNIFORM CORROSION AT 40X
20Cb-3	0.2410	1.7420	LARGE VISIBLE PITS, NO SHEEN AT 1X - VERY LARGE PITS, SEVERE CORROSION AT 40X
INCONEL 400	a3233	2.1180	NO PITTING, NO SHEEN AT 1X - NUMEROUS PITS, SEVERE UNIFORM CORROSION AT 40X

4.2.4 Following another 4-week cycle, the specimens were returned to the laboratory for the 16-week analysis. The 16-week data is presented in Table 18.

TABLE 18

RESULTS OF 16 WEEK EXPOSURE TO A SALT FOG AND J6 DIP9 IN 1.01 HCL - ALUMINA

MATERIAL NAME	WGT LOSS(g)	CORR. RATE(MPY)	REMARKS - OBSERVATIONS AT 1X AND 40X
HASTELLOY C-22	0.0014	3.3068	NO PITTING, BRIGHT SHEEN AT 1X - SOME VERY SMALL PITS, NO DEPOSITS AT 40X
INCONEL 625	0.0022	0.0110	NO PITTING, BRIGHT SHEEN AT 1X - FEW MEDIUM SIZED PITS AT 40X
ZIRCONIUM 702	0.0018	0.0119	SLIGHT PITTING, SEMI BRIGHT SHEEN AT 1X - NO PITS, PATCHES OF CORROSION AT 40X
HASTELLOY c-276	0.0032	0.0151	NO PITTING, BRIGHT SHEEN AT 1X - SOME VERY SMALL PITS, NO DEPOSITS AT 40X
HASTELLOY C-4	0.0035	0.0170	NO PITTING, BRIGHT SHEEN AT 1X - SOME VERY SMALL PITS, NO DEPOSITS AT 40X
INCOLOY S-3	0.0086	0.0442	NO PITTING, BRIGHT SHEEN AT 1X - FEW SMALL PITS, NO DEPOSITS AT 40X
HASTELLOY B-2	0.1126	0.5390	NO PITTING, DISCOLORATION, NO SHEEN AT 1X - SHALLOW LARGE PITS, UNIFORM CORROSION AT 40X
FERRALUM 255	0.1506	0.8381	VISIBLE PITTING, NO SHEEN AT 1X - NUMEROUS LARGE AND SMALL PITS, NO DEPOSITS AT 40X
SS304L	0.1672	0.8761	VISIBLE PITTING, NO SHEEN AT 1X - NUMEROUS LARGE AND DEEP PITS AT 40X
INCONEL 825	0.1684	0.4819	NUMEROUS PITS, NO SHEEN AT 1X - NUMEROUS LARGE AND DEEP PITS, WELD DECAY AT 40X
SS304LN	0.1881	0.3176	SMALL PITS, DISCOLORED, NO SHEEN AT 1X - NUMEROUS PITS, SOME DEPOSITS AT 40X
SS304L	0.1864	0.9573	VISIBLE PITTING, NO SHEEN AT 1X - MANY PITS, SOME WELD DECAY AT 40X
INCONEL 600	0.1931	0.9942	NO PITTING, DISCOLORATION, NO SHEEN AT 1X - UNIFORM CORROSION, SMALL PITS AT 40X
SS317L	0.1862	1.0018	VISIBLE PITTING, NO SHEEN AT 1X - NUMEROUS LARGE AND DEEP PITS AT 40X
SS316L	0.1918	1.0210	VISIBLE PITTING, NO SHEEN AT 1X - NUMEROUS LARGE AND DEEP PITS AT 40X
7Mo + N	0.1863	1.0526	FEW PITS, DISCOLORATION, NO SHEEN AT 1X - FEW LARGE PITS WELD DECAY, UNIFORM CORROSION AT 40X
ES 2205	0.2309	1.2228	VISIBLE PITTING, DARK COLOR, NO SHEEN AT 1X - SOME LARGE AND MANY SMALL PITS AT 40X
20Cb-3	0.3352	1.8022	EXTENSIVE PITTING, NO SHEEN AT 1X - EXTENSIVE LARGE, DEEP PITS, NO DEPOSITS AT 40X
INCONEL 400	0.4864	2.4009	NO PITTING, NO SHEEN AT 1X - UNIFORM CORROSION, PITS IN WELD, NO DEPOSITS AT 40X

As can be seen from the table, several materials displayed increased attack and fell lower in the rankings. Most notable were the 304L, 316L, and 317L stainless steels. This allowed several materials to move up in the rankings, most notably the Inconel 600, Inconel 825, and the Ferralium 255. The visual observations continued to be helpful in characterizing the alloy surface and type of corrosive attack. The top materials did not display any increase in pitting, and the weight loss data confirms this fact.

- 4.2.5 At the completion of another 4-week exposure cycle, the specimens were returned to the laboratory for the 20-week analysis. The 20-week data is presented in Table 19. A graphical presentation of the corrosion rate data is shown in Figure 8.

TABLE 19

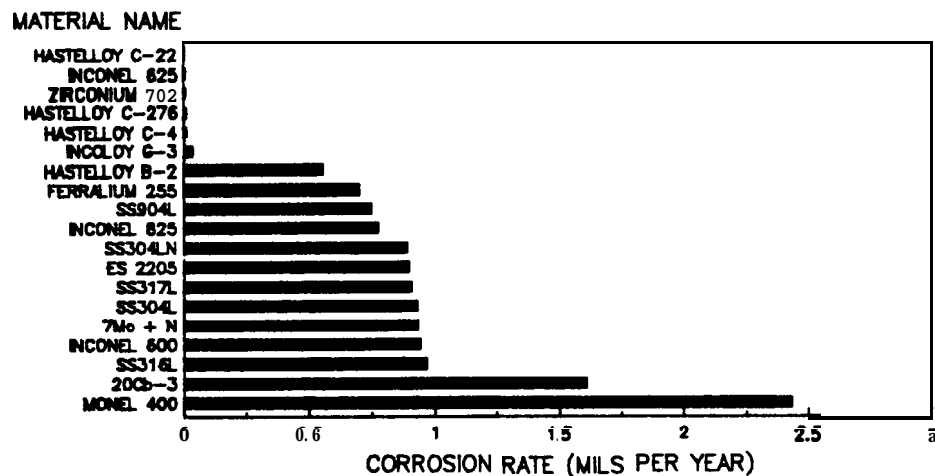
RESULTS OF 20 WEEKS EXPOSURE IN 5% SALT FOG AND 20 DIPS IN 1.0N HCL - ALUMINA

MATERIAL NAME	WGT LOSS(g)	CORR. RATE(MPY)	REMARKS - OBSERVATIONS AT 1X AND 40X
HASTELLOY C-22	0.0009	0.0035	NO PITTING, BRIGHT SHEEN AT 1X - VERY FEW TINY PITS, NO DEPOSITS AT 40X
INCONEL 600	0.0025	0.0100	NO PITTING, BRIGHT SHEEN AT 1X - VERY FEW SMALL PITS AT 40X
ZIRCONIUM 702	0.0020	0.0106	SLIGHT PITTING, SEMI BRIGHT SHEEN AT 1X - NO PITS, SURFACE CORROSION PATCHES AT 40X
HASTELLOY C-276	0.0035	0.0132	NO PITTING, BRIGHT SHEEN AT 1X - VERY FEW TINY PITS AT 40X
HASTELLOY C-4	0.0037	0.0143	NO PITTING, BRIGHT SHEEN AT 1X - FEW VERY SMALL PITS, NO DEPOSITS AT 40X
INCOLOY G-3	0.0093	0.0383	NO PITTING, BRIGHT SHEEN AT 1X - SOME SHALLOW PITTING AT 40X
HASTELLOY B-2	0.1547	0.5625	NO PITTING, DISCOLORATION, ML SHEEN AT 1X - SHALLOW LARGE PITS, UNIFORM CORROSION AT 40X
FERRALIUM 255	0.1581	0.7039	NUMEROUS PITS, NO SHEEN AT 1X - NUMEROUS SHALLOW PITTING AT 40X
SS304L	0.1795	0.7525	VISIBLE PITTING, DISCOLORED, NO SHEEN AT 1X - MANY WIDE SHALLOW AND SMALL DEEP PITS AT 40X
INCONEL 825	0.1858	0.7775	VISIBLE HEAVY PITTING, NO SHEEN AT 1X - MANY DEEP PITS, SEVER WELD ATTACK AT 40X
SS304LN	0.2288	0.8929	VISIBLE SMALL PITS, DISCOLORED, NO SHEEN AT 1X - NUMEROUS PITS, MANY DEEP AT 40X
ES 2205	0.2518	0.9001	VISIBLE PITTING, NO SHEEN AT 1X - SOME MEDIUM PITTING, UNIFORM CORROSION AT 40X
SS317L	0.2122	0.9088	VISIBLE PITTING, DISCOLORED, NO SHEEN AT 1X - MANY WIDE SHALLOW AND SMALL DEEP PITS AT 40X
SS304L	0.2269	0.9323	VISIBLE SMALL PITS, DISCOLORED, NO SHEEN AT 1X - NUMEROUS PITS, SOME DEEP ON WELD AT 40X
7Mo + N	0.2072	0.9365	VISIBLE PITTING ON WELD, NO SHEEN AT 1X - NUMEROUS PITS, SOME DEEP, WELD ATTACK AT 40X
INCONEL 600	0.2298	0.9465	NO PITTING, NO SHEEN AT 1X - TINY PITS, UNIFORM CORROSION AT 40X
SS316L	0.2276	0.9700	VISIBLE HEAVY PITTING, DISCOLORED, NO SHEEN AT 1X - MANY WIDE SHALLOW AND SMALL DEEP PITS AT 40X
20Cb-3	0.3746	1.6112	VISIBLE VERY HEAVY PITTING, NO SHEEN AT 1X - EXTREME PITTING, MANY VERY DEEP AT 40X
INCONEL 400	0.6196	2.4325	NO PITTING, DISCOLORED, NO SHEEN AT 1X - TINY PITS WITH UNIFORM CORROSION AT 40X

As can be seen from the table, the materials generally remained in their respective positions when compared to the 16-week data. The 304L stainless steel dropped slightly in the rankings due to severe weld attack.

When the corrosion rate data is graphed, as in Figure 8, the great differences in performance can easily be seen. The level of performance of the top alloys is much higher than that of the lower materials. The cutoff line between the **Incoloy G-3** and the Hastelloy B-2 shows a 15 fold increase in the corrosion rate. The corrosion rate of **304L** stainless steel is approximately 260 times higher than that of Hastelloy C-22 in the salt fog/acid dip exposure test. The slight weight gains for Hastelloy C-22 and Inconel 625 in weeks 16 and 20 were unexpected. This could have been caused by slight errors in measurement or differences in cleaning and weighing procedures. However, this did not upset the relative rankings, and the gains were considered insignificant.

FIGURE 8 - SALT **FOG/ACID** DIP DATA
20 WEEKS/20 ACID DIPS



- 4.2.6 In conjunction with the standard alloy coupons, specimens were tested in the composite welded configuration. These specimens were produced by joining dissimilar metals by welding the candidate alloys to **304L** stainless steel. The resulting composite coupons were exposed to the same conditions as the standard specimens to determine any undesirable galvanic effects at the weld area. This was considered necessary since the successful new alloy would be installed in an existing

304L stainless steel piping system, and galvanic corrosion in the weld area could become a source of system failure. The composite welded coupons were cleaned prior to examination in the same manner as described earlier. The 16-week observations are presented in Table 20.

TABLE 20

RESULTS OF 16 WEEK EXPOSURE IN 5% SALT FDS AND 16 #1D DIPS

COMPOSITE GALVANIC WELD SPECIMENS

MATERIAL NAME	REMARKS - OBSERVATIONS AT 1X AND 40X
SS304L - C-276	SOME WELD DECAY ON BOTH SIDES AT 1X - LARGE PITS ALONG 304L SIDE AT 40X
SS304L - B-2	SOME DECAY ON 304L SIDE AT 1X - 304L SIDE HAS SOME WELD DECAY AT 40X
SS304L - C-4	SOME WELD DECAY AT 1X - LARGE PITS AND DECAY ON 304L SIDE AT 40X
SS304L - C-22	SOME WELD DECAY ON 304L SIDE AT 1X - LARGE PITTING ALONG 304L SIDE AT 40X
SS304L - HA00	EXTREME WELD DECAY ON 304L SIDE AT 1X - WELD DECAY ON BOTH SIDES AT 40X
SS304L - 304LN	SLIGHT WELD PITTING AT 1X - SMALL PITS AND DEPOSITS ON WELD AT 40X
SS304L - 316L	SOME DECAY ON 304L SIDE AT 1X - SMALL PITS ON WELD AT 40X
SS304L - 317L	SOME PITTING OF WELD AT 1X - WELD DECAY AND PITTING AT 40X
SS304L - 904L	SLIGHT WELD DECAY ON 304L SIDE AT 1X - SMALL PITS ON WELD AT 40X
SS304L - I-600	WELD DECAY ON 304L SIDE AT 1X - 304L SIDE WELD DECAY AT 40X
SS304L - I-625	WELD PITTING AT 1X - 304L SIDE WELD DECAY AND PITTING AT 40X
SS304L - I-825	WELD PITTING AT 1X - WELD PITTING ON BOTH SIDES AT 40X
SS304L - S-3	SOME PITTING ON WELD AT 1X - PITS ON S-3 SIDE OF WELD AT 40X
SS304L - 20Cb-3	SOME PITTING, 304L SIDE WELD DECAY AT 1X - LARGE PITS AND DECAY ON BOTH SIDES AT 40X
SS304L - 7Mo+N	VISIBLE WELD PITTING AT 1X - LARGE PITS AND WELD DECAY ON BOTH SIDES AT 40X
SS304L - ES 2205	VISIBLE WELD PITTING AT 1X - PITTING AND DECAY OF WELD ON BOTH SIDES AT 40X
SS304L - F-255	WELD DECAY ON 304L SIDE AT 1X - PITTING AND DECAY OF WELD ON BOTH SIDES AT 40X

As can be seen from the table, most of the specimens suffered some type of weld decay. For the alloys under consideration from a corrosion resistance standpoint (Hastelloy C-22 and Inconel 625), the deterioration was mostly on the 304L surfaces adjacent to the weld. Since 304L stainless steel is anodic to these two alloys, this result was expected. The 304L is corroding preferentially and cathodically protecting the more corrosion resistant alloy. Since the particular application of the corrosion resistant alloy is to form thin wall convolutes welded to a heavy wall 304L stainless steel pipe, the galvanic effect will be minimal. The effects can be further lessened by welding using the corrosion resistant alloy as the weld filler and coating the weld area with AR-7 to block any electrolyte from reaching the galvanic

couple. The AR-7 material is readily available from KSC stock and is described fully in KSC-STD-C-0001B.

4.2.7 Further testing was conducted during the study to determine if any of the alloys under consideration would be susceptible to stress corrosion cracking in the Shuttle launch environment. This was considered important due to the forming operations used in fabricating flexible convoluted bellows. The convolutes are severely deformed during manufacture, and high residual tensile stresses could be present. This situation combined with a corrosive environment created concern to properly define the stress corrosion behavior of the candidate alloys. For this testing, standard U-bend specimens were exposed to the same set of conditions as the corrosion coupons. These U-bend specimens were welded in the middle of the bend to create the worst case condition. As of the time of this report, only two of the stress corrosion specimens have failed. The 304L stainless steel specimen cracked after 8 weeks and eight acid dips. The Ferralium 255 specimen cracked after 12 weeks and 12 acid dips. All other materials are continuing to display stress corrosion cracking resistance in the salt fog/acid dip environment.

4.3 BEACH EXPOSURE/ACID SPRAY

4.3.1 After 60 days of beach exposure and 5 acid **sprays**, the coupons were returned to the laboratory for analysis. After the cleaning procedure, the specimens were weighed, corrosion rate calculations were made, and visual examinations were conducted as described for the salt fog/acid dip process. The results of these analyses for each of the alloys for the 60 day/5 spray cycle are presented in Table 21. As can be seen from the table, several materials clearly separated from the rest and displayed excellent corrosion resistance. The **Hastelloy** C-22 and Inconel 625 showed no

detectable weight loss, while the Hastelloy C-4 and C-276 were on **the** limits of measurement. The calculated corrosion rates for these materials are considered insignificant, and any one should be considered acceptable. The observations confirmed the resistance of these alloys, with no visual deterioration at 40x. These results were considered important but premature, and the specimens were returned to the beach for further exposure.

TABLE 21

RESULTS OF 60 DAY EXPOSURE TO BEACH CORROSION SITE AND 5 SPRAYS WITH 10% VOL. HCL - ALUMINA

MATERIAL NAME	WGT LOSS(g)	CORR. RATE(MPY)	REMARKS - OBSERVATIONS AT 1X AND 40X
HASTELLOY C-22	0.0000	0.0000	NO PITTING, BRIGHT SHEEN AT 1X - NO PITTING, NO WELD DECAY AT 40X
INCONEL 625	0.0000	0.0000	NO PITTING, BRIGHT SHEEN AT 1X - NO PITTING, NO WELD DECAY AT 40X
HASTELLOY C-L26	0.0001	0.0009	NO PITTING, BRIGHT SHEEN AT 1X - NO PITTING, NO WELD DECAY AT 40X
HASTELLOY C-4	0.0001	0.0009	NO PITTING, BRIGHT SHEEN AT 1X - NO PITTING, NO WELD DECAY AT 40X
ZIRCONIUM 702	0.0007	0.0080	STAINED, NO SEEN AT 1X - UNIFORM CORROSION, NO PITTING AT 40X
INCOLOY G-3	3.0015	0.0140	NO PITTING, BRIGHT SEEN AT 1X - MINOR PITTING, UNIFORM CORROSION OF WELD AT 40X
ES 2205	0.0121	0.0990	NO PITTING, NO SEER AT 1X - MODERATE SHALLOW PITTING AT 40X
FERRALTIUM 255	0.0105	0.1100	NO PITTING, BRIGHT SHEEN AT 1X - UNIFORM CORROSION, PITTING AT EL9 AT 40X
INCONEL 825	0.0124	0.1200	VISIBLE PITTING, SLIGHT SHEEN AT 1X - SLIGHT PITTING, MINOR PITTING OF WELD AT 40X
7Mo + N	0.3130	0.1387	NO PITTING, NO SHEEN AT 1X - UNIFORM CORROSION, SEVERE PITTING OF WELD AT 40X
SS304L	0.0147	0.1440	VISIBLE PITTING, SLIGHT SEEN AT 1X - SHALLOW PITTING, UNIFORM DECAY L-F WELD AT 40X
SS317L	0.0188	0.1979	VISIBLE PITTING, SLIGHT SHEEN AT 1X - SLIGHT PITTING/SOME DEEP, NO WELD DECAY AT 40X
INCONEL 600	0.0203	0.1950	VISIBLE PITTING, NO SHEEN AT 1X - SHALLOW PITTING, NO WELD DECAY AT 40X
SS316L	0.0247	0.2450	VISIBLE PITTING, NO SHEEN AT 1X - MODERATE PITTING, SLIGHT PITTING OF WELD AT 40X
SS304L	0.0277	0.2780	VISIBLE PITTING, NO SHEEN AT 1X - MODERATE PITTING, SUE PITTING OF WELD AT 40X
HASTELLOY B-2	0.0329	0.2600	NO PITTING AT 1X - FEW PITS WITH UNIFORM CORROSION, SOME WELD DECAY AT 40X
SS304LN	0.0348	0.3200	VISIBLE PITTING, NO SHEEN AT 1X - SLIGHT PITTING, SOME PITTING OF WELD AT 40X
20Cb-3	0.0431	0.4350	VISIBLE PITTING, SLIGHT SHEEN AT 1X - HEAVY PITTING/SOME DEEP, SEVERE PITTING OF WELD AT 40X
MONEL 400	0.0954	0.9710	NO PITTING, NO SHEEN AT 1X - UNIFORM CORROSION, NO PITTING AT 40X

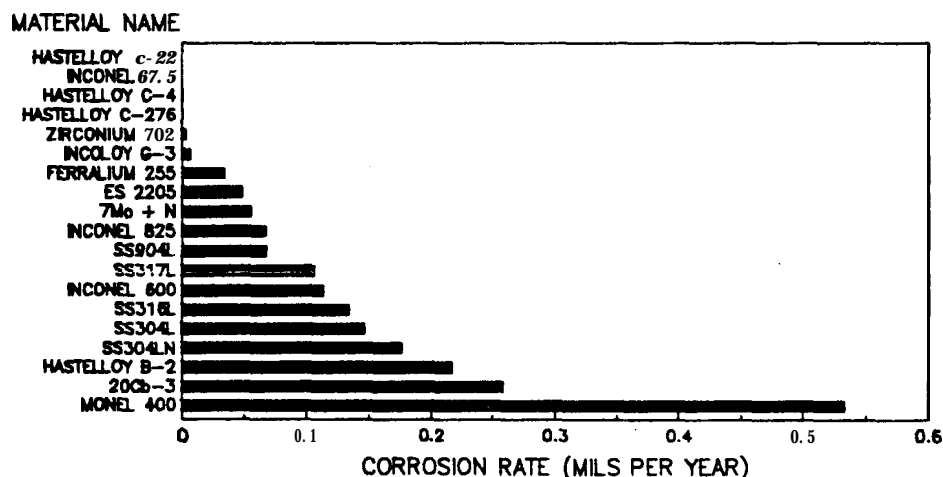
4.3.2 After 251 days of beach exposure with 13 acid sprays, the specimens were returned to the laboratory for analysis. The same procedures were conducted to clean, weigh, calculate, and observe the coupons. The 251-day data is shown in Table 22. A graphical presentation of the corrosion rate data is shown in Figure 9. Following the **251-day** exposure cycle, the same four materials displayed excellent corrosion resistance and were clearly superior to the remainder of the alloys. The same reduction in corrosion rate phenomenon **was** experienced as in the salt fog testing. This **is** probably due to a reduction in pitting rates over time as explained previously. The

corrosion rates shown in Figure 9 display the same cutoff as for the salt fog data, except that the increase in corrosion rate is not as pronounced. Between the Incoloy G-3 and the Ferralium 255, there is only a 5 fold increase in corrosion rate. Since the corrosion rates of Hastelloy C-22 and Inconel 625 were not measurable, no numerical comparison factor can be found with respect to the other alloys. However, these two alloys are clearly superior to the stainless steel alloys in the beach exposure/acid spray testing.

TABLE 22

RESULTS OF 251 DAY EXPOSURE TO BEACH CORROSION SITE AND 13 SPRAYS WITH 10% VOL. HCL - ALUMINA

MATERIAL NAME	WT LOSS(g)	CORR. RATE(MPY)	REMARKS - OBSERVATIONS AT 1X AND 40X
HASTELLOY C-22	0.0000	0.0000	NO PITTING, BRIGHT SHEEN AT 1X - NO PITTING, NO CORROSION AT 40X
INCONEL 625	0.0000	0.0000	NO PITTING, BRIGHT SHEEN AT 1X - NO PITTING, NO WELD DECAY AT 40X
HASTELLOY C-4	0.0001	0.0009	NO PITTING, BRIGHT SHEEN AT 1X - NO PITTING AT 40X
HASTELLOY C-276	0.0001	0.0009	NO PITTING, BRIGHT SHEEN AT 1X - VERY FEW SMALL PITS, NO WELD DECAY AT 40X
ZIRCONIUM 702	0.3014	0.0040	SLIGHT PITTING, SLIGHT SHEEN AT 1X - UNIFORM CORROSION, NO PITTING AT 40X
INCOLOY G-3	0.0034	0.0037	NO PITTING, BRIGHT SHEEN AT 1X - FEW SMALL PITS, UNIFORM WELD DECAY AT 40X
FERRALIUM 255	0.0139	0.0343	SLIGHT PITTING, MEDIUM SHEEN AT 1X - UNIFORM CORROSION, WELD DECAY AT 40X
ES 2205	0.0251	0.0490	SLIGHT PITTING, NO SHEEN AT 1X - SMALL PITS, UNIFORM CORROSION SEVERE WELD DECAY AT 40X
7Mo + N	0.0220	0.0561	SLIGHT PITTING, NO SHEEN AT 1X - UNIFORM CORROSION, LARGE DEEP PITS ON WELD AT 40X
INCONEL 825	0.0288	0.0600	VISIBLE PITTING, SLIGHT SHEEN AT 1X - MANY SMALL SHALLOW PITS, PITS ON WELD AT 40X
SS904L	0.0293	0.0685	VISIBLE PITTING, LOW SHEEN AT 1X - MANY SMALL PITS, WELD PITTING AT 40X
SS317L	0.0450	0.1069	VISIBLE PITTING, NO SHEEN AT 1X - SOME SMALL PITS, SURFACE CORROSION, WELD PITTING AT 40X
INCONEL 600	0.0497	0.1140	SLIGHT PITTING, NO SHEEN AT 1X - UNIFORM SMALL PITS, NO WELD DECAY AT 40X
SS316L	0.0566	0.1344	NUMEROUS PITS, NO SHEEN AT 1X - MANY SMALL PITS, SOME WELD PITTING AT 40X
SS304L	0.0612	0.1467	VISIBLE PITTING, NO SHEEN AT 1X - LARGE AND SMALL SHALLOW PITS, WELD DECAY AT 40X
SS304LN	0.0816	0.1768	VISIBLE PITTING, NO SHEEN AT 1X - SOME PITTING WITH DEPOSITS, WELD DECAY AT 40X
HASTELLOY B-2	0.1064	0.2177	NO PITTING, NO SHEEN AT 1X - FEW PITS, UNIFORM CORROSION, NO WELD DECAY AT 40X
20Cb-3	0.1074	0.2590	EXTENSIVE PITTING, NO SHEEN AT 1X - EXTENSIVE PITTING, SOME LARGE, UNIFORM WELD DECAY AT 40X
MONEL 400	0.2447	0.5340	NO PITTING, NO SHEEN AT 1X - NO PITTING, UNIFORM CORROSION AT 40X

FIGURE 9 - BEACH CORROSION DATA
251 DAYS/13 ACID SPRAYS

- 4.3.3 When the beach results are compared to the salt fog results, many materials change positions relative to each other. In general, the materials at the top (**Hastelloy C-22** and **Inconel 625**) and at the bottom (**20Cb-3** and **Monel 400**) of each list remained in their respective positions. However, the standard stainless steel alloys such as **304L**, **304LN**, **316L**, and **317L** declined in relative performance while the duplex stainless alloys such as **Ferrallium 255**, **7Mo+N**, and **ES 2205** improved in the rankings. This was an interesting occurrence and could be explained as follows. The main difference between the two tests is oxygen availability. While the specimens are in the salt fog chamber, the surfaces are continually wet, and this film of water could reduce the oxygen available to the metal surface. Since most corrosion resistant alloys depend on oxide films on their surface for protection, the suspicion is that the salt fog conditions could be hindering the formation of these protective oxide films on the duplex stainless steels, allowing accelerated corrosion to take place. The beach data, in contrast to the salt fog data, supports the electrochemical findings in regard to the **Ferrallium 255**. The reasons for this are unclear but could be due to the formation of the protective oxide films.
- 4.3.4 For reasons stated earlier, composite welded coupons were tested in conjunction with the standard specimens to determine any undesirable effects of the galvanic couple. The composite specimens were cleaned in the same manner before the examination. The **251-day** beach exposure observations are shown in Table 23, As can be seen from the table, most specimens were suffering from weld decay. The severity was generally less than that observed in the salt fog testing, but the results are similar in nature with most of the attack concentrated on the **304L** stainless steel surfaces. As stated before, coating of the weld area with the **AR-7** material should reduce the galvanic effects to a minimum.

TABLE 23

RESULTS OF 251 DAY EXPOSURE TO BEACH CORROSION SITE AND 13 SPRAYS WITH 10% VOL. HCL - ALUMINA

COMPOSITE GALVANIC WELD SPECIMENS

MATERIAL NAME	REMARKS - OBSERVATIONS AT 1X AND 40X
98304L - C-276	PITTING ON 304L SIDE AT 1X - SEVERE WELD DECAY ON 304L SIDE AT 40X
98304L - B-2	NO VISIBLE DECAY AT 1X - SLIGHT WELD DECAY ALONG 304L SIDE AT 40X
98304L - C-4	NO VISIBLE DECAY AT 1X - SLIGHT WELD DECAY ON 304L SIDE AT 40X
98304L - C-22	SLIGHT WELD DECAY ON 304L SIDE AT 1X - SLIGHT WELD DECAY ON 304L SIDE AT 40X
98304L - H400	SLIGHT WELD DECAY ON 304L SIDE AT 1X - WELD DECAY ON 304L SIDE AT 40X
98304L - 304LN	NO VISIBLE DECAY AT 1X - PITTING OF WELD ON BOTH SIDES AT 40X
98304L - 316L	NO VISIBLE DECAY AT 1X - PITTING AND WELD DECAY ON BOTH SIDES AT 40X
98304L - 317L	NO VISIBLE DECAY AT 1X - WELD DECAY AND PITTING ON 304L SIDE, PITTING ONLY ON 317L SIDE AT 40X
98304L - 904L	NO VISIBLE DECAY AT 1X - UNIFORM WELD DECAY ON 304L SIDE AT 40X
98304L - 1400	NO VISIBLE DECAY AT 1X - WELD DECAY ON 304L SIDE, SLIGHT DECAY ON 1-600 SIDE AT 40X
98304L - 1-625	NO VISIBLE DECAY AT 1X - WELD DECAY AND PITTING ON 304L SIDE AT 40X
98304L - 1-825	NO VISIBLE DECAY AT 1X - WELD DECAY AND PITTING ON 304L SIDE, SLIGHT DECAY ON 1-825 SIDE AT 40X
98304L - G-3	NO VISIBLE DECAY AT 1X - WELD DECAY AND PITTING ON 304L SIDE, SLIGHT DECAY ON G-3 SIDE AT 40X
98304L - 20Cb-3	VISIBLE PITTING ON WELD AT 1X - WELD DECAY AND PITTING ON BOTH SIDES AT 40X
98304L - 7Mo-N	VISIBLE PITTING ON WELD AT 1X - HEAVY PITTING ALONG WELD AT 40X
98304L - ES 2205	WELD DECAY ON 304L SIDE AT 1X - SEVERE WELD DECAY ON 304L SIDE, PITTING ON ES-2205 SIDE AT 40X
98304L - F-255	WELD DECAY ON 304L SIDE AT 1X - SEVERE WELD DECAY ON 304L SIDE, SLIGHT PITTING ON F-255 SIDE AT 40X

4.3.5 In conjunction with the salt fog testing, duplicate U-bend stress corrosion cracking specimens were exposed at the beach corrosion test site to determine the stress corrosion cracking susceptibility of the candidate alloys. As of the time of this report, none of the specimens exposed to the naturally occurring conditions at the beach site have experienced failure. Exposure of these specimens will continue, to determine if any specimens will crack in the future.

4.3.6 By comparing results from the salt fog to the beach testing, many differences have been noted. The beach testing is still considered the best judge of an alloy's performance since it has naturally occurring conditions that reflect the conditions experienced at Launch Complex 39. However, the accelerated testing does give insight into which materials have a good chance of performing well. In all the testing, by electrochemical methods, salt fog/acid dip, beach exposure/acid spray, and ferric chloride immersion, the same materials are at the top of the list. The Hastelloy C-22

has displayed superior corrosion resistance during all the testing. This work concentrated on one specific environment that contains sodium chloride and hydrochloric acid. Since all these alloys are very environment specific, altering that environment even slightly may produce extreme changes in alloy performance. Other chemical environments such as high pH (basic), stronger acids, other corrosives, or high temperatures may cause failure of the materials identified in this study. When dealing with high performance corrosion resistant alloys, thorough testing is an absolute requirement for choosing the right material for the job. The long term history received from the continued beach testing will be invaluable to completely characterize alloy behavior.

4.3.7 Photos of some salt fog chamber and beach exposure samples are shown in Appendix B. These photos are representative of the types and extent of corrosion experienced by the candidate alloys. Photos are at about 1x, 40x, and 500x. The alloys in the photos are Hastelloy C-22, 304L, 316L, Monel 100, and 20Cb-3. The Hastelloy C-22 experienced no corrosion. The Monel 400 samples show uniform corrosion, and the other three alloys show pitting corrosion.

4.4 FERRIDRIDE . IMMERSION

4.4.1 Results for the samples with an autogenous weld are summarized in Table 21. Some samples showed no signs of corrosion. Others showed uniform corrosion, pitting corrosion, weld decay, or corrosive attack in the heat affected zone. Some representative photos are shown in Figure 10. Figure 10a, of Inconel 625, shows no corrosion. The 316L in Figure 10b shows severe pitting corrosion. Hastelloy D-2, seen in Figure 10c, suffered uniform corrosion, and the Inconel 825 sample of Figure 10d shows severe pitting attack at the weld and in the heat affected zone.

**TABLE 24 FERRIC CHLORIDE IMMERSION RESULTS
AUTOGENOUS WELD SAMPLES**

ALLOY	HOURS IMMERSED	RESULTS
HASTELLOY C-4	912	NO CORROSION
HASTELLOY C-22	72	NO CORROSION
HASTELLOY C-276	912	NO CORROSION
HASTELLOY B-2	72	UNIFORM CORROSION
INCONEL 600	72	MODERATE PITTING
INCONEL 625	912	NO CORROSION
INCONEL 825	72	SEVERE PITTING IN HEAT AFFECTED ZONE
INCO G-3	912	NO CORROSION
MONEL 400	72	UNIFORM CORROSION
ZIRCONIUM 702	72	MODERATE PITTING
SS 304L	72	SEVERE PITTING
SS 304LN	72	SEVERE PITTING
SS 316L	72	SEVERE PITTING
SS 317L	72	MILD PITTING AND WELD DECAY
SS 904L	72	NO CORROSION
20 Cb-3	72	SEVERE PITTING IN HEAT AFFECTED ZONE
7Mo	72	WELD DECAY
ES 2205	72	WELD DECAY
FERRALIUM 255	72	NO CORROSION

4.4.2 Results for the samples welded to 304L stainless steel are given in Table 25. It was not possible to obtain a sample of Zirconium 702 welded to 304L; so Zirconium 702 does not appear in Table 25. The effect of galvanic corrosion can be seen clearly by noticing that the 304L part of each sample suffered severe pitting corrosion. This can be seen visually in Figure 11.

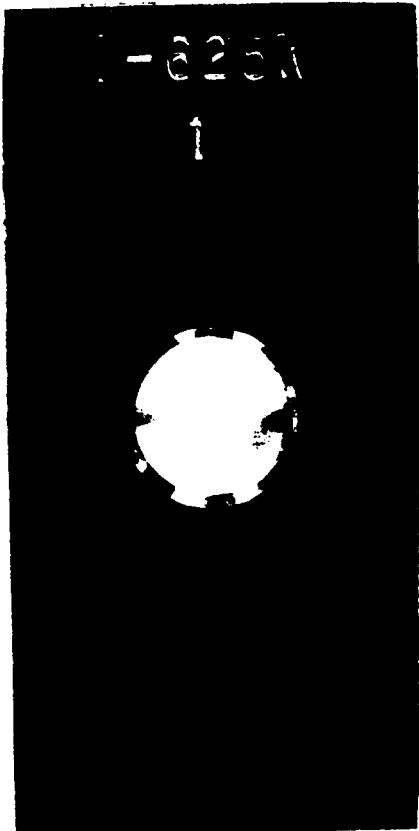
**TABLE 25 FERRIC CHLORIDE IMMERSION RESULTS
SAMPLES WELDED TO 304L STAINLESS**

ALLOY	OBSERVATIONS ON CANDIDATE ALLOY	ALLOY	OBSERVATIONS ON CANDIDATE ALLOY
HASTELLOY C-4	NO CORROSION	SS 304LN	SEVERE PITTING
HASTELLOY C-22	NO CORROSION	SS 316L	SOME PITTING
HASTELLOY C-276	NO CORROSION	SS 317L	NO CORROSION
HASTELLOY B-2	UNIFORM CORROSION	SS 904L	NO CORROSION
INCONEL 600	UNIFORM CORROSION	20Cb-3	SLIGHT PITTING
INCONEL 625	NO CORROSION	7 Mo + N	NO CORROSION
INCONEL 825	NO CORROSION	ES 2205	NO CORROSION
INCO G-3	NO CORROSION	FERRALIUM 255	NO CORROSION
MONEL 400	UNIFORM CORROSION		

NOTE: All samples were immersed for 72 hours.
In each case, the 304L portion of the sample
suffered severe pitting.

Figure 10 Photos After Ferric Chloride Immersion, 2.2x

a) Inconel 625



b) 316L



c) Hastelloy B-2



d) Inconel 825



Figure 11 Ferric Chloride Immersion - Galvanic Samples



a) 304L Welded to
Hastelloy C-276

<--- 304L
Severe Pitting

<--- Hastelloy C-276
No Corrosion



b) 304L Welded to 904L

<--- 304L
Severe Pitting

<--- 904L
No Corrosion

5.0 CONCLUSIONS

- 5.1 Several alloys were found that have superior resistance to pitting and crevice corrosion, compared to the **304L** stainless steel that was originally used for construction of convoluted flexible joints.
- 5.2 Good agreement was found between all 4 of the corrosion tests. In particular, the cyclic polarization technique was found to give **excellent** agreement with the beach exposure and salt fog chamber results. This electrochemical method may be used as a very quick way to evaluate alloys before performing long term field exposure tests.
- 5.3 Using the conditions found at the Space Shuttle launch site (high chloride content plus hydrochloric acid), the most resistant alloys were found to be, in order, Hastelloy C-22, Inconel 625, Hastelloy C-276, Hastelloy C-4, and **Inco** Alloy G-3.
- 5.4 On the basis of corrosion resistance, combined with weld and mechanical properties, Hastelloy C-22 was determined to be the best material for construction of flex hoses for use at the Space Shuttle launch site.

REFERENCES

1. J. J. Dundas, A. P. Bond, Corrosion Resistance of Stainless Steels in Seawater, Materials Performance, Vol.24, No.10, p.54, 1985.
2. A. P. Bond, H. J. Dundas, Resistance of Stainless Steels to Crevice Corrosion in Seawater, Materials Performance, Vol.23, No.7, p.39, 1984.
3. A. Garner, Crevice Corrosion of Stainless Steels in Sea Water: Correlation of Field Data With Laboratory Ferric Chloride Tests, Corrosion, Vol.37, No.3, p.178, 1981.
4. W. F. Bogaerts, A. A. **VanHaute**, Chloride Pitting and Water Chemistry Control in Cooling or Boiler Circuits, Corrosion Science, Vol.25, No.12, p.1149, 1985.
5. A. Kawashima, K. Hashimoto, The Pitting Corrosion Behavior of Rapidly Solidified Fe-Cr Alloys in 0.5 M NaCl Solution,

Corrosion Science, Vol.26, **No.6**, p.467, 1986.

6. R. F. Wilde, The Influence of Silicon on the Pitting Corrosion Resistance of an **18Cr-8Ni** Stainless Steel, Corrosion, Vol.42, **No.3**, p.147, 1986.

7. J. R. Park, Z. Szklarska-Smialowska, Pitting Corrosion of Inconel 600 in High-Temperature Water Containing **CuCl₂**, Corrosion, Vol.41, **No.11**, p.665, 1985.

8. 4. I. Asphahani, Corrosion Resistance of High Performance Alloys, Materials Performance, Vol.19, No.12, p.33, 1980.

9. P. B. Lindsay, Effect of Heat Treatment on the Corrosion Resistance of High-Alloy Stainless Steel and Nickel-Base Alloys, Materials Performance, Vol.25, No.12, p.23, 1986.

10. A. I. Asphahani, Effect of Acids on the Stress Corrosion Cracking of Stainless Materials in Dilute Chloride Solutions, Materials Performance, Vol.19, **No.11**, p.9, 1980.

11. A. 1. Asphahani, Localized Corrosion of High Performance Alloys, Materials Performance, Vol.19, **No.8**, p.9, 1980.

12. D. R. Knittel, A. Bronson, Pitting Corrosion on Zirconium - A Review, Corrosion, **Vol.40, No.1**, p.9, 1984.

13. R. Bandy, D. Van Rooyen, Pitting-Resistant Alloys in Highly Concentrated Chloride Media, Corrosion, Vol.39, **No.6**, p.227, 1983.

14. T. S. Lee, III, F. G. Hodge, Resistance of "Hastelloy" Alloys to Corrosion by Inorganic Acids, Materials Performance, **Vol.15, No.9**, p.29, 1976.

15. F. E. Manning, J. D. Smith, J. L. Nickerson, New Versatile Alloys for the Chemical Process Industry, Materials Performance, **Vol.27, No.6**, p.67, 1988.

16. P. E. Manning, Comparison of Several Accelerated Laboratory Tests for the Determination of Localized Corrosion Resistance of High-Performance Alloys, Corrosion, Vol.39, **No.3**, p.98, 1983.

17. ASTM **G59-78**, Standard Practice for Conducting **Potentiodynamic** Polarization Resistance Measurements, 1986 Annual Book of ASTM Standards, Volume 03.02, ASTM, Philadelphia, PA, 1986.

18. **ASTM G61-78**, Standard Practice For Conducting Cyclic Potentiodynamic Polarization Measurements For Localized **Corrosion**, 1986 Annual Book of ASTM Standards, Volume 03.02, ASTM, Philadelphia, PA, 1986.
19. **ASTM B117-85**, Standard Method of Salt **Spray** (Fog) Testing, 1986 Annual Book of ASTM Standards, Volume 03.02, ASTM, Philadelphia, PA, 1986.
20. **ASTM G1-81**, Standard Practice for Preparing, Cleaning, and Evaluating Corrosion Test Specimens, 1986 Annual Book of ASTM Standards, Volume 03.02, ASTM, Philadelphia, PA, 1986.
21. **ASTM G50-76**, Standard Practice for Conducting Atmospheric Corrosion Tests on Metals, 1986 Annual Book of XSTM Standards, Volume 03.02, ASTM, Philadelphia, PA, 1986.
22. **ASTM G48-76**, Standard **Test** Methods For Pitting and Crevice Corrosion Resistance of Stainless Steels and Related **Alloys** By The Use Of Ferric Chloride Solution, 1986 Annual Book of ASTM Standards, Volume 03.02, ASTM, Philadelphia, PA, 1986.
23. Princeton Applied Research Application Note **CORR 1**, **EG&G** Princeton Applied Research, Princeton, New Jersey, 1982.
24. R. **Baboian**, G. S. Haynes, Cyclic Polarization Measurements - Experimental Procedure and Evaluation of Test Data, in Electrochemical Corrosion Testing, ASTM STP 727, F. Mansf'eld, U. Bertocci, Eds., ASTM, Philadelphia, Pennsylvania, p.274, 1981.
25. **F. L. Liening**, Practical Applications of Electrochemical Techniques to Plant Localized Corrosion Problems, Materials Performance, Vol.19, **No.2**, p.35, 1980.

APPENDIX A

Corrosion Potential and Cyclic
Polarization Graphs

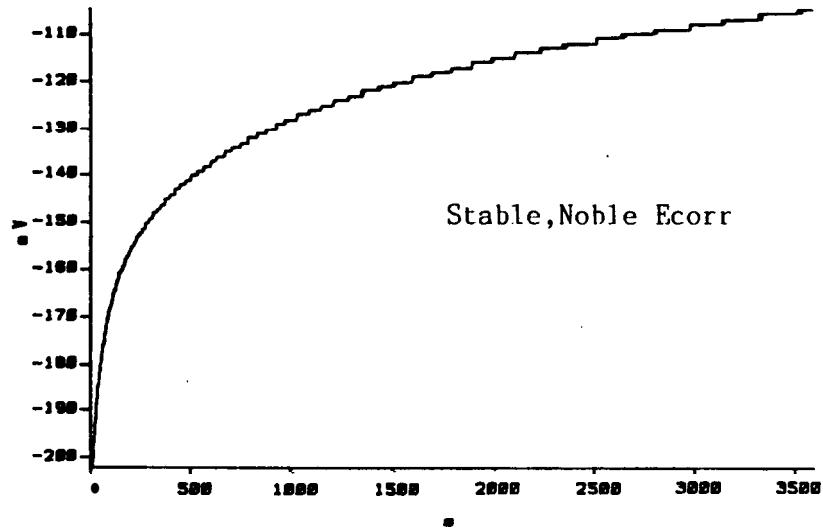


Figure A1 Hastelloy C-4 Corrosion Potential
in Aerated 3.55% NaCl + 0.1N HCl

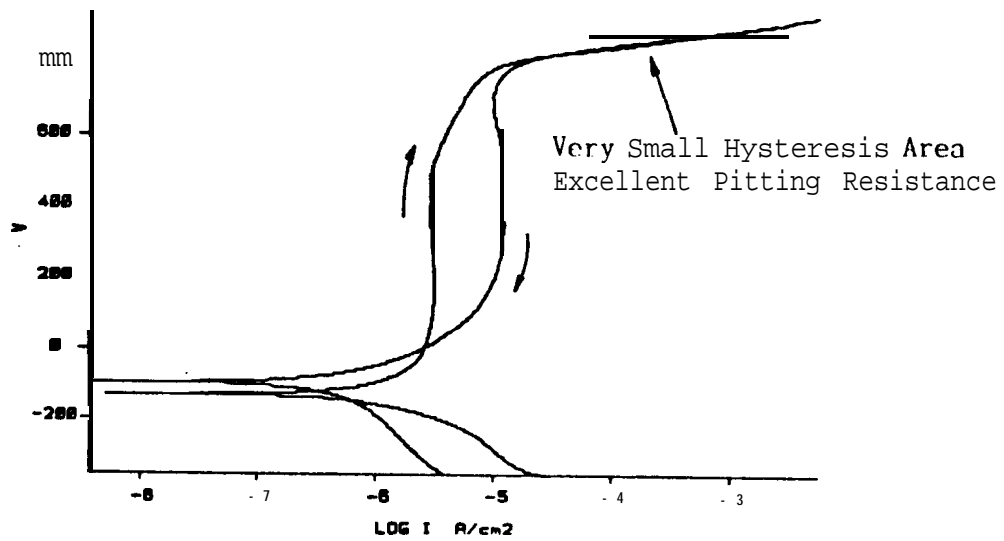


Figure A2 Hastelloy C-4 Cyclic Polarization
in Aerated 3.55% NaCl + 0.1N HCl

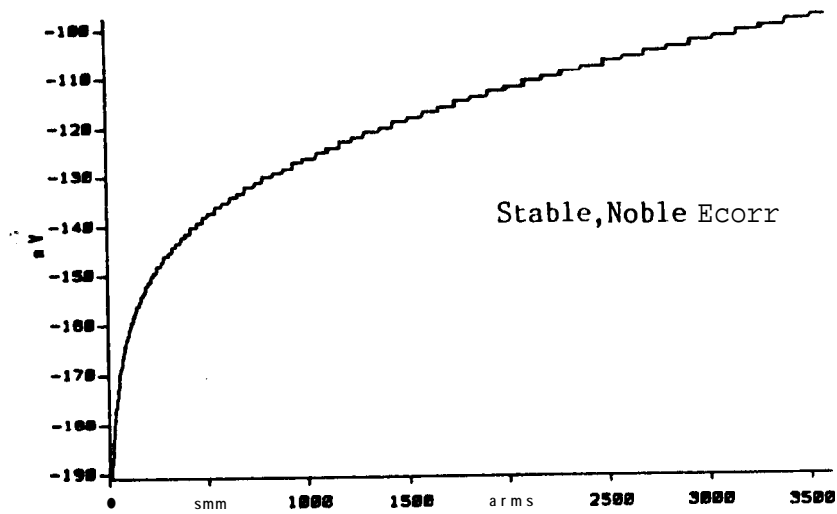


Figure A3 Hastelloy C-4 Corrosion Potential
in Aerated 3.55% NaCl + 1.0N HCl

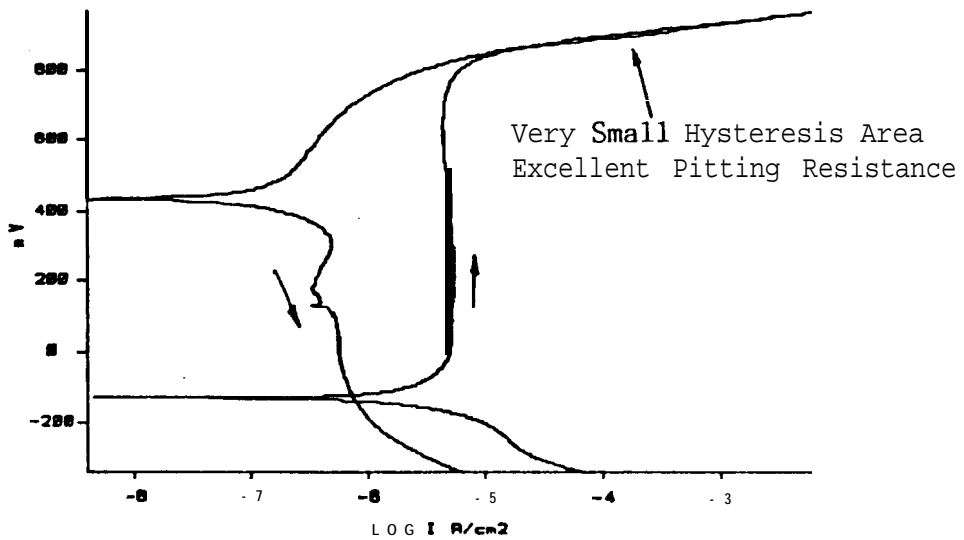


Figure A4 Hastelloy C-4 Cyclic Polarization
in Aerated 3.55% NaCl + 1.0N HCl

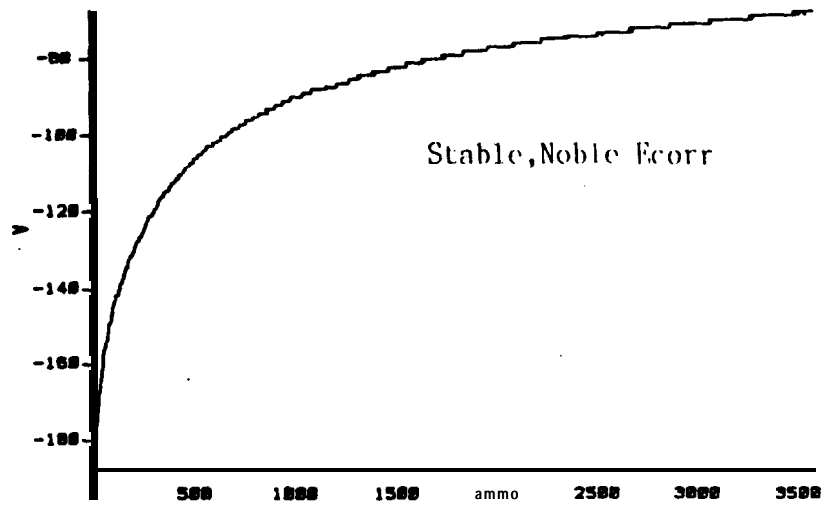


Figure A5 Hastelloy C-22 Corrosion Potential
in Aerated 3.55% NaCl + 0.1N HCl

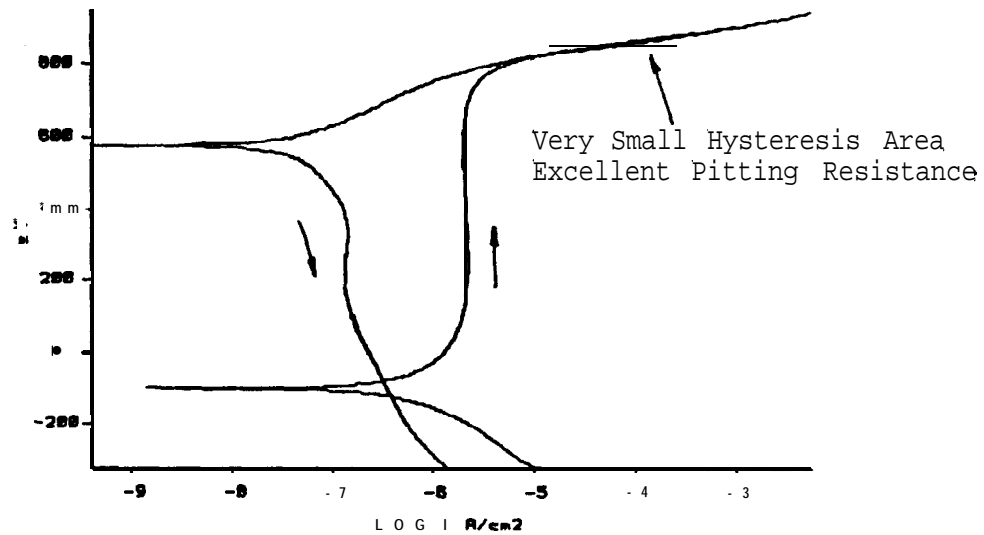


Figure A6 Hastelloy C-22 Cyclic Polarization
in Aerated 3.55% NaCl + 0.1N HCl

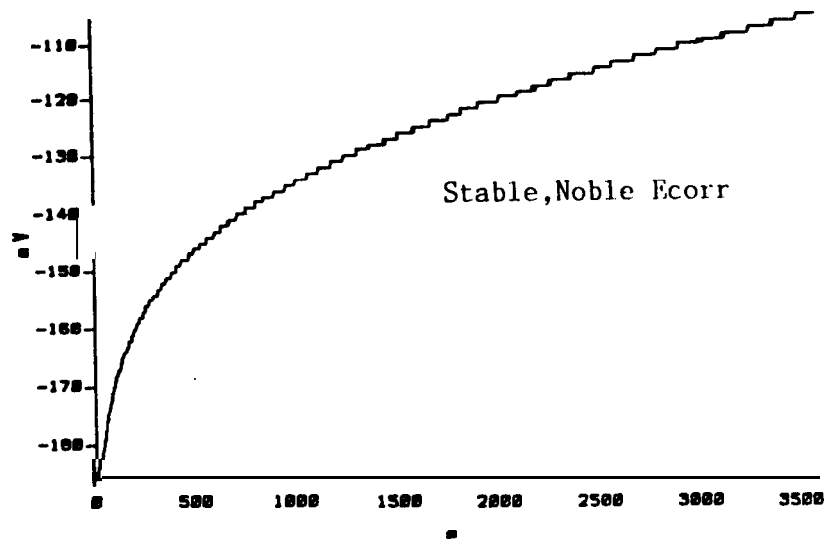


Figure A7 Hastelloy C-22 Corrosion Potential
in Aerated 3.55% NaCl + 1.0N HCl

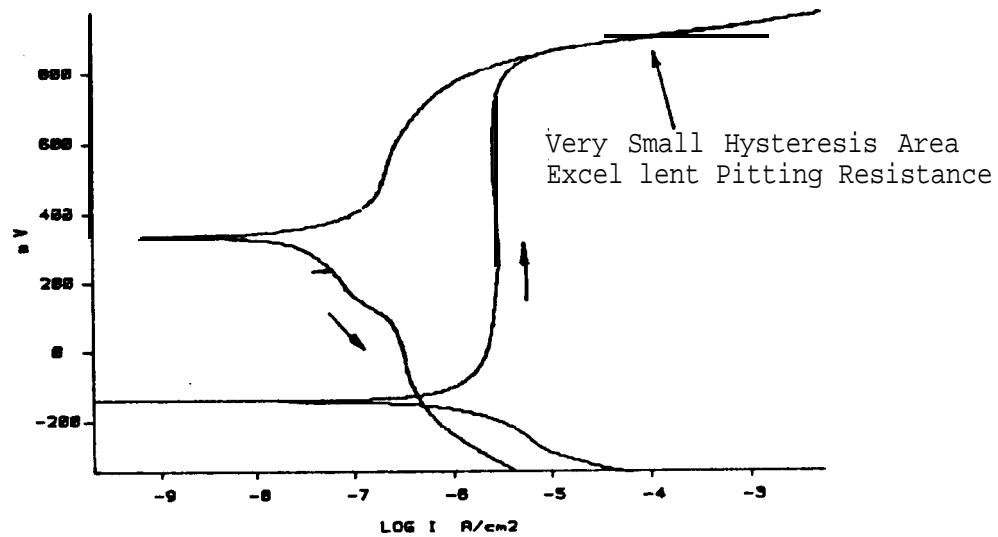


Figure A8 Hastelloy C-22 Cyclic Polarization
in Aerated 3.55% NaCl + 1.0N HCl

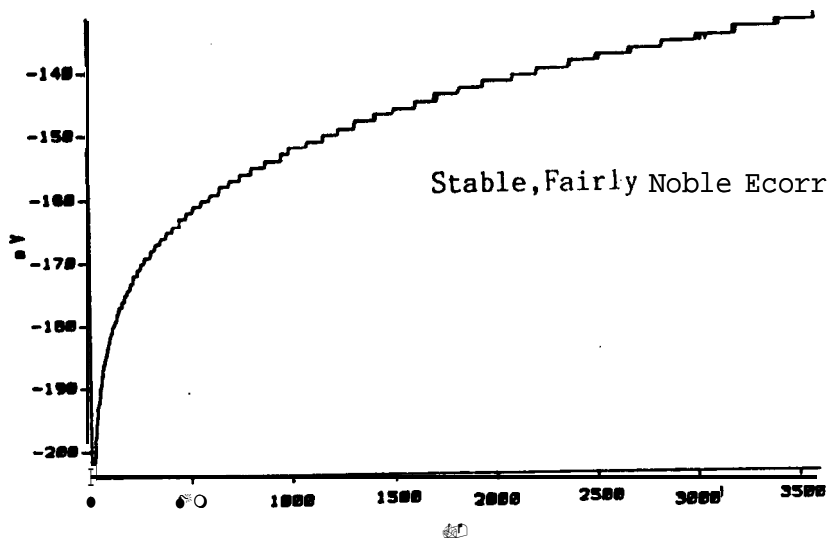


Figure A9 Hastelloy C-276 Corrosion Potential
in Aerated 3.55% NaCl + 0.1N HCl

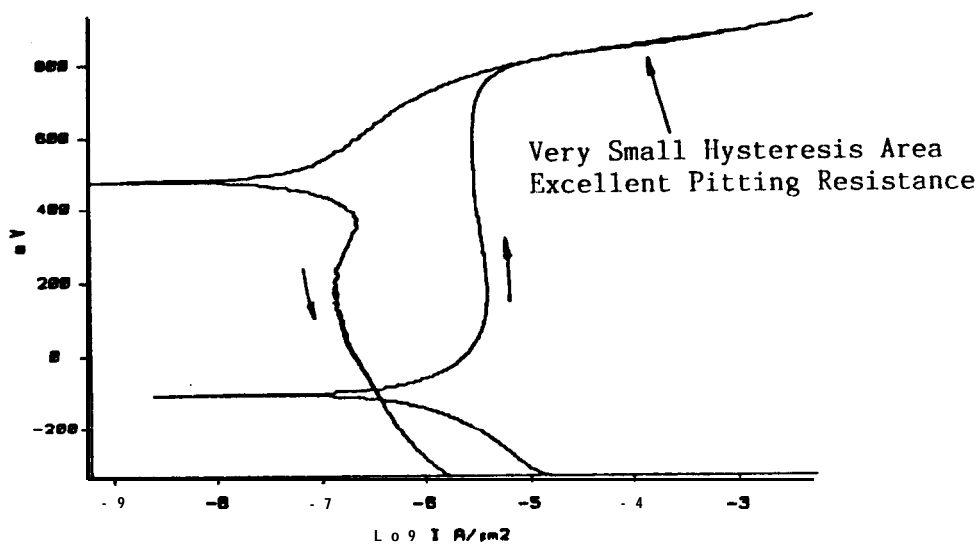


Figure A10 Hastelloy C-276 Cyclic Polarization
in Aerated 3.55% NaCl + 0.1N HCl

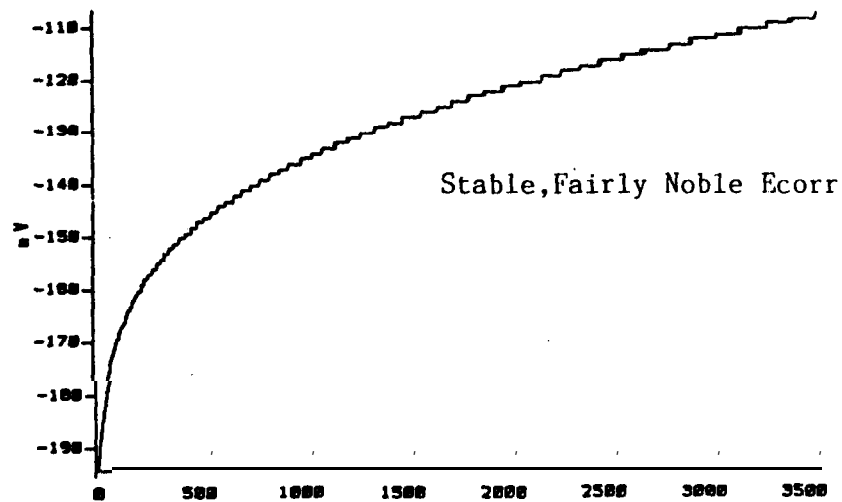


Figure A11 **Hastelloy C-276** Corrosion Potential
in Aerated 3.55% **NaCl** + 1.0N **HCl**

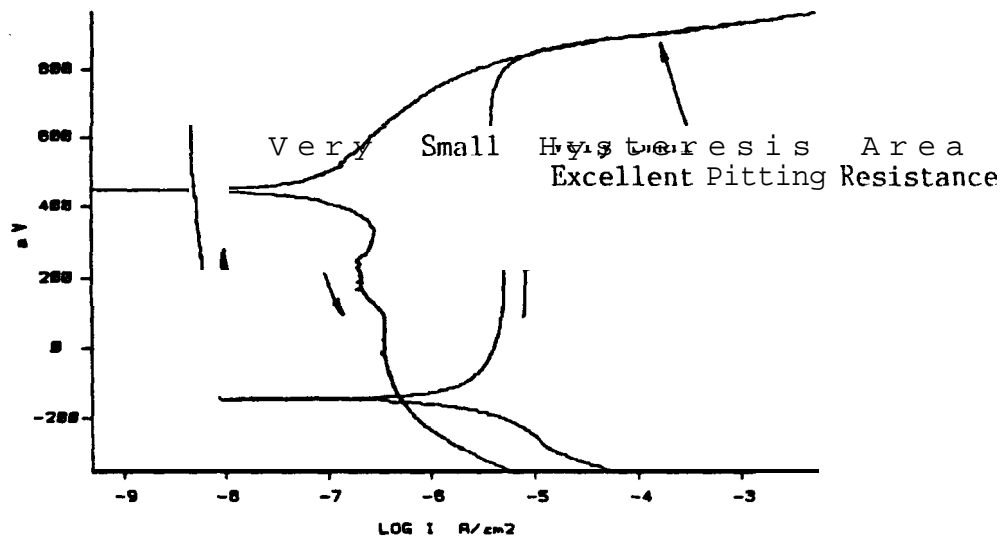


Figure A12 **Hastelloy C-276** Cyclic Polarization
in Aerated 3.55% **NaCl** + 1.0N **HCl**

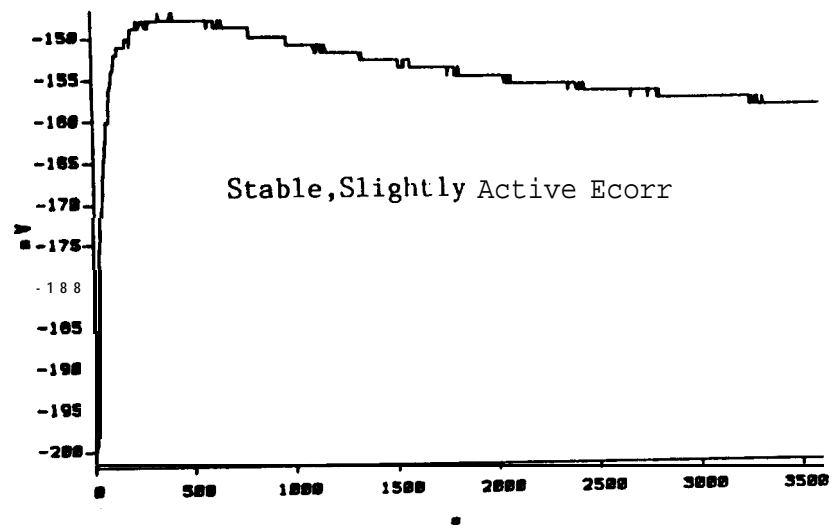


Figure A13 Hastelloy B-2 Corrosion Potential
in Aerated 3.55% NaCl + 0.1N HCl

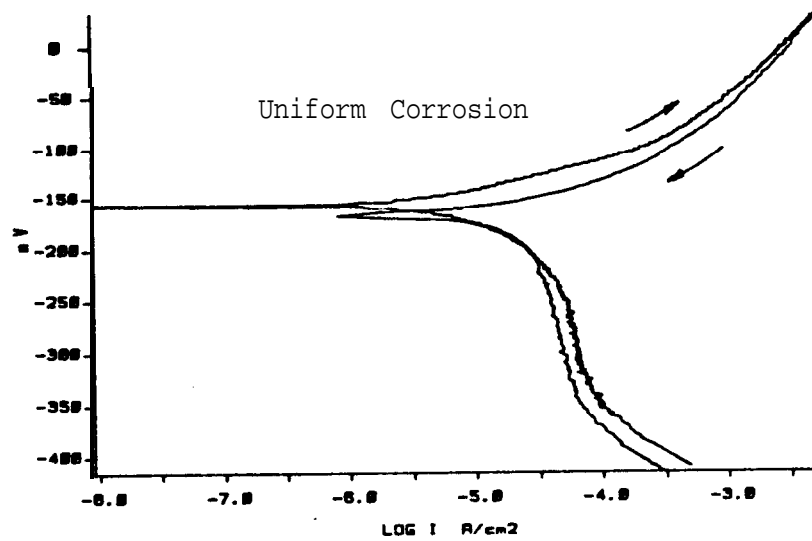


Figure A14 Hastelloy B-2 Cyclic Polarization
in Aerated 3.55% NaCl + 0.1N HCl

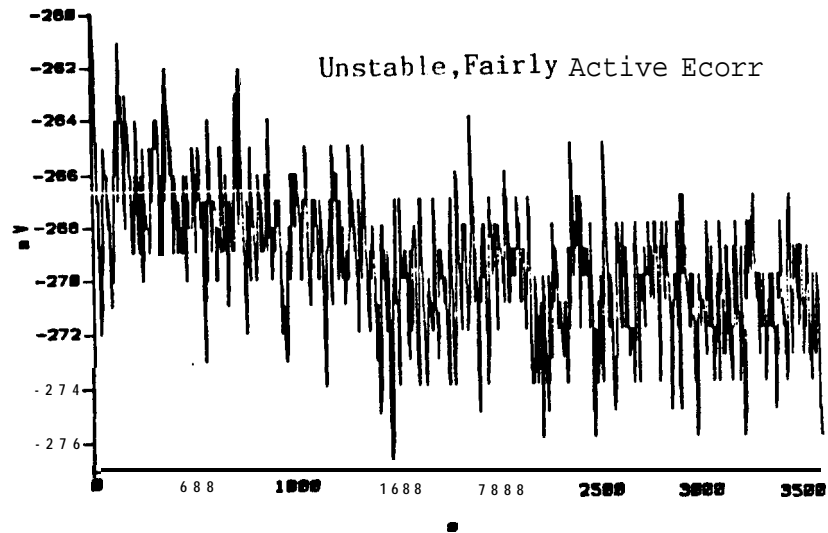


Figure A15 Inconel 600 Corrosion Potential
in Aerated 3.55% NaCl + 0.1N HCl

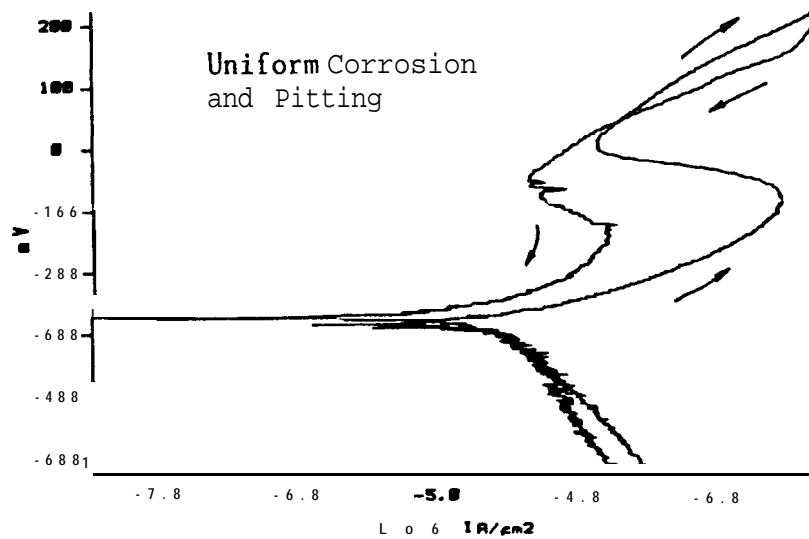


Figure A16 Inconel 600 Cyclic Polarization
in Aerated 3.55% NaCl + 0.1N HCl

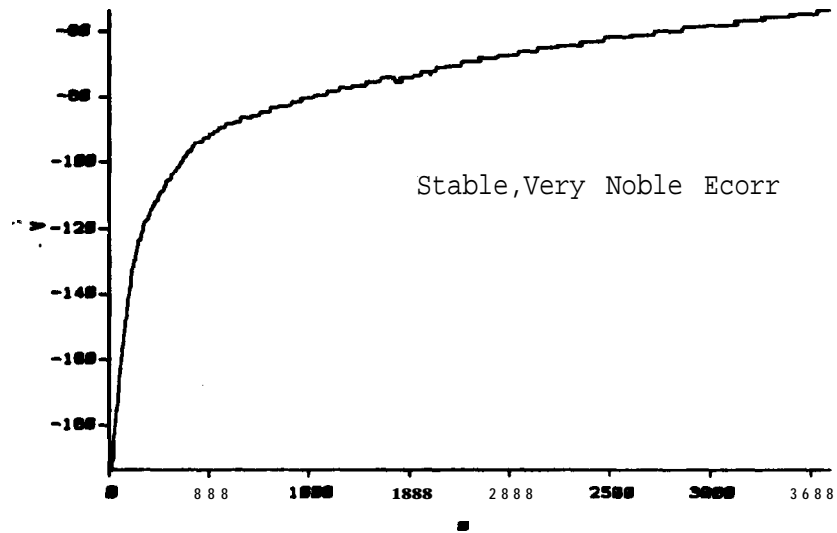


Figure A17 Inconel 625 Corrosion Potential
in Aerated 3.55% NaCl + 0.1N HCl

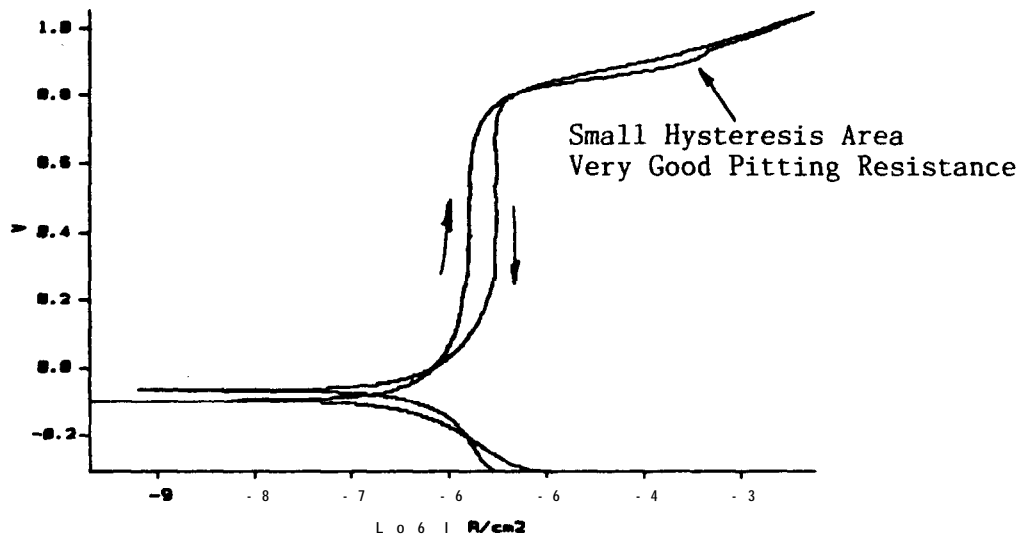


Figure A18 Inconel 625 Cyclic Polarization
in Aerated 3.55% NaCl + 0.1N HCl

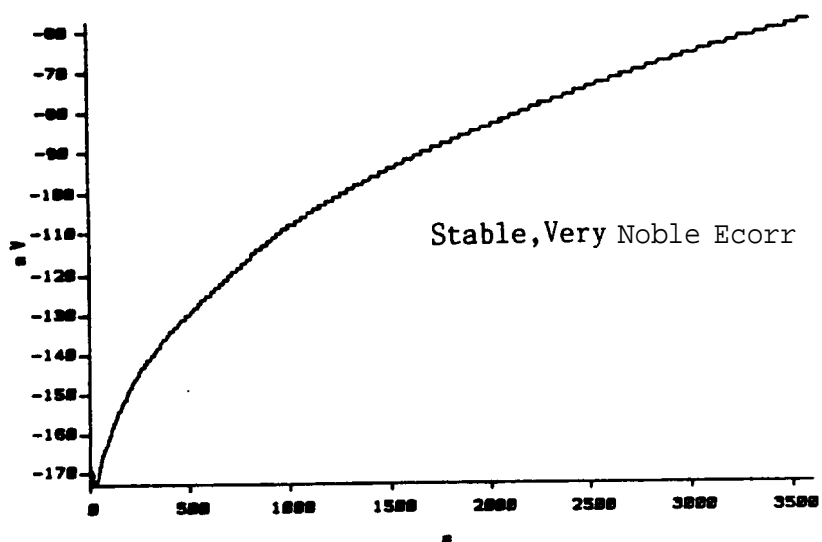


Figure A19 Inconel 625 Corrosion Potential
in Aerated 3.55% NaCl + 1.0N HCl

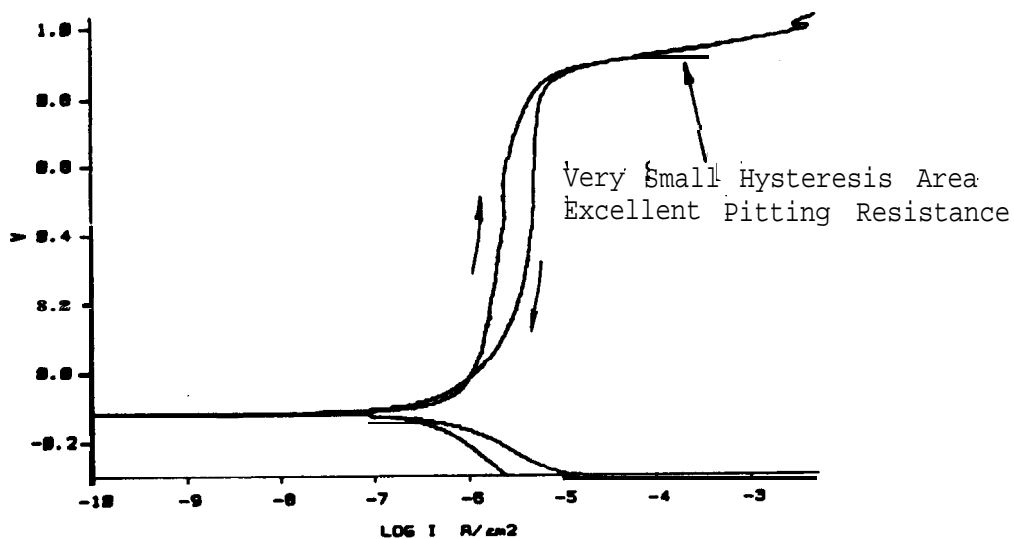


Figure A20 Inconel 625 Cyclic Polarization
in Aerated 3.55% NaCl + 1.0N HCl

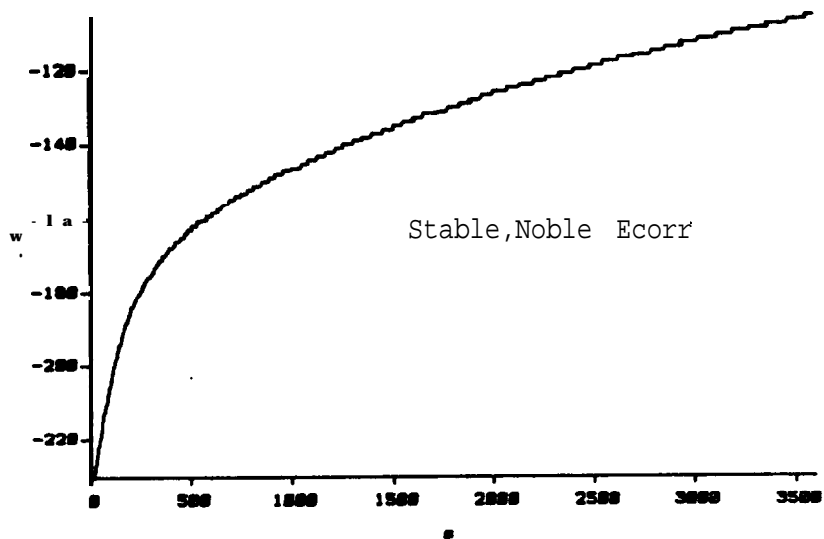


Figure A21 Inconel 825 Corrosion Potential
in Aerated 3.55% NaCl + 0.1N HCl

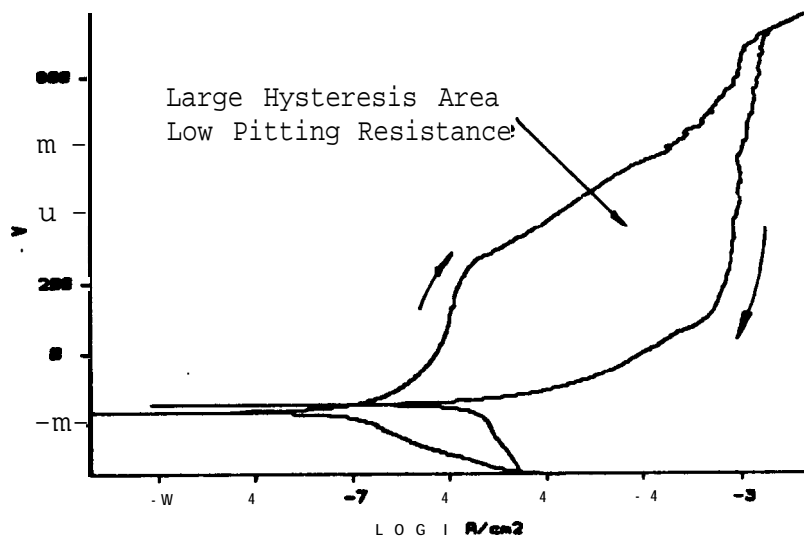


Figure A22 Inconel 825 Cyclic Polarization
in Aerated 3.55% NaCl + 0.1N HCl

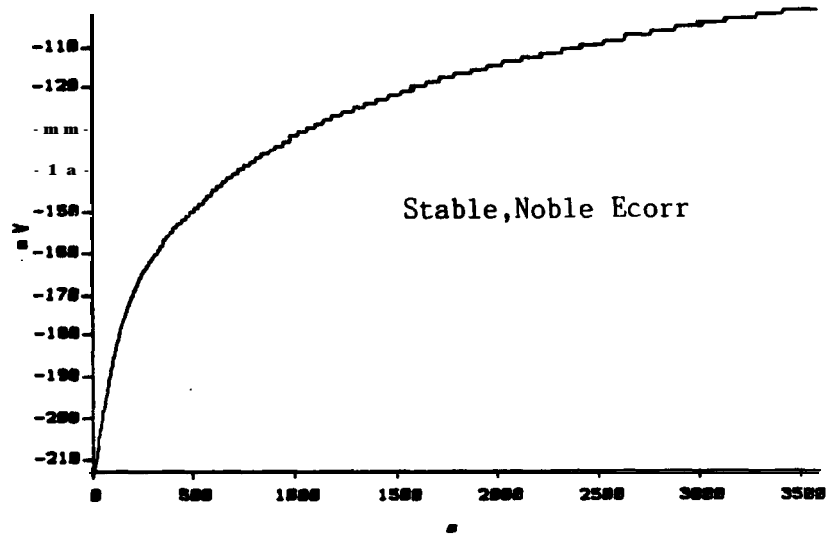


Figure A23 Inco G-3 Corrosion Potential
in Aerated 3.55% NaCl + 0.1N HCl

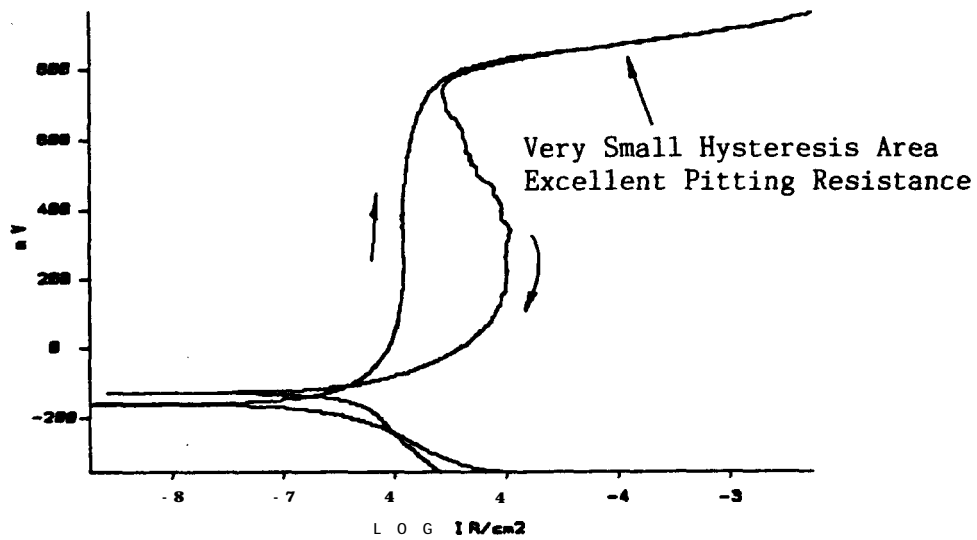


Figure A24 Inco G-3 Cyclic Polarization
in Aerated 3.55% NaCl + 0.1N HCl

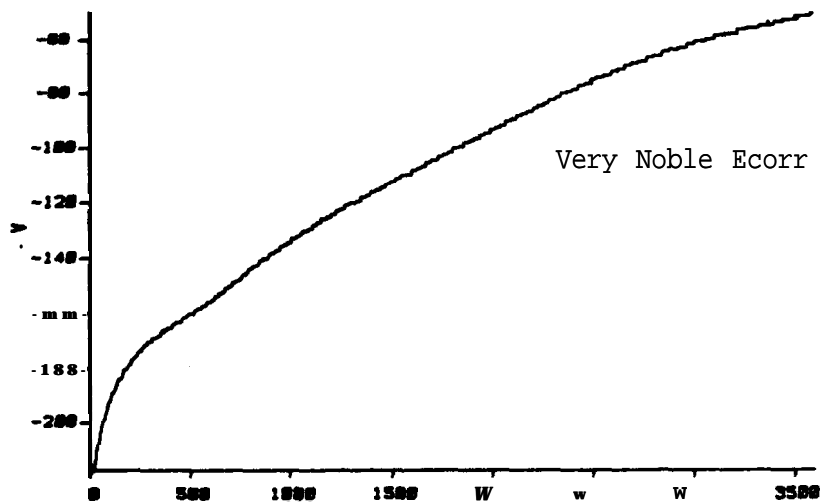


Figure A25 Inco G-3 Corrosion Potential
in Aerated 3.55% NaCl + 1.0N HCl

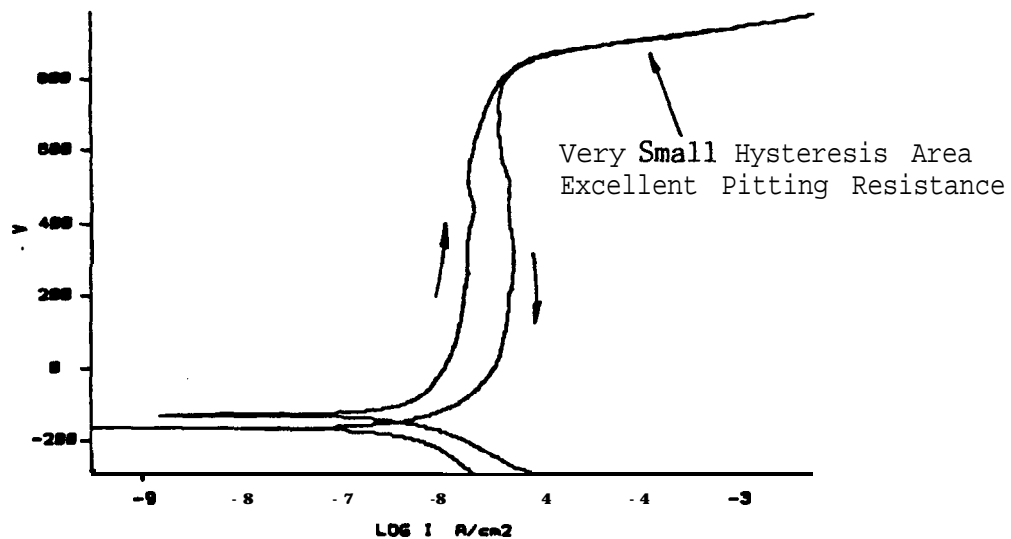


Figure A26 Inco G-3 Cyclic Polarization
in Aerated 3.55% NaCl + 1.0N HCl

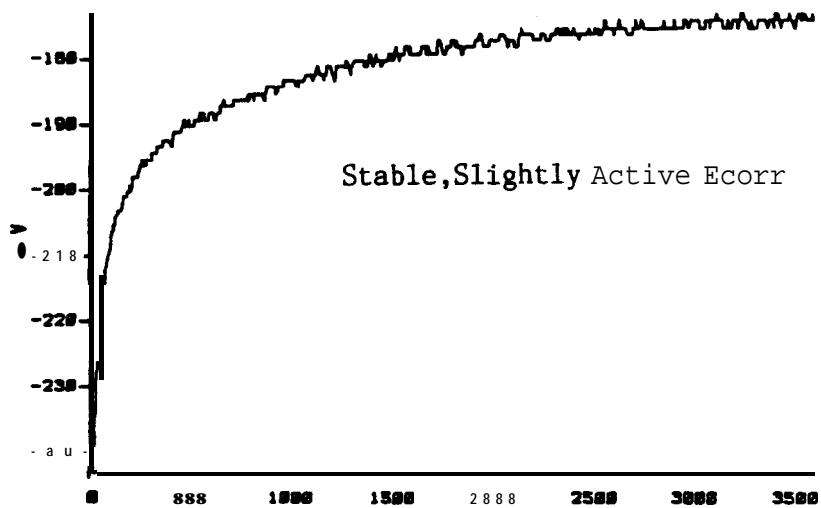


Figure A27 Monel 400 Corrosion Potential
in Aerated 3.55% NaCl + 0.1N HCl

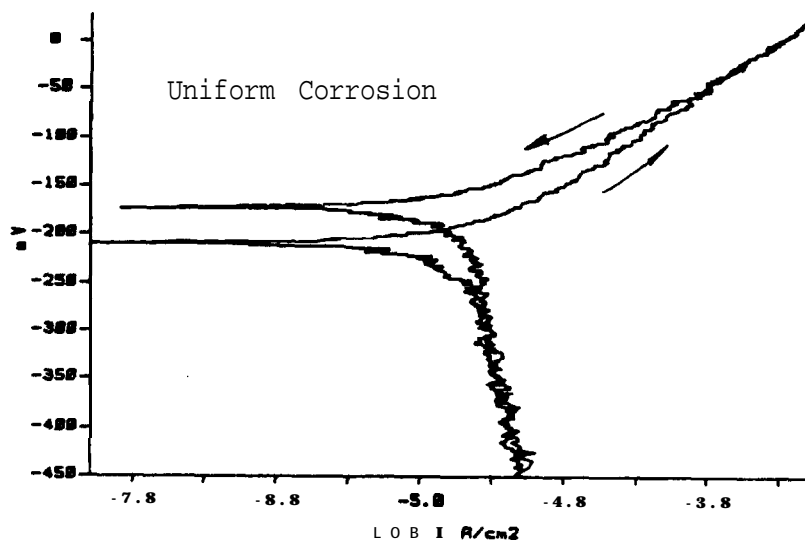


Figure A28 Monel 400 Cyclic Polarization
in Aerated 3.55% NaCl + 0.1N HCl

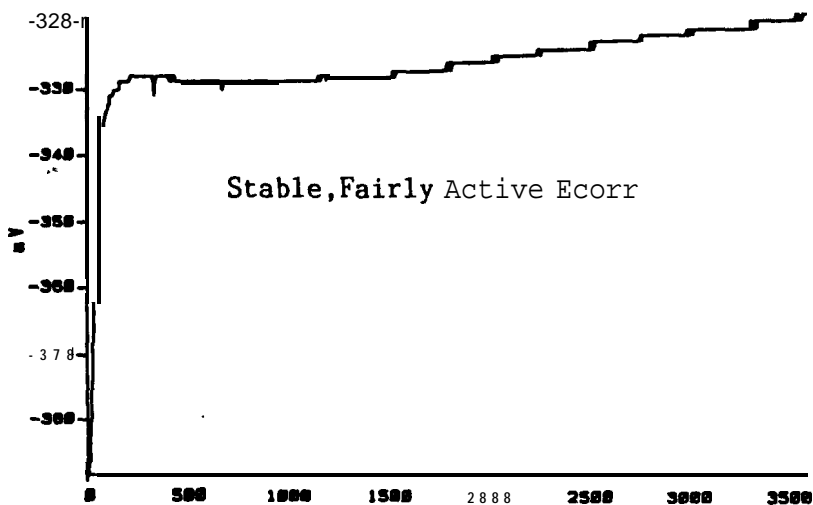


Figure A29 Zirconium 702 Corrosion Potential
in Aerated 3.55% NaCl + 0.1N HCl

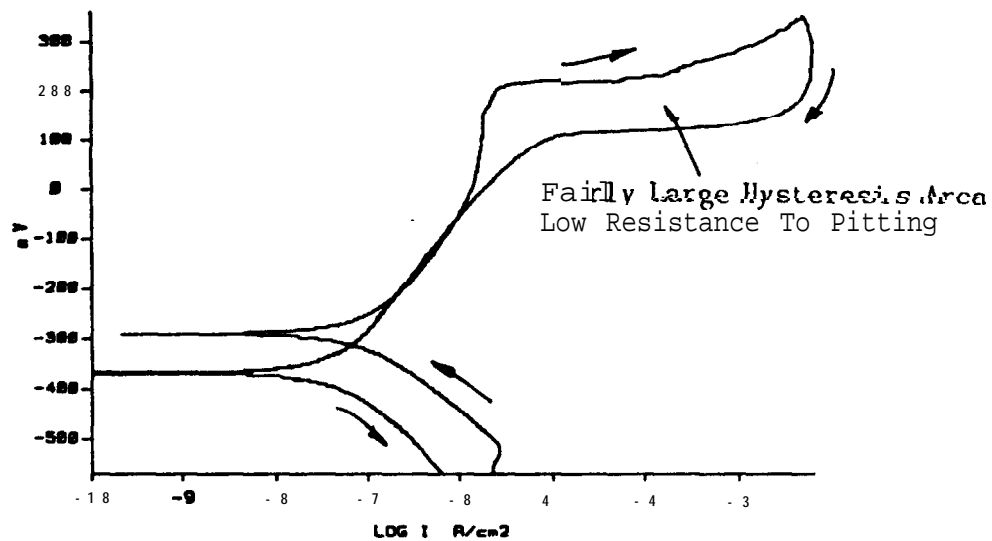


Figure A30 Zirconium 702 Cyclic Polarization
in Aerated 3.55% NaCl + 0.1N HCl

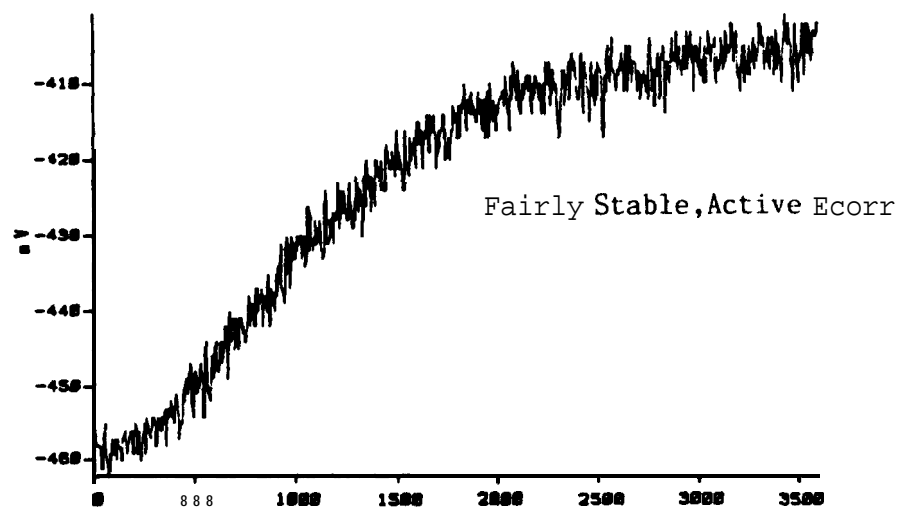


Figure A31 304L Corrosion Potential
in Aerated 3.55% NaCl + 0.1N HCl

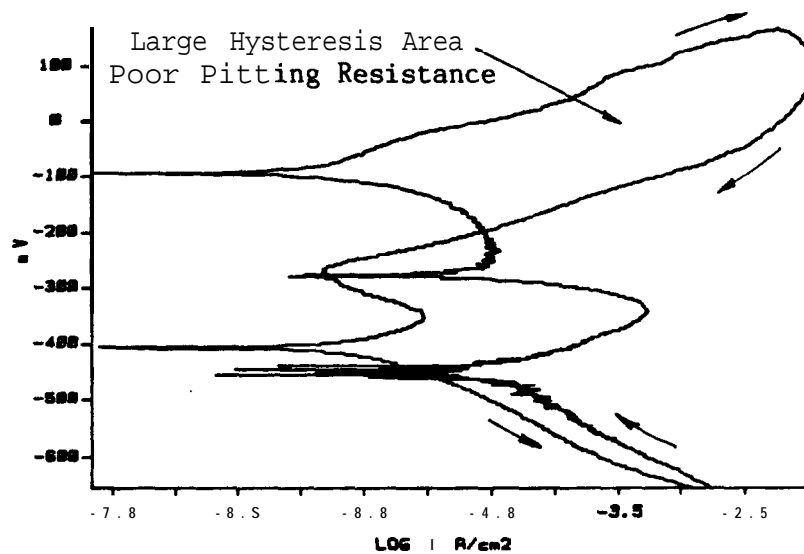


Figure A32 304L Cyclic Polarization
in Aerated 3.55% NaCl + 0.1N HCl

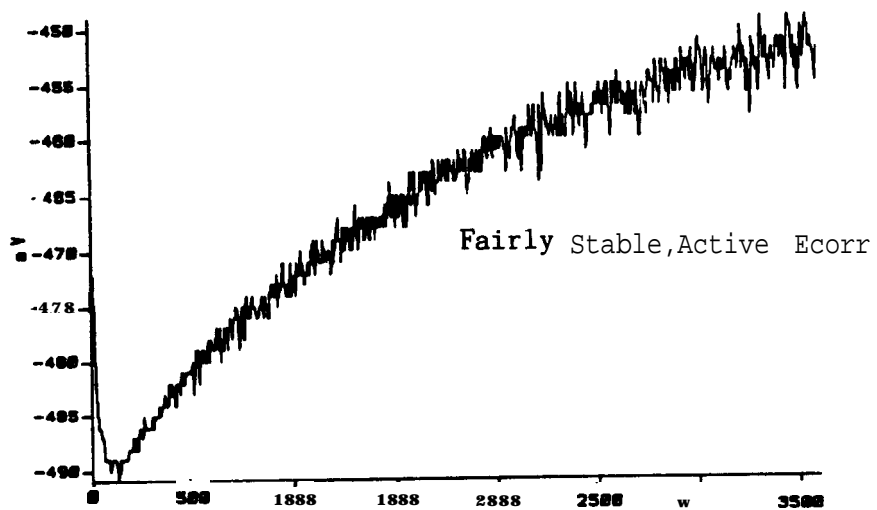


Figure A33 304L Corrosion Potential
in Aerated 3.55% NaCl + 1.0N HCl

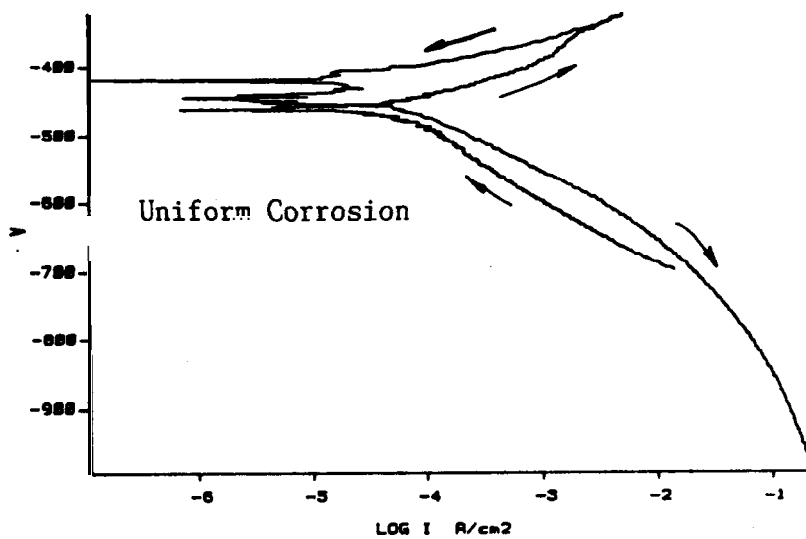


Figure A34 304L Cyclic Polarization
in Aerated 3.55% NaCl + 1.0N HCl

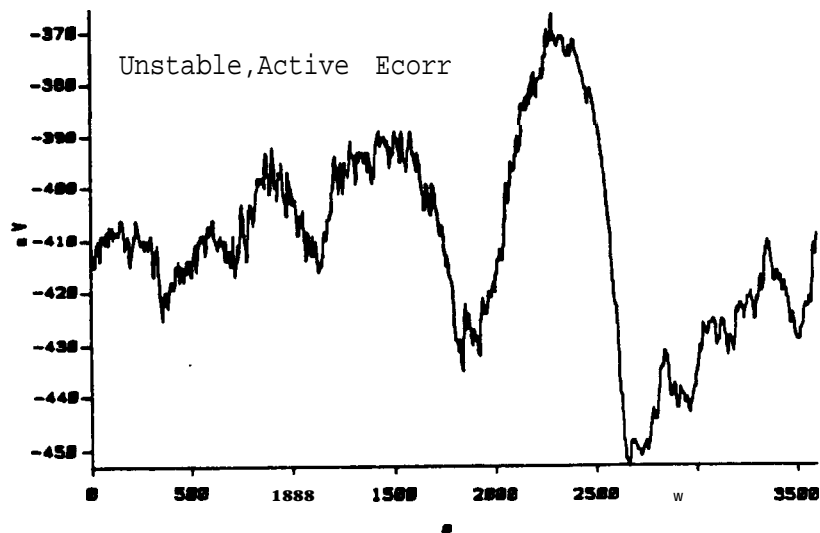


Figure A35 304LN Corrosion Potential
in Aerated 3.55% NaCl + 0.1N HCl

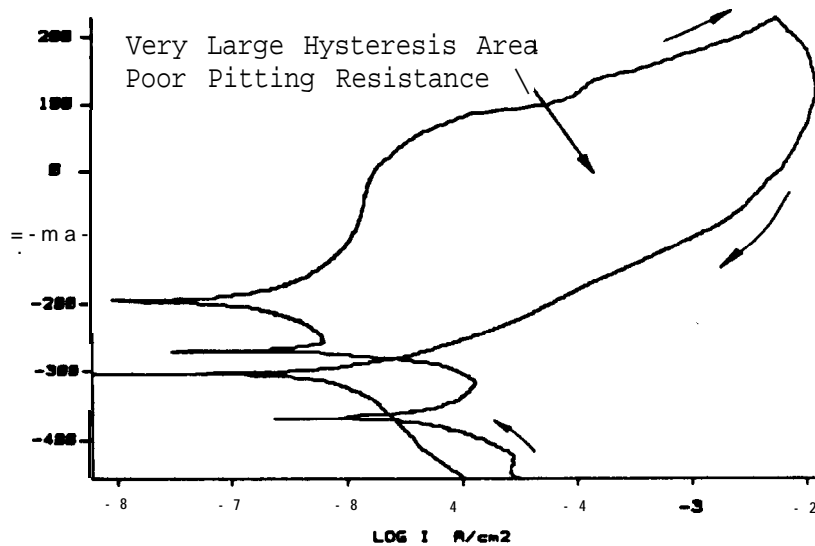


Figure A36 304LN Cyclic Polarization
in Aerated 3.55% NaCl + 0.1N HCl

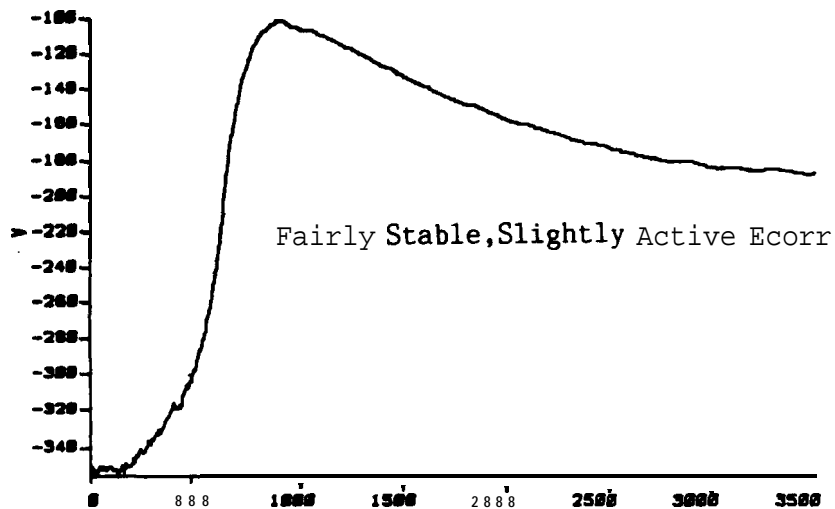


Figure A37 316L Corrosion Potential
in Aerated 3,553 NaCl + 0.1N HCl

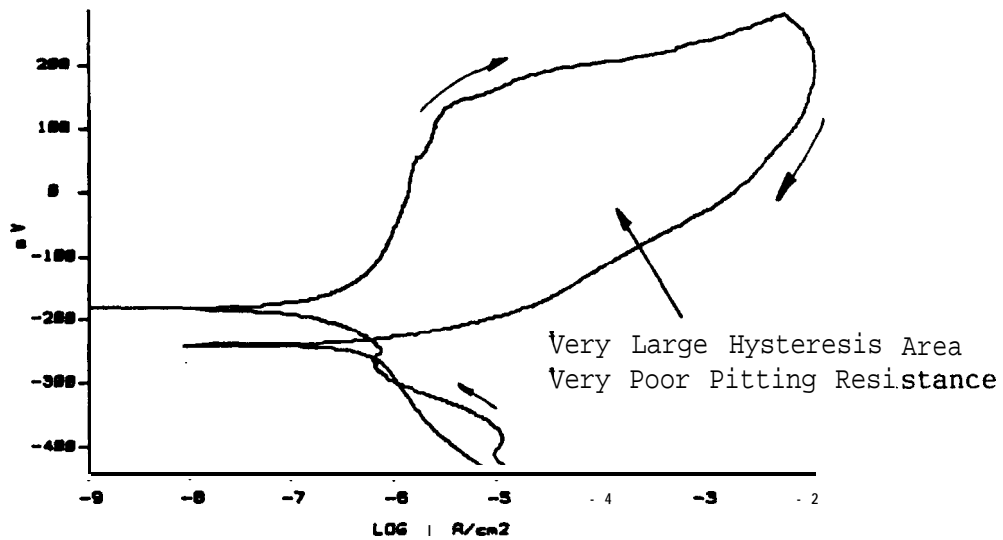


Figure A38 316L Cyclic Polarization
in Aerated 3.55% NaCl + 0.1N HCl

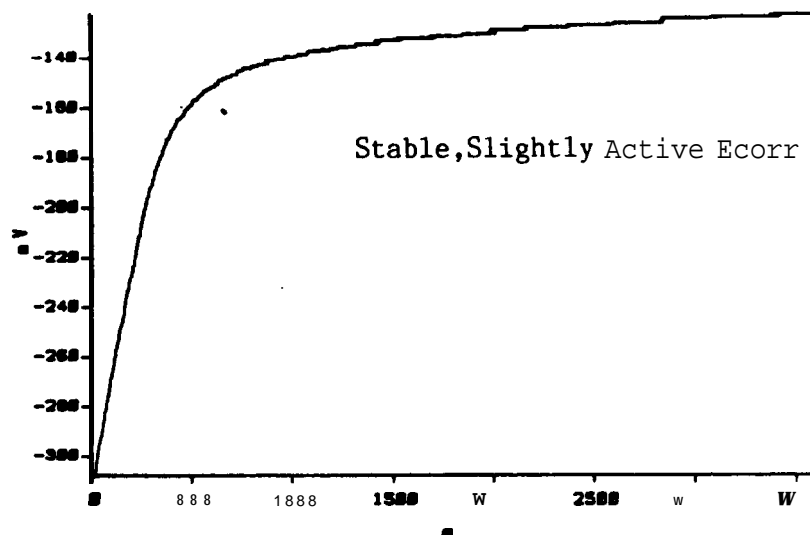


Figure A39 317L Corrosion Potential
in Aerated 3.55% NaCl ± 0.1N HCl

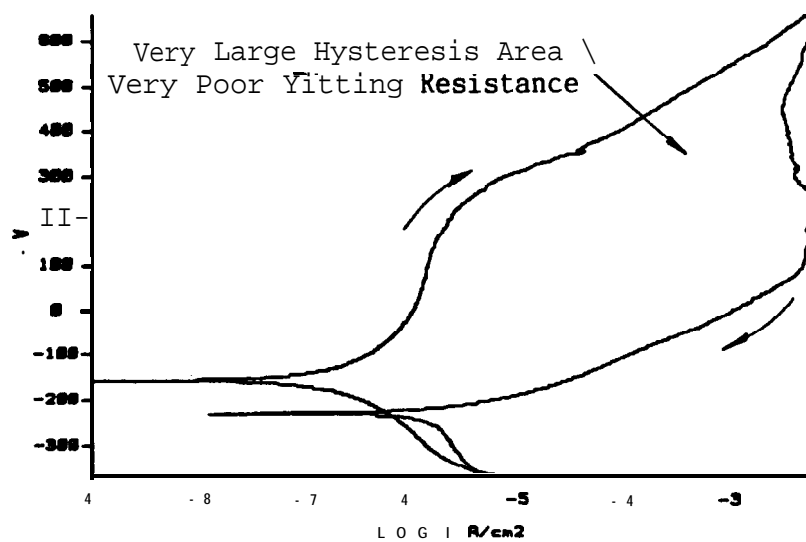


Figure A40 317L Cyclic Polarization
in Aerated 3.55% NaCl ± 0.1N HCl

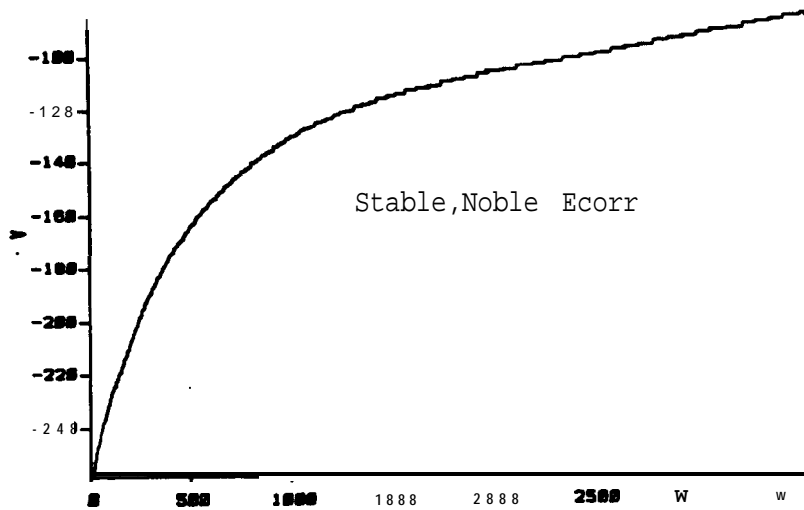


Figure A41 904L Corrosion Potential
in Aerated 3.55% NaCl + 0.1N HCl

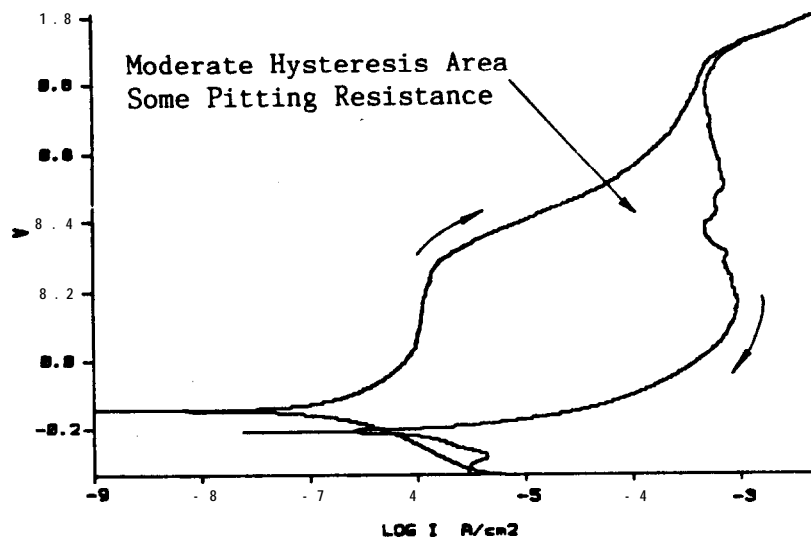


Figure A42 904L Cyclic Polarization
in Aerated 3.55% NaCl + 0.1N HCl

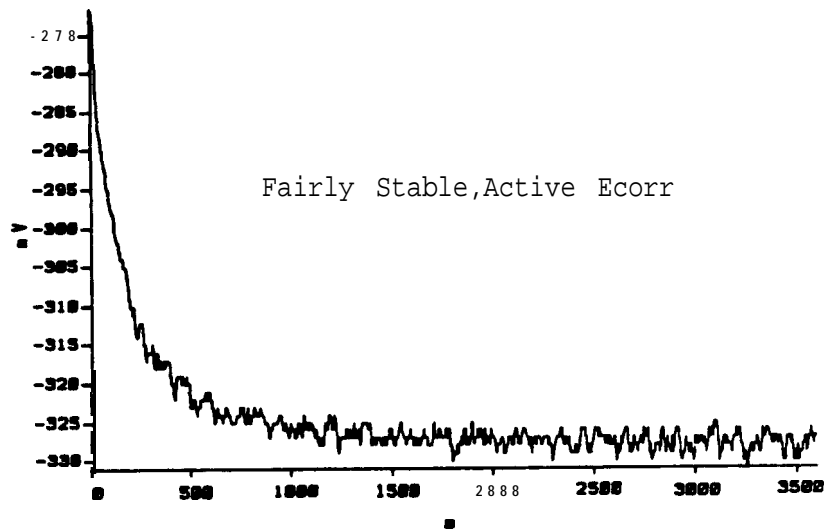


Figure A43 904L Corrosion Potential
in Aerated 3.55% NaCl + 1.0N HCl

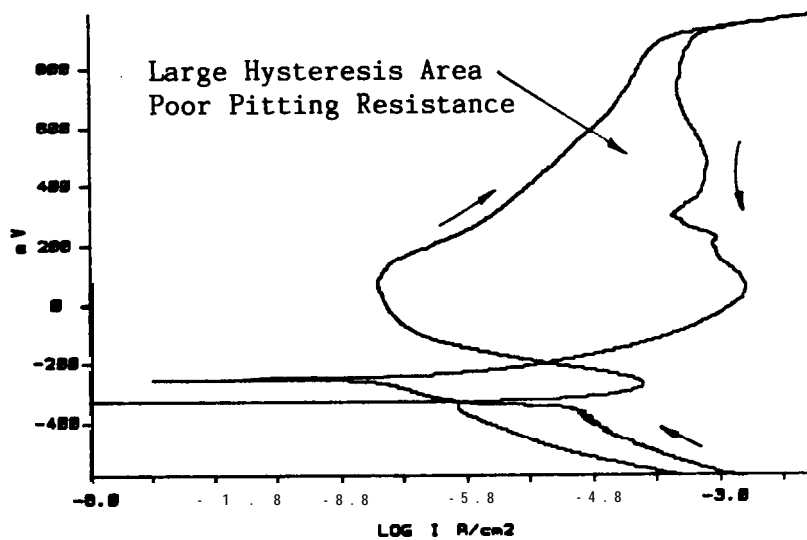


Figure A44 904L Cyclic Polarization
in Aerated 3.55% NaCl + 1.0N HCl

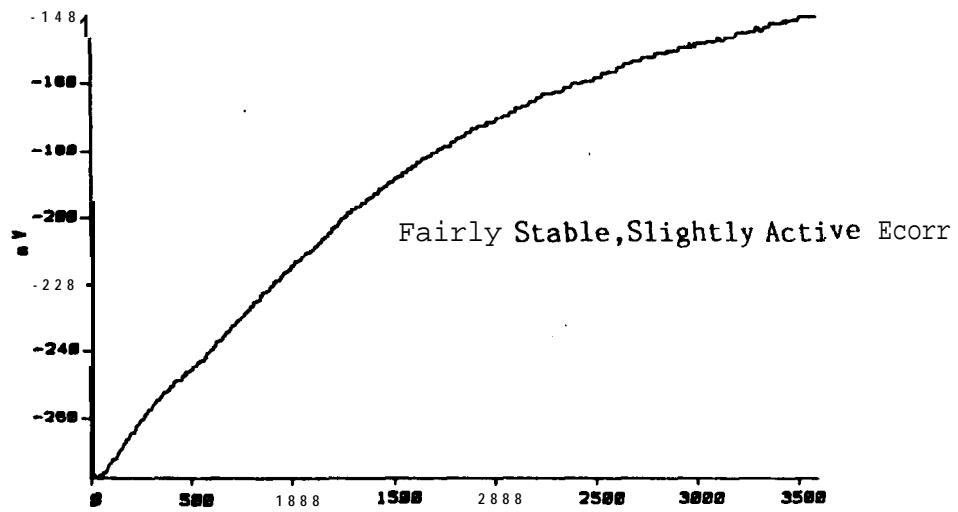


Figure A45 20 Cb-3 Corrosion Potential
in Aerated 3.55% NaCl + 0.1N HCl

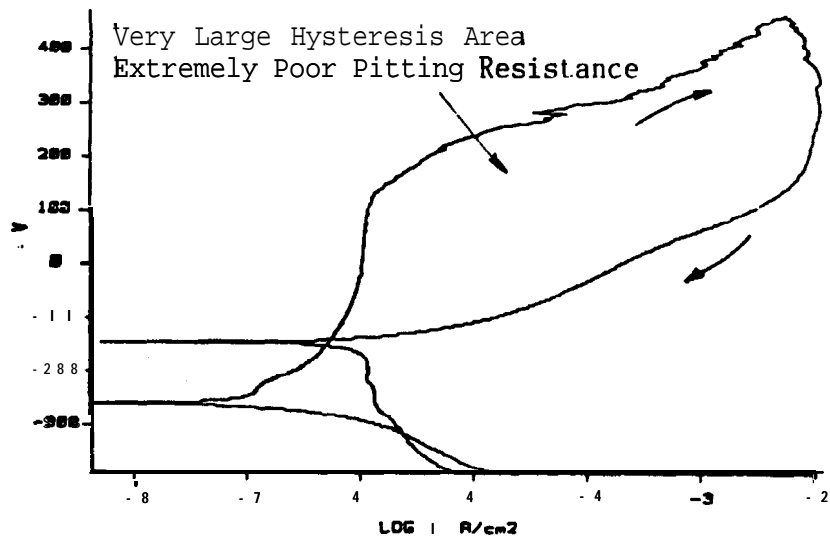


Figure A46 20 Cb-3 Cyclic Polarization
in Aerated 3.55% NaCl + 0.1N HCl

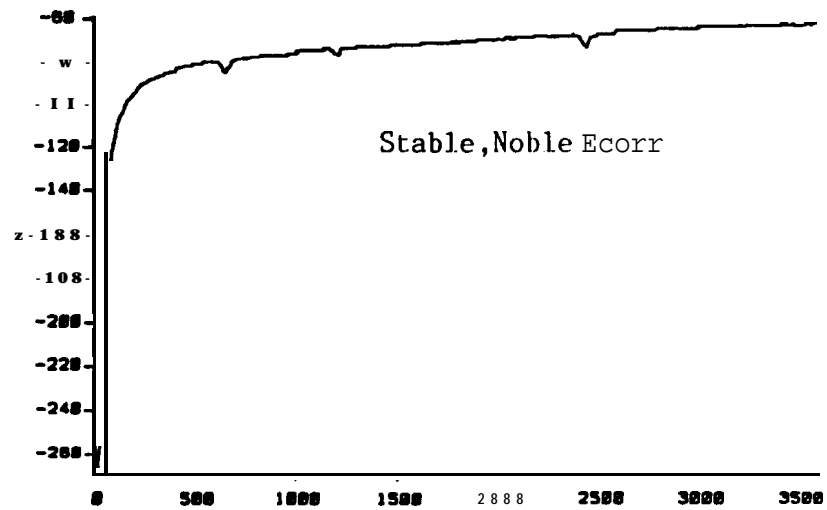


Figure A47 7MotN Corrosion Potential
in Aerated 3.55% NaCl + 0.1N HCl

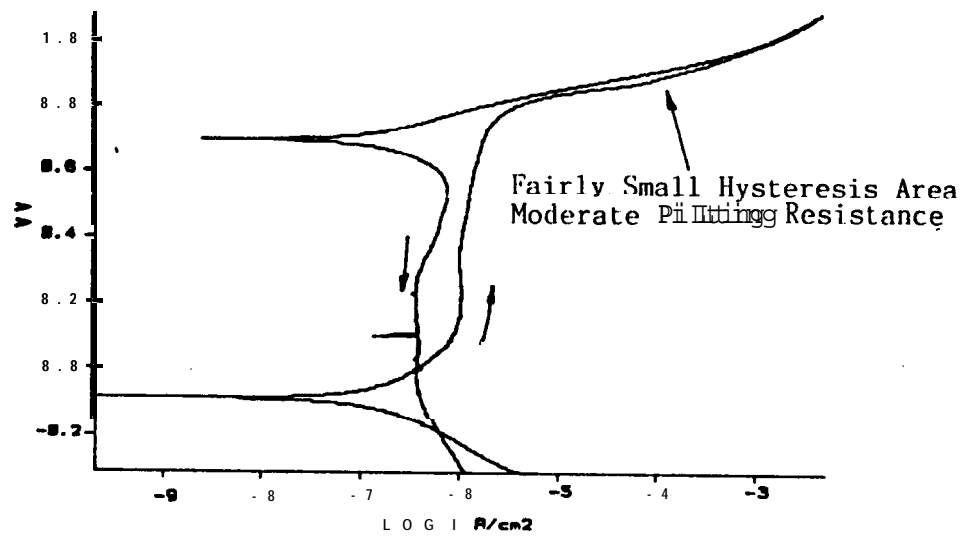


Figure A48 7MotN Cyclic Polarization
in Aerated 3.55% NaCl + 0.1N HCl

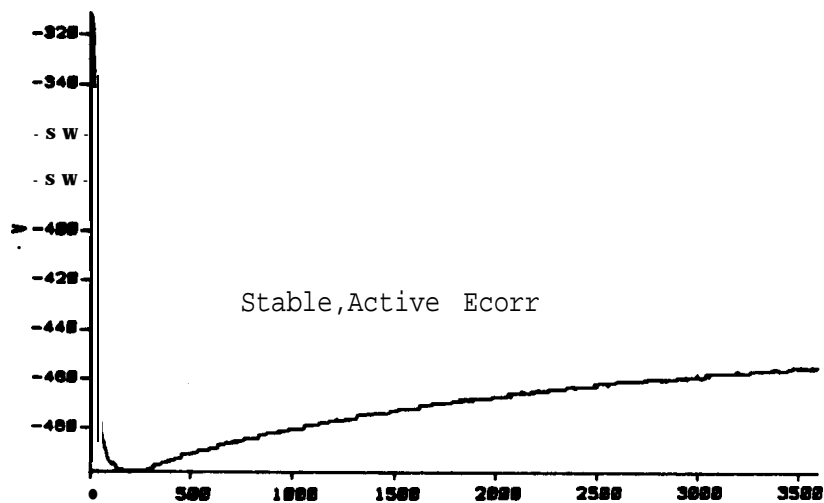


Figure A49 7MotN Corrosion Potential
in Aerated 3.55% NaCl + 1.0N HCl

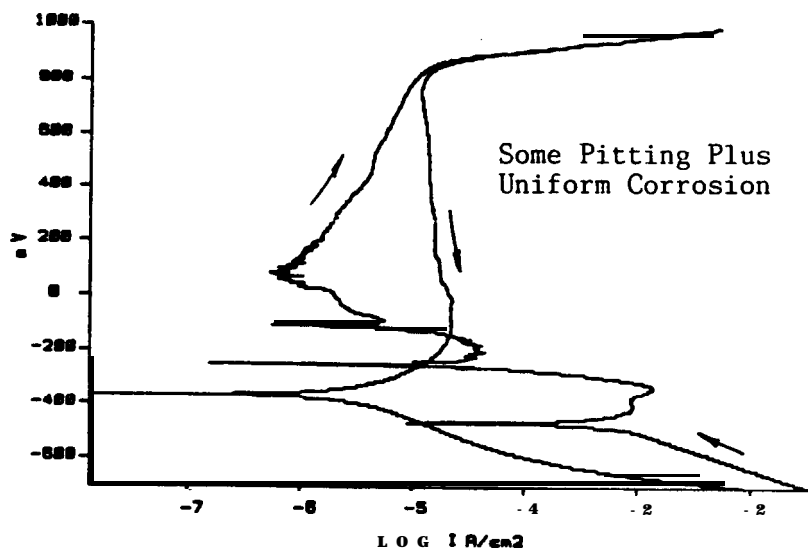


Figure A50 7MotN Cyclic Polarization
in Aerated 3.55% NaCl + 1.0N HCl

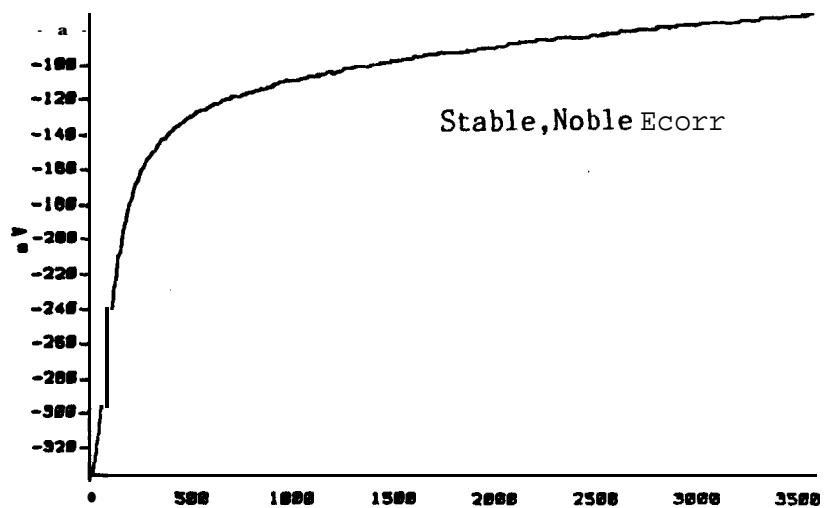


Figure A51 ES 2205 Corrosion Potential
in Aerated 3.55% NaCl + 0.1N HCl

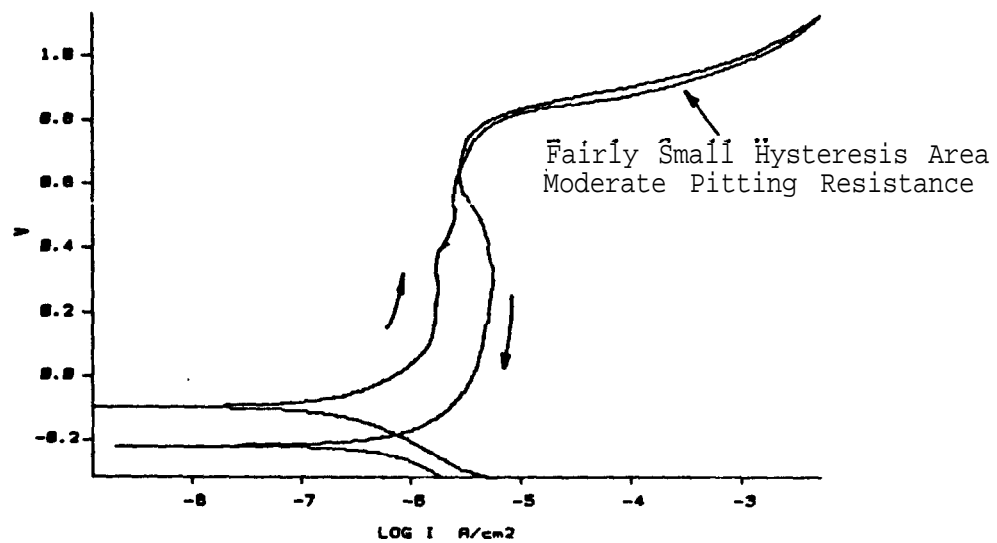


Figure A52 ES 2205 Cyclic Polarization
in Aerated 3.55% NaCl + 0.1N HCl

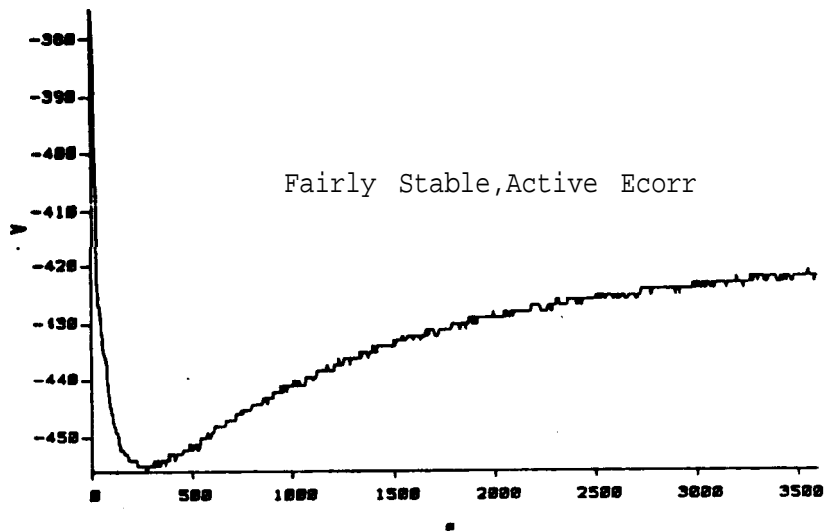


Figure A53 ES 2205 Corrosion Potential
in Aerated 3.55% NaCl + 1.0N HCl

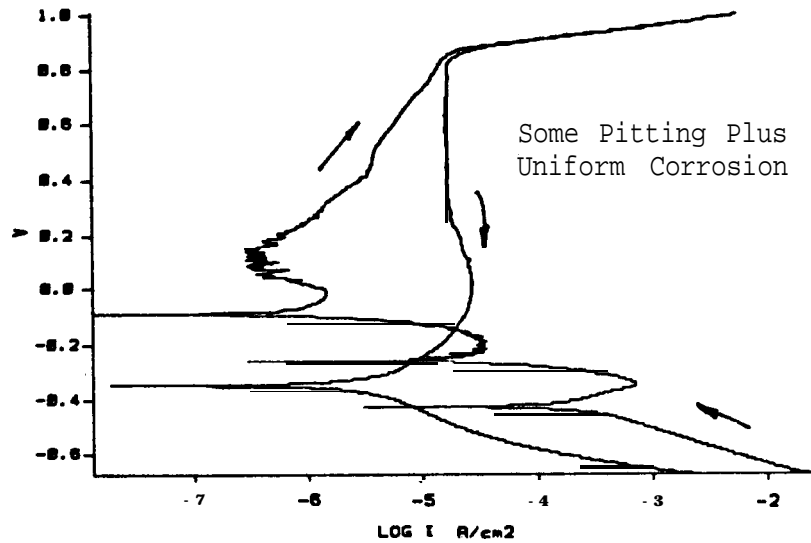


Figure A54 ES 2205 Cyclic Polarization
in Aerated 3.55% NaCl + 1.0N HCl

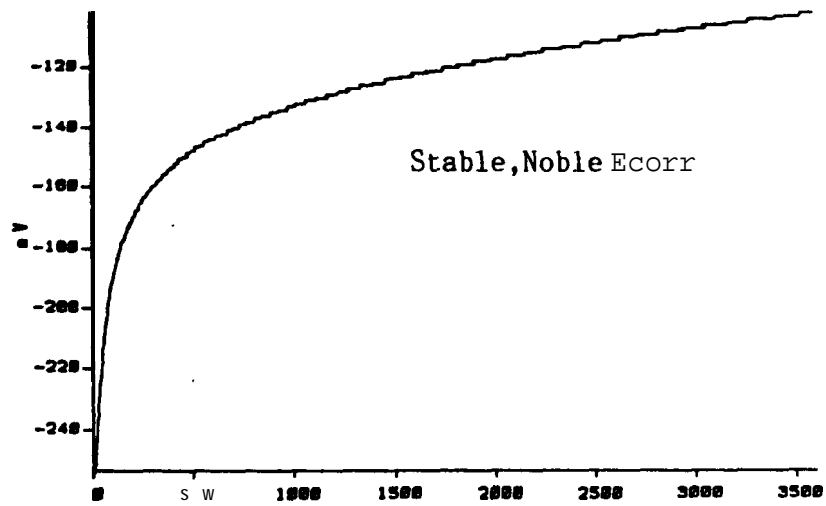


Figure A55 Ferralium 255 Corrosion Potential
in Aerated 3.55% NaCl + 0.1N HCl

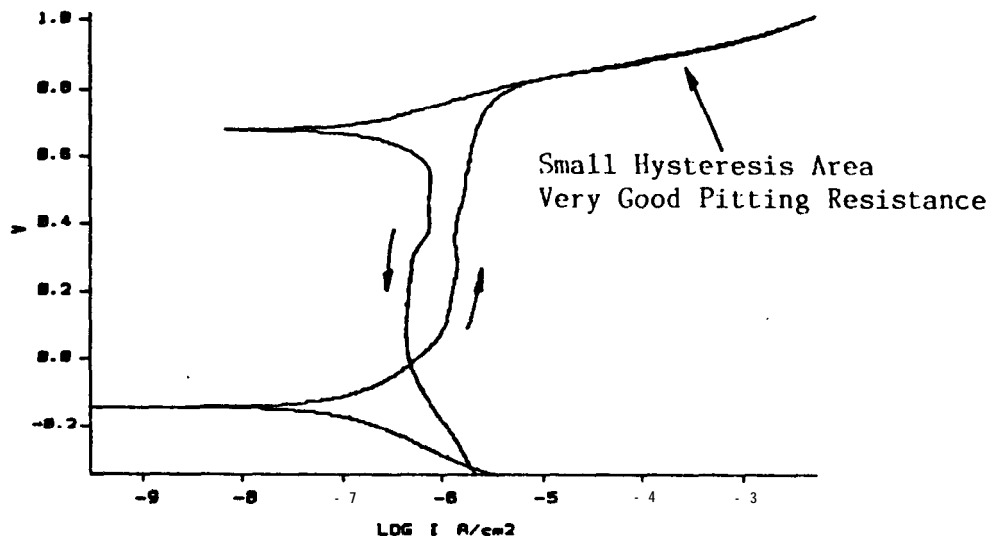


Figure A56 Ferralium 255 Cyclic Polarization
in Aerated 3.55% NaCl + 0.1N HCl

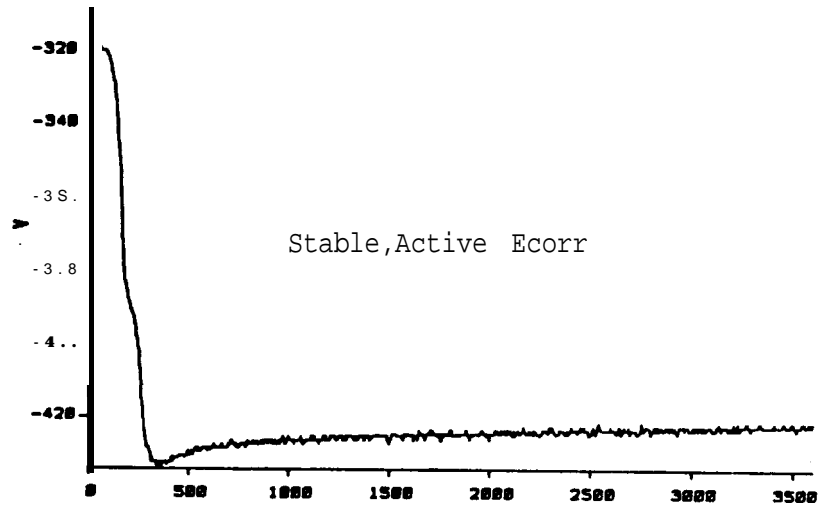


Figure A57 Ferralium 255 Corrosion Potential
in Aerated 3.55% NaCl + 1.0N HCl

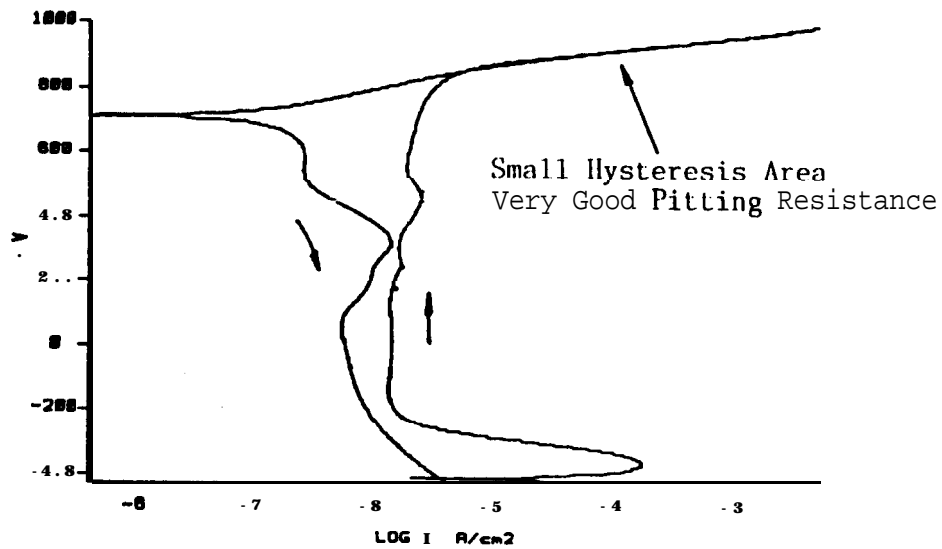
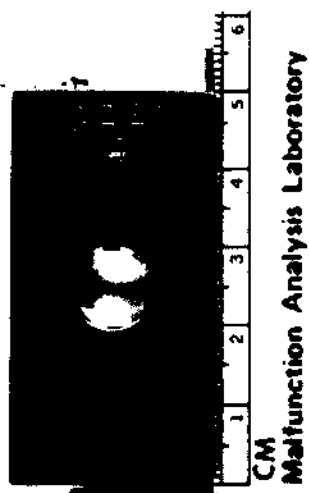
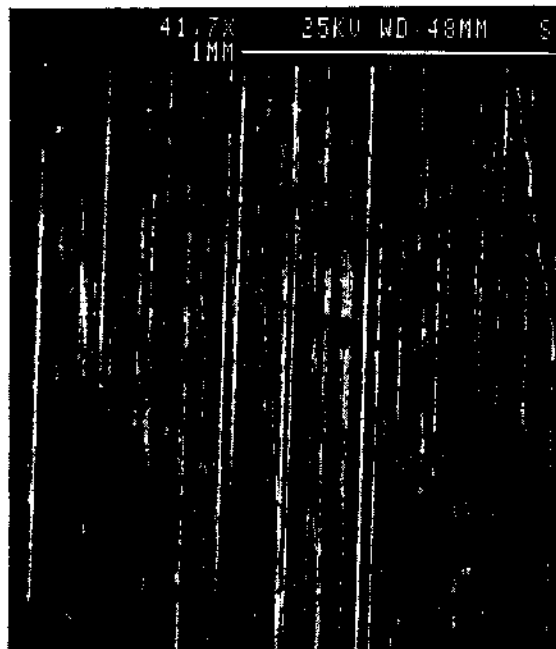


Figure A58 Ferralium 255 Cyclic Polarization
in Aerated 3.55% NaCl + 1.0N HCl

APPENDIX B
Salt Fog and Beach Exposure
Sample Photos



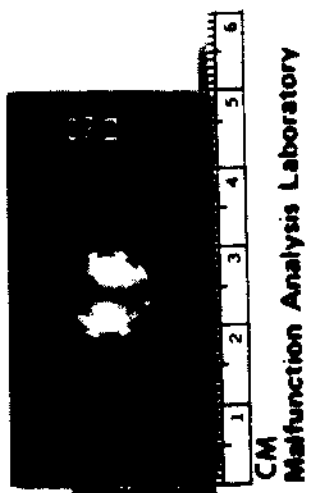
1x



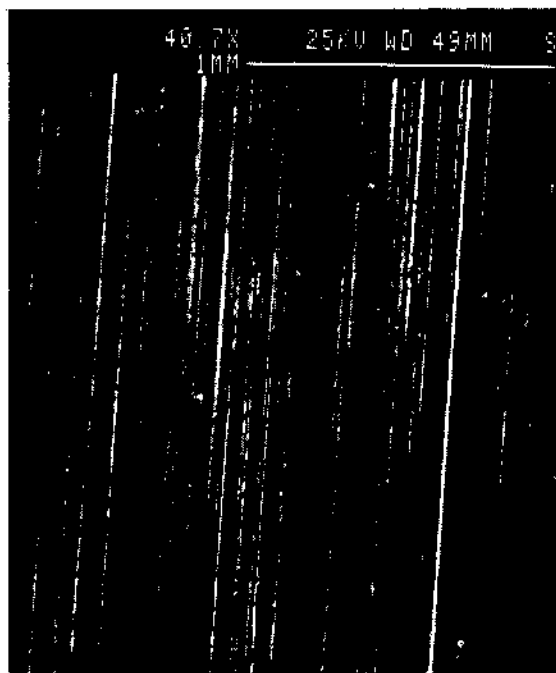
41.7x

Figure B1

Hastelloy C-22 After 20-Week Salt Fog Exposure and 20 Acid Dips



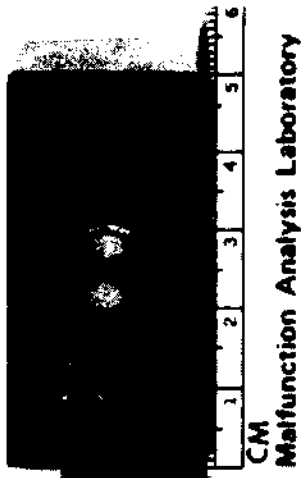
1x



40.7x

Figure B2

Hastelloy C-22 After 251-Day Beach Exposure and 13 Acid Sprays



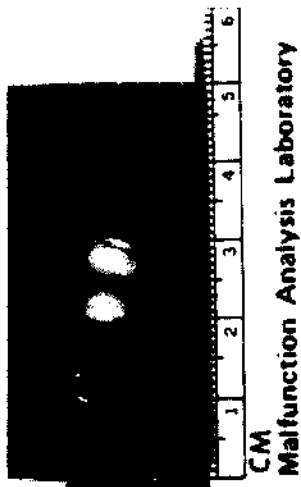
1x

Figure B3



40.7x

304L After 20-Week Salt Fog Exposure and 20 Acid Dips



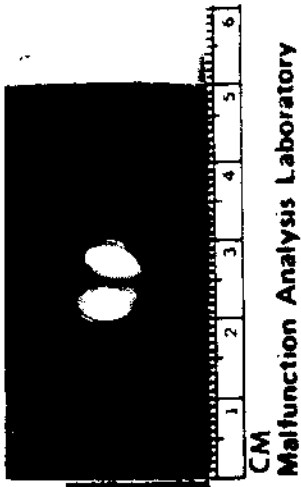
1x

Figure B4



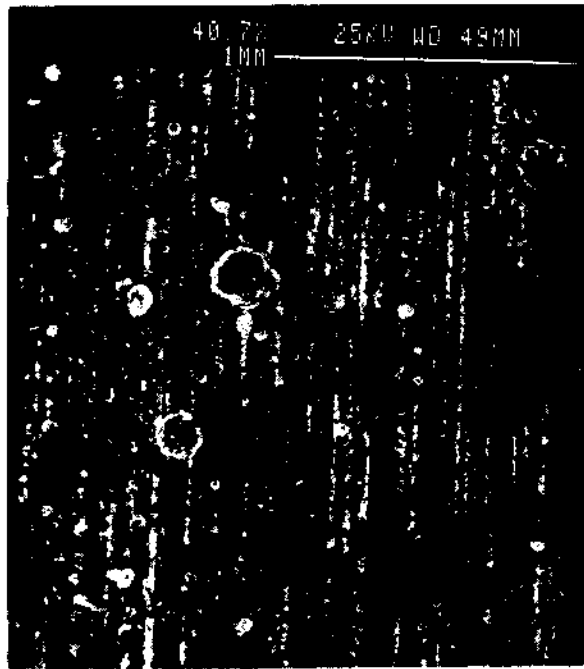
38.3x

304L After 251-Day Beach Exposure and 13 Acid Sprays



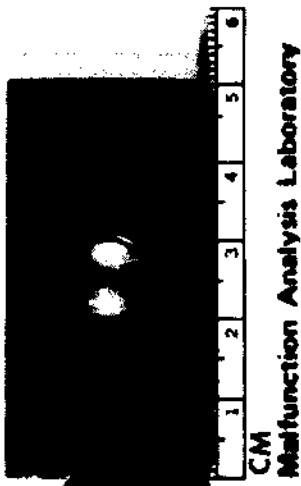
1x

Figure B5



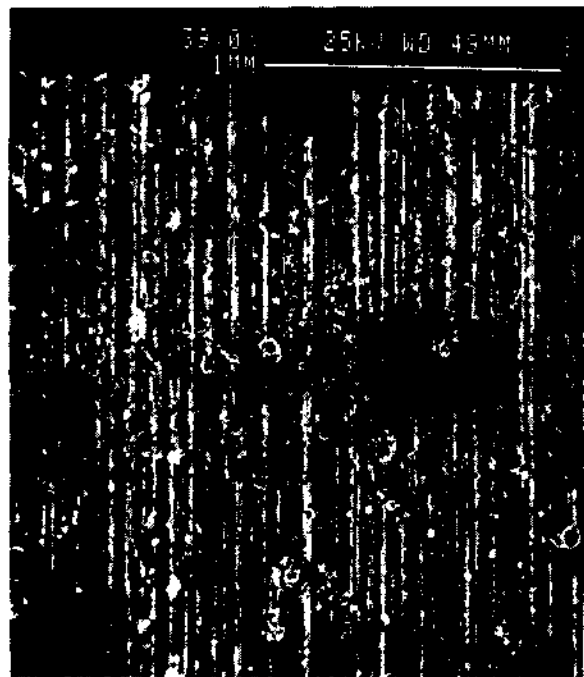
40.7x

316L After 20-Week Salt Fog Exposure and 20 Acid Dips



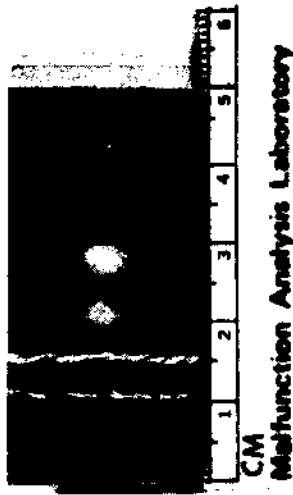
1x

Figure B6



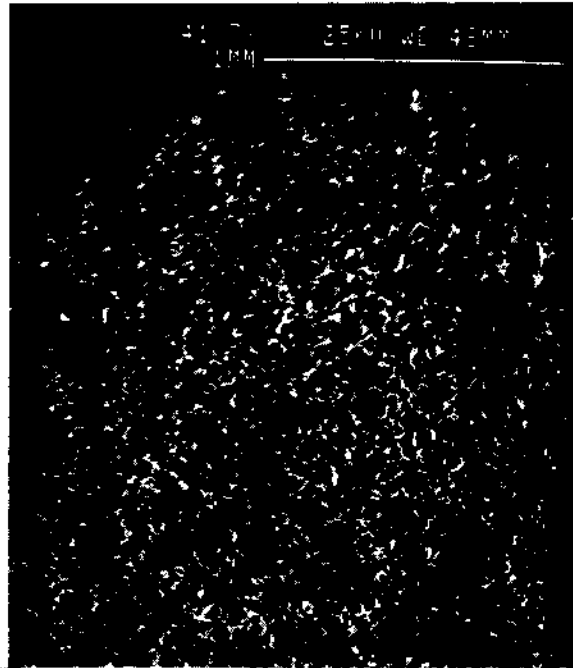
39.0x

316L After 251-Day Beach Exposure and 13 Acid Sprays



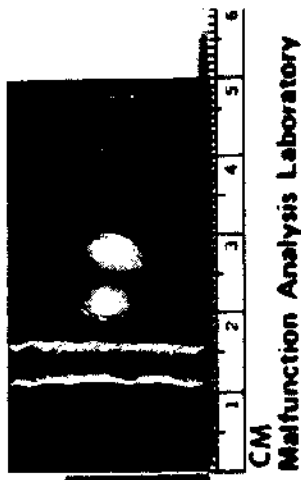
1x

Figure B7



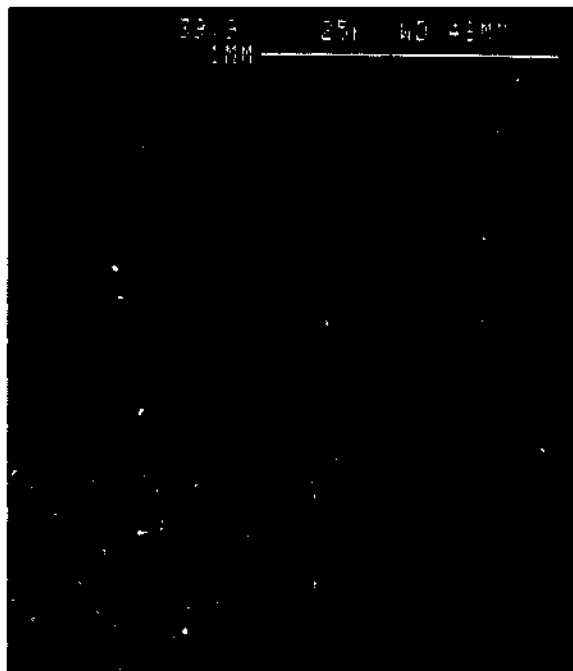
41.7x

Monel 400 After 20-Week Salt Fog Exposure and 20 Acid Dips



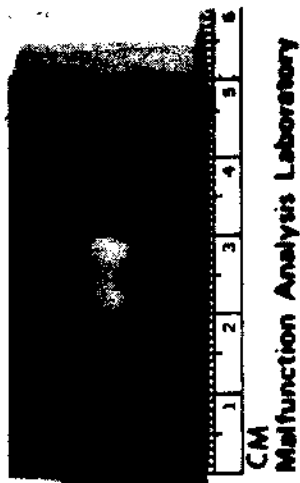
1x

Figure B8



39.9x

Monel 400 After 251-Day Beach Exposure and 13 Acid Sprays



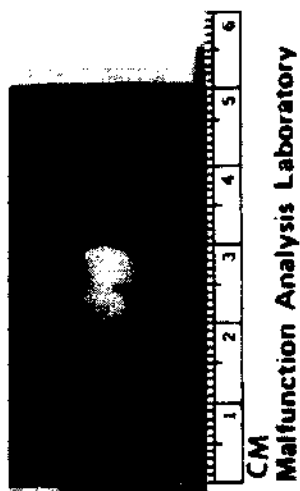
1x

Figure B9



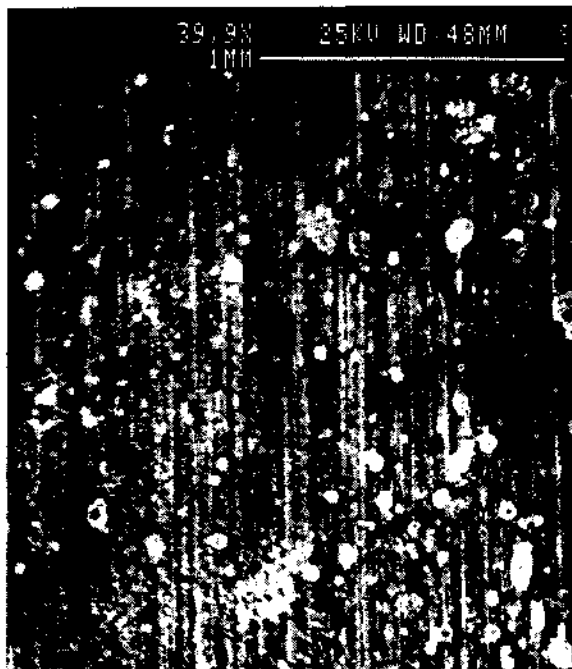
41.4x

20 Cb-3 After 20-Week Salt Fog Exposure and 20 Acid Dips



1x

Figure B10



39.9x

20 Cb-3 After 251-Day Beach Exposure and 13 Acid Sprays

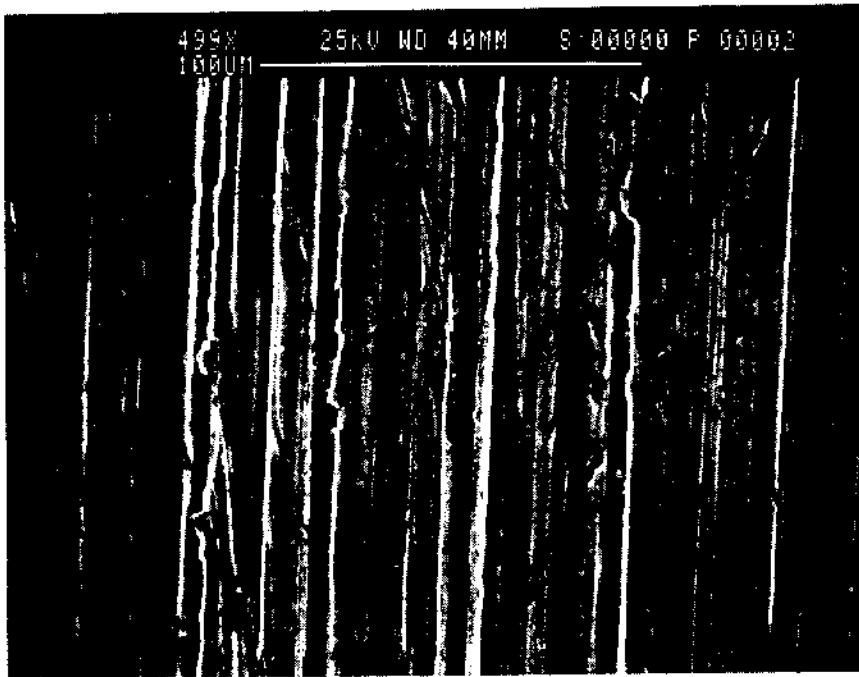


Figure B11 Hastelloy C-22 After 20-Week Salt Fog Exposure and 20 Acid Dips 400x

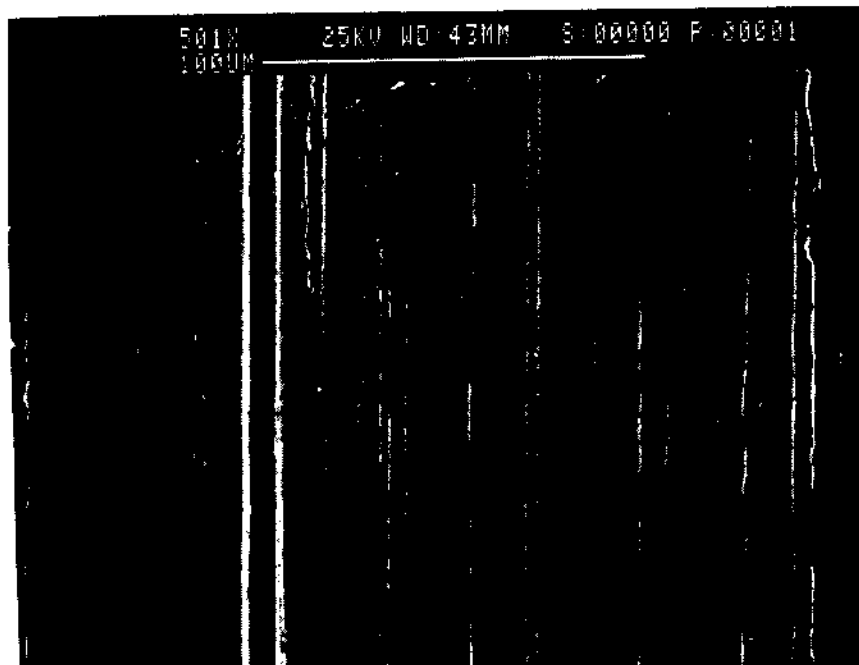


Figure B12 Hastelloy C-22 After 251-Day Beach Exposure and 13 Acid Sprays, 501x

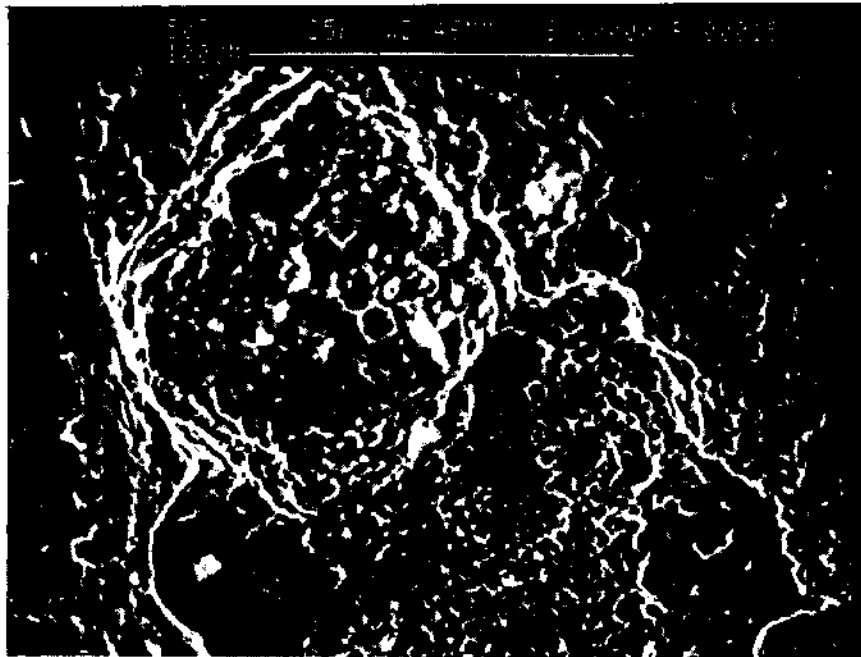


Figure B13 304L After 20-Week Salt
Fog Exposure and 20 Acid Dips, 507x

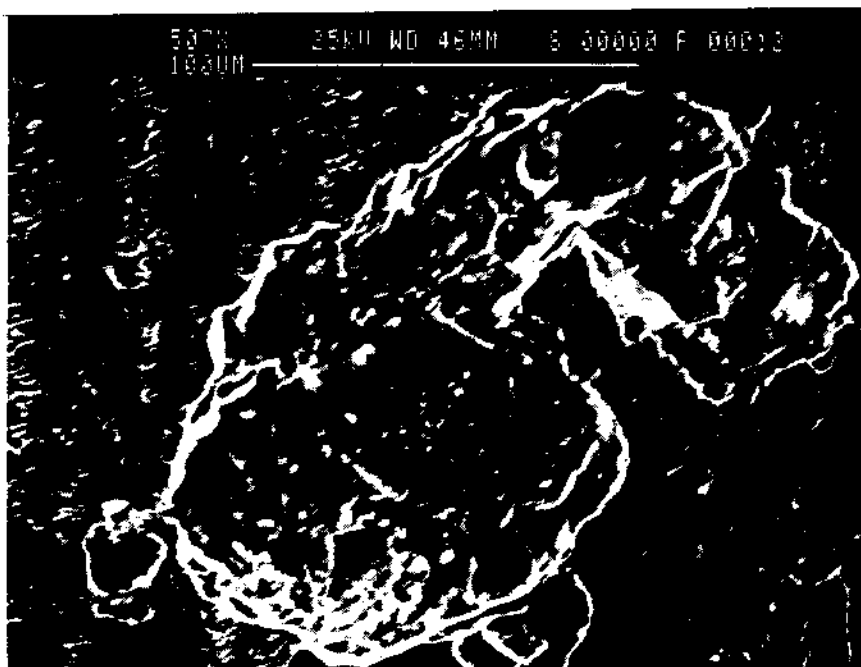


Figure B14 304L After 251-Day Beach
Exposure and 13 Acid Sprays, 507x

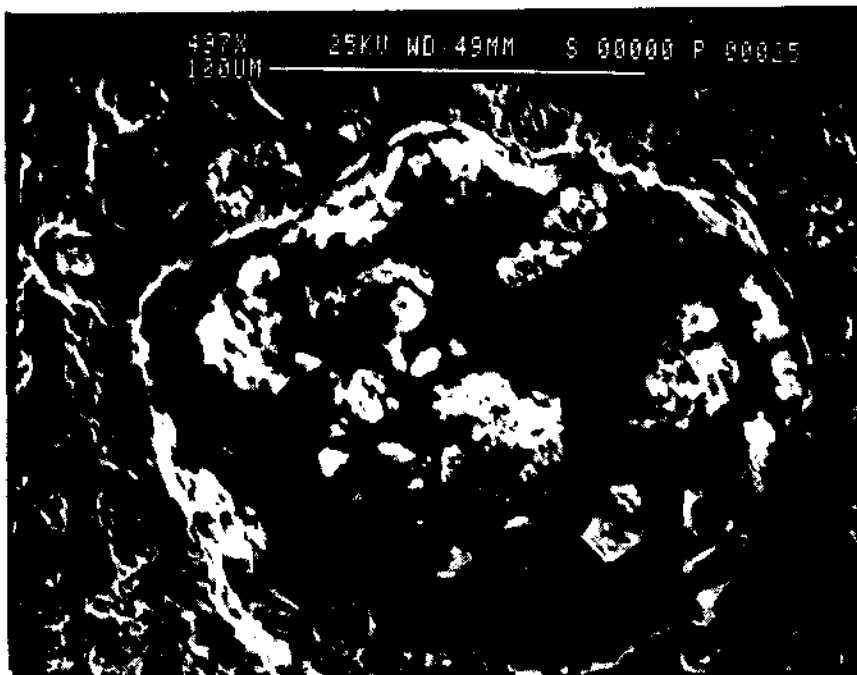


Figure B15 316L After 20-Week Salt
Fog Exposure and 20 Acid Dips, 497x

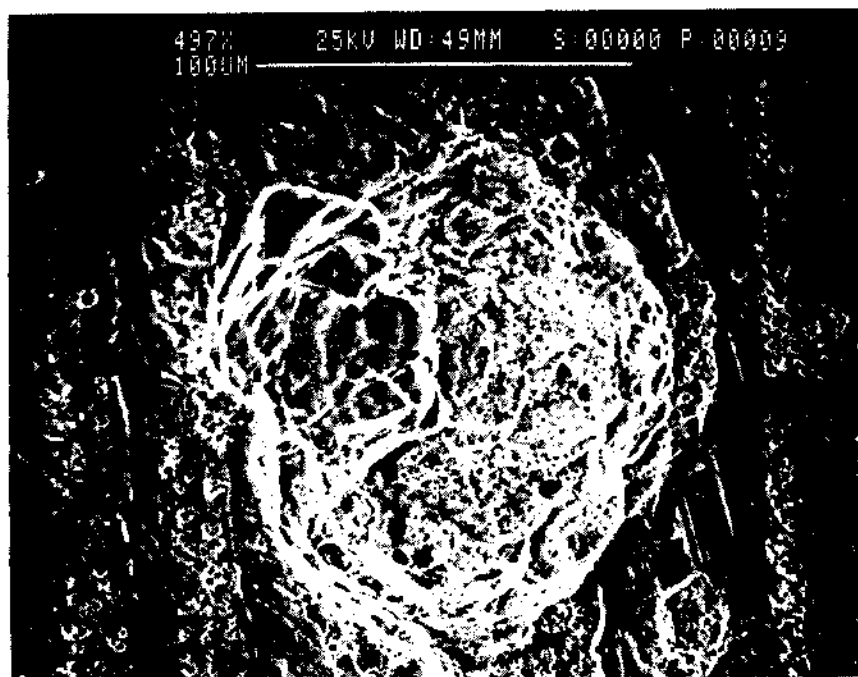


Figure B16 316L After 251-Day Beach
Exposure and 13 Acid Sprays, 497x

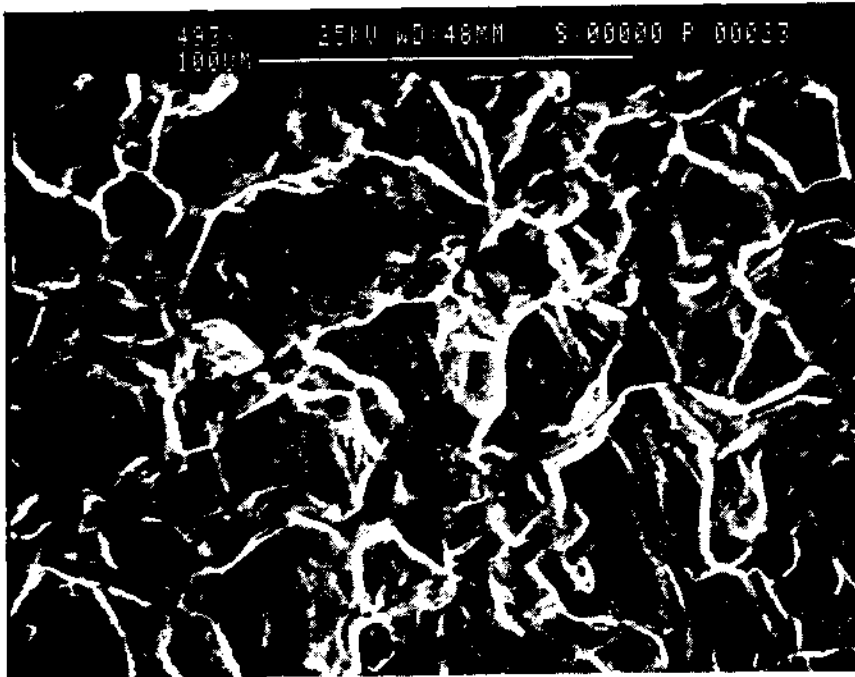


Figure B17 Monel 400 After 20-Week Salt Fog Exposure and 20 Acid Dips, 493x

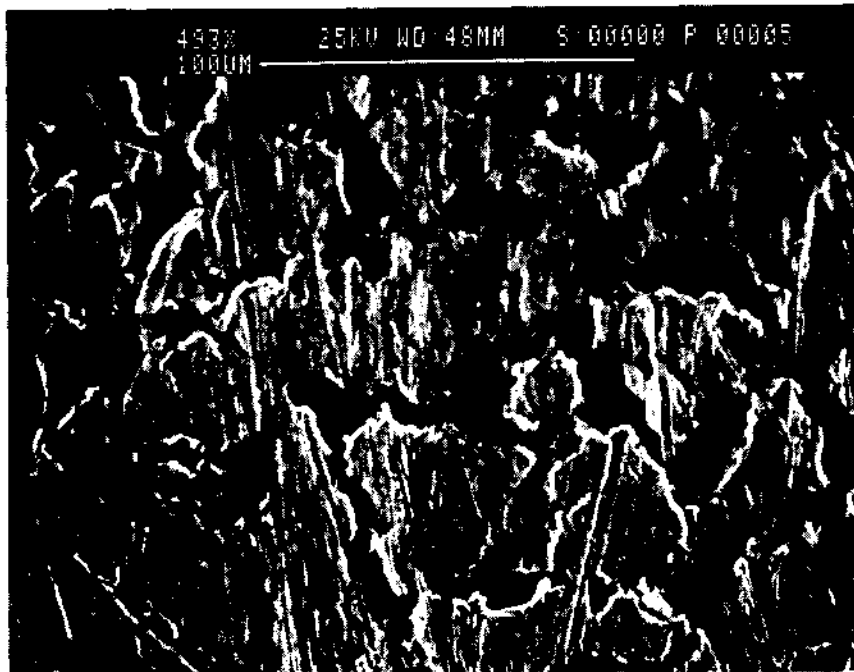


Figure B18 Monel 400 After 251-Day Beach Exposure and 13 Acid Sprays, 493x

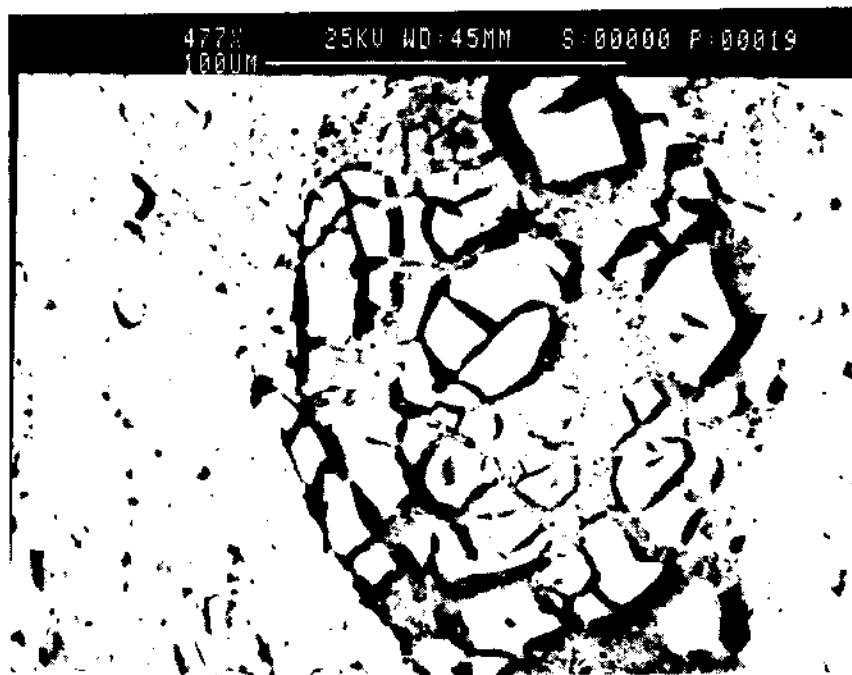


Figure B19 20 Cb-3 After 20-Week Salt
Fog Exposure and 20 Acid Dips, 477x

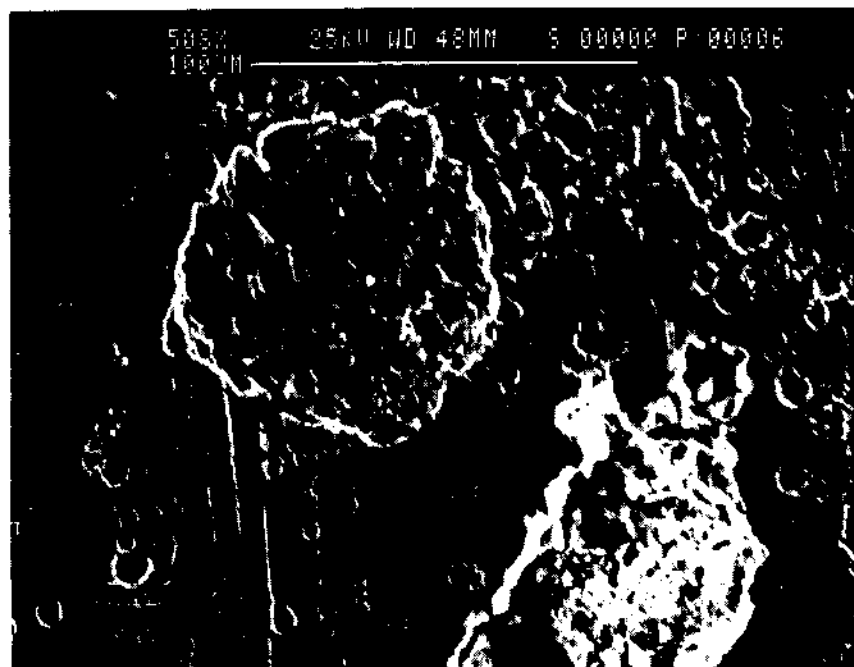


Figure B20 20 Cb-3 After 251-Day Beach
Exposure and 13 Acid Sprays, 508x